PRESSURE SENSING IN VICINITY OF LEAKS FOR LEAK DETECTION

BY

SUARA, KABIR ADEWALE

A Thesis Presented to the

DEANSHIP OF GRADUATE STUDIES

KING FAHD UNIVERSITY OF PETROLEUM & MINERALS

DHAHRAN, SAUDI ARABIA

In Partial Fulfillment of the
Requirements for the Degree of

MASTER OF SCIENCE

In

MECHANICAL ENGINEERING

APRIL 2013

KING FAHD UNIVERSITY OF PETROLEUM & MINERALS

DHAHRAN 31261, SAUDI ARABIA

DEANSHIP OF GRADUATE STUDIES

This thesis, written by **SUARA, KabirAdewale** under the direction of his thesis advisor and approved by his thesis committee, has been presented to and accepted by the Dean of Graduate Studies, in partial fulfillment of the requirements for the degree of **MASTER OF SCIENCE IN MECHANICAL ENGINEERING**.

Thesis Committee

Dr. Rached Ben-Mansour (Advisor)

Dr. Mohamed A. Habib (Member)

Dr. Atia Khalifa (Member)

Dr. Zuhair Gasem
Department Chairman

Dr. Salam A. Zummo
Dean of Graduate Studies

4/5/13

Date

ACKNOWLEDGEMENT

First and foremost, my gratitude goes to the KFUPM authorities for giving me the opportunity to do my MS program in KFUPM and for providing me with funds in the cause of my research. I am very grateful to my Advisor and Supervisor, Dr. Rached Ben-Mansour for his unquantifiable support, guidance and encouragement throughout my program. Indeed, I would like to express my gratitude to Dr. Habib Mohamed and Dr. Atia Khalifa for their immense contributions and supports to my research work. I would like to extend my gratefulness to all the staff and faculty members of Mechanical Engineering Department of the school. I also wish to sincerely thank Mr. Bahaaeldin and Mr. Romeo for their moral, intellectual supports and great contributions to the work.

My heartfelt thanks go to family. This work couldn't have been completed without their pure devotion, sacrifice and continued prayers to my success. Their encouragements kept me going where there seemed to be no way. I also like to extend these heartfelt thanks to my fiancée, Ebunoluwa, for her steady mental support, consideration, patience, help, and encouragement. Furthermore, I wish to thank my colleagues and friends in KFUPM for their supports and their great concern in the course of my study, indeed I had their soft shoulders to lean on. In the same way, I wish to give my sincere appreciation to my brother and Mentor, Engr. Tesleem Asafa and his family for their perpetual supports and encouragements.

Ultimately, my highest gratitude goes to the God Almighty, the knower of unseen and the Master of the day of accountability for giving me life, wisdom, knowledge and for making my MS program a success.

TABLE OF CONTENTS

LIST OF TABLES

Table

LIST OF FIGURES

LIST OF SYMBOLS

a	acceleration	[m/s^2]
g	acceleration due to gravity	[m/s^2]
k	turbulence kinetic energy	[m^2/s^2]
P	line pressure	[Pascal]
Q	Volumetric flow rate	[L/min]
R	Reynolds stresses	[m^2/s^4]
u, v, w	components of velocity	[m/s]
V	velocity magnitude	[m/s]

Greek symbols

δ	delta function	[-]
ρ	density	[kg/m^3]
μ	dynamic viscosity	[Pa/s]
α	leak exponent	[-]
ε	turbulent dissipation rate	[m^2/s^3]

Subscripts

i, j	vector notation for coordinates	[-]
t	turbulence	[-]
x,y,z	position coordinates	[m]

THESIS ABSTRACT (ENGLISH)

NAME: SUARA, KABIR ADEWALE

TITLE: PRESSURE SENSING IN VICINITY OF LEAKS FOR LEAK DETECTION

MAJOR: MECHANICAL ENGINEERING

DATE: APRIL 2013

Leaks account for the largest amount of water lost in distribution pipelines. Cause of leakages in water pipelines ranges from the damage on pipes to improper designs and installations of water pipe networks. Also, leaks are as results of failure in joint, corrosion in pipes, overtime deterioration of pipes amongst others. In a quest for saving the amount of water loss due to delayed detection of leaks in pipelines, a non- acoustic, in-pipe monitoring technique is sought. This eliminates the interference of the environmental factors such as noise with the detection mechanism.

The present work is on experimental and numerical investigation of pressure variation within the vicinities of leaks. Three-dimensional CFD turbulent flow calculations were used to investigate the flow characteristics close to simulated small cylindrical leaks (<1% of the total flow) in a typical water distribution pipelines. In which pressure related characteristics and acceleration were identified to change greatly in the vicinities of leaks. The experimental and numerical works were carried out to investigate the effectiveness of using differential pressure as sensing component in an in-pipe detection mechanism. The comparison between the computational and experimental results gave a good agreement with deviation limited to 30% of the experimental result. In all the cases, the differential pressure reduces exponentially from the line pressure, 30 psi, at the wall of the pipe to 0 psi at distances away from the wall. In order to test the method against flow condition numerically, the flow velocity of a typical pipe was varied between 0.5m/s and 2m/s. The pipe flow increase has positive if any significant on the measurable value of differential pressure within the vicinities of the leaks; therefore the method can be used for monitoring pipe under operation. In addition, mobility module was redesigned with incorporation of propeller propulsion unit and high pressure rotary seal.

THESIS ABSTRACT (ARABIC)

الاسم: أديوالي كبير سوارا

العنوان: إستشعار الضغط بالقرب من التسريبات لكشف التسرب

التخصص: الهندسة الميكانيكية

التاريخ: إبريل 2013

يعتبر التسريب هو اكبر مساهم فى كمية المياه المفقودة فى انابيب شبكات التوزيع و يحدث التسريب في انابيب المياه نتيجة لأسباب عدة منها تلف الانابيب وسوء التصميم والتركيب وأيضا بسبب انهيار الوصلات والتآكل فى الانابيب إضافة الى عوامل اخرى. من أجل توفير الماء المفقود نتيجة تأخر الكشف عن التسريبات في خطوط الأنابيب، فقد تم دراسة تقنية كشف لا صوتية لمراقبة الانابيب من الداخل بحيث تلغى تداخل العوامل البيئية مع آلية الكشف المستخدمة و دقتها مثل الضوضاء على سبيل المثال.

فى هذة الرسالة , تمت دراسة تجريبية معملية وعددية لتغير الضغط فى المناطق المجاورة للتسريبات من داخل الانابيب حيث تم بناء أنموذج عددى ثلاثى الابعاد لمحاكاة التدفق المضطرب فى الانابيب مع وجود فتحات تسرب صغيرة فى الانبوب (أقل من 1 في المائة من معدل التصرف الاجمالى للانبوب) اسطوانية الشكل لدراسة خصائص و تحديد الخصائص التى تؤثر على الضغط والتسارع في المناطق المجاورة للتسريبات حيث استخدمت الدراسة التجريبيه والعدديه للتحقق من فعالية استخدام تغير الضغط كآلية لكشف التسريب فى الانابيب.

أوضحت المقارنة بين النتائج المعمليه والعدديه وجود توافق جيد مع انحراف محدودة (حوالى 30%) عن النتائج المعمليه فى بعض الحالات وفى جميع الحالات يتغير فرق الضغط المقاس بالقرب من مكان التسريب بشكل الدالة الأسية (مثلا من فرق ضغط 30 رطل/بوصة مربعة عند جدار الانبوبه الى 0 عند مسافات بعيداً عن الجدار الى منتصف الانبوب)

من أجل إختبار هذه الطريقه عدديا عند ظروف السريان النمطية تم دراسة تغيير سرعة التدفق فى الأنبوب ما بين 0.5 الى 2 متر/ثانية وقد وجد أن زيادة سريان المائع لها تاثير ايجابى – إن وجد - على فرق الضغط المقاس بجوار التسريبات.

لذلك هذه الطريقة يمكن استخدامها لمراقبة الانابيب تحت ظروف التشغيل وبالإضافة إلى ذلك، أعيد تصميم الوحدة النمطية المتنقلة مع استخدام وحدة الدفع المروحية و الوحدة الدوارة المعزولة للعمل تحت ضغوط عالية.

درجة الماجستير في العلوم
جامعة الملك فهد للبترول والمعادن
الظهران، المملكة العربية السعودية

CHAPTER 1

INTRODUCTION

1.1 Leaks in Water pipelines

Water is essential for every living thing; therefore there is need for regular supply of potable water. For countries that depend on water distribution networks, water scarcity is one challenge; also challenging is the assurance of supply of uncontaminated water. For such a system, an almost leak-free distribution is required which ensures that there is no unintentional supply from the network and there is no infiltration of contaminants into the network. Cause of leakages in water pipelines ranges from the damage on pipes to improper designs and installations of water pipe networks. Also, leaks are as results of failure in joint, corrosion in pipes, overtime deterioration of pipes amongst others. Larry [28].

Figure 1.1: Typical crack in a pipeline leading to content leakages. Hunaidi and Chu [3]

A proper monitoring of health of pipe, damage detection and control must be in place. Monitoring the health of a pipeline network includes tasks such as determining the current roughness parameters of pipes, identifying leakages and blockages, etc. Mohan et al. [1]. Leaks can account for, on average, 10,000 gallons of water wasted in the home every year, which is enough to fill a backyard swimming pool (EPA, 2011)[2]. As a result, pipe damage control and water distribution management have become high priorities for water utilities and authorities because there were greater understandings of the economic, social, and environmental costs associated with water losses. In many water distribution systems, a significant amount of water is lost due to leakage from distribution pipes, to reduce this water loss, system operators conduct systematic programs to locate and repair leaks, Hunaidi and Chu [3]. With the global awareness on addressing the socio-economic effect of leakages in water pipe networks, studies are

being carried out on daily basis on optimizing the methods of leaks detection for early detection and control. Methods have been developed for -experimental studies, field works and simulation/ computational works –the detection. Several devices have been developed for pipe damage detection in water distribution networks among which is acoustic leak detection equipment-listening rods, aqua phones, hydrophones, etc.-, leak noise correlators.

1.2 Overview of the Thesis

The overall thesis is presented as follow. Chapter 1 presents the literature survey likewise defines the objectives of the study. In chapter 2, details about the experimental set up are presented with calibration of components used for the work. Chapter 3 presents the mathematical models used for the computation; mesh independence studies are presented likewise the model tests. Chapter 4 presents the details of both the computation and experimental results; results comparison and discussion of parametric studies are also presented. In chapter 5, the contribution on the in-pipe mobility module is present. Finally, chapter 5 gives summary of the work as conclusion and recommendations for future studies are also made.

1.3 Literature Review

Several mechanisms are being used in detection of pipe damages and leakages. These mechanisms utilize the advantage that flow in pipes exhibit special properties at the point of leaks among which are, flow rates, pressure and sound generation. These properties

make it possible to detect leaks by applying a relevant measuring device. Among these devices are flow tracer, pressure transducers, accelerometer and others. In the earliest period when leak detection became inevitable, visual inspection of pipes was in vogue as used by most inspection officers but in later years when need for more accurate means for location of leaks in buried pipes were required, some devices were developed. Among the first of these devices are the inventions of Wilsky [13] and Reid and Michael [23]. These devices used the sonic signal from flow within the pipe to locate leakages.

1.3.1 Acoustic Detection Methods

Acoustic being the leading technology in leak detection due to the vast number of sensor and devices that can be incorporated has been used by many researchers in the past. Leaks in water pipes create acoustic emissions, which can be sensed to identify and localize leaks Chatzigeorgiou et al. [30].

This acoustic equipment includes: *Listening devices* which may be either mechanical or electronics. They use to be sensitive mechanisms or materials such as piezoelectric elements to sense leak-induced sound or vibration while some modern electronic listening devices incorporate signal amplifiers and noise filters to make the leak signal stand out. The acoustic equipment may also involve the *noise loggers* which serve as the data acquisition unit. They are used for large area leak survey with the incorporation of devices like accelerometers and hydrophones for sensing. Other component of acoustic equipment is the leak *noise correlator*- a microprocessor–based device which compares signals from two locations to effectively correlate the source of signal by calculating how close the source is from both receivers.

In the work of Hunaidi and Chu [3] in which he examined the acoustic characteristics of leak signals in plastic water distribution pipes by carrying out a test of leak detection on the facility of National Research Council (NRC); vibration and acoustic sensors were used to measure the leak signals in the test pipe, he found out that the higher the pipe pressure the more significant the frequency of transmission of signal and that, the flow rates have a significant effect on the amplitude measured signal but have a negligible effect on the frequency. They also found out that the effectiveness of the correlation techniques is affected by the selection of acoustic/ vibration sensors. The cut off frequency of high and low pass digital filters are used to remove noise and they concluded that accelerometer measured leak signals have higher levels of frequency than hydrophone measured signals and that the propagation velocity is independent of the frequency below 50Hz. This conclusion was also supported by Gao et al. [11] that the accelerometers are most suitable in multi-leak system and coherent noise situation. Theoretical predictions of correlations coefficients of pressure, velocity and acceleration responses were carried out. However for location of leaks having small signal to noise ratio (SNR), the measure of pressure using hydrophones would be suitable. Gao et al. [11]

Figure 1.2: Monitoring Officers using listening devices for leak location

(a)

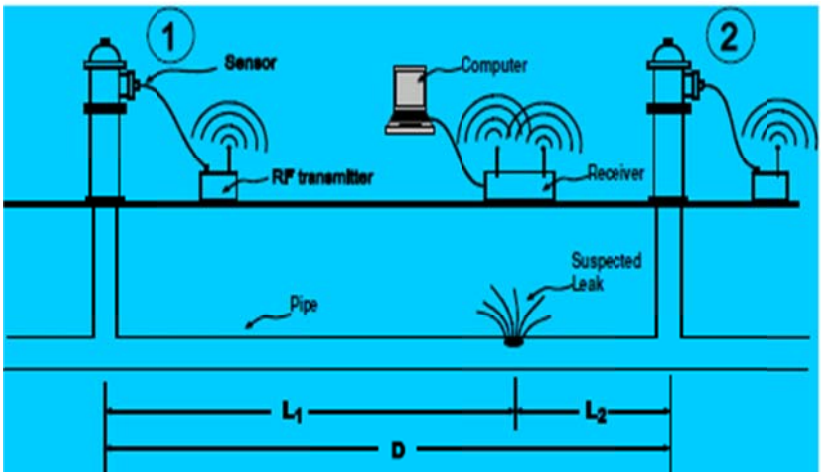

(b)

Figure 1.3: Some acoustics equipment with correlation scheme. Hunaidi and Wang [12]

The behavior of a leak in water pipe depends on the material of the pipe and the surrounding [5-8]. In the work of Hunaidi and Chu [3] on characteristics of leak signals in plastic water pipes, it was found that the frequency content of leaks signals in the setup used measured with hydrophone were below 50Hz. Also, the leak noise amplitude in plastic pipes can be characterized as diminishing at the rate of 0.25dB/m with a possible variation due to weather condition. Also the findings of Martin et al. [8] described the leak behavior of having a uniform excitation in broad band frequency with characterized low frequency not more than 200Hz for plastic homogeneous pipes. In the work of Maninder [9] on leak detection in water distribution polyethylene pipes, it was found that leak made signals are below 250Hz with the high amplitude leak signals concentrated in the range of 60Hz and 150Hz. Leak signals up to 100Hz are highly affected by ambient noise while 250Hz above brings about uncertainty depending on the pipe material and ambient conditions.

1.3.2 Non-Acoustic Detection Methods

Some **non-acoustic non measurement based methods** of leak detection include:

Tracer gas technique: - the principle behind this is the ability of some gases to penetrate through the soil. This kind of gas is deployed into the pipe. The pipeline is then pressurized so as to allow the gas to exit through the leaks with the network. Regions of high concentration of the gas are then used to locate the leakages within the distribution system. Typical application is shown in Figure 4 below.

Figure 1. 4: Gas tracer used in leak detection. [Picture from http://www.leakbusters.net/gas-tracer.html]

Thermography: - This technique takes the advantage of the property changes in the soil in region of leak to locate where leak is eminent. Thermal anomalies above pipes are detected with a ground or air-deployed infrared camera. The method involves scanning through the pipe network using an infrared camera either land or air deployed. In the work of Fahmy et al, [14] a study was conducted to investigate the factors that affect the use of IR camera in detecting and locating water leaks in underground water mains such as weather conditions, soil and pavement surface conditions, ground water level and distance of sensor (i.e. IR camera) from source and it was found out that there were constraints when it comes to pipe network being adjacent to a drainage line.

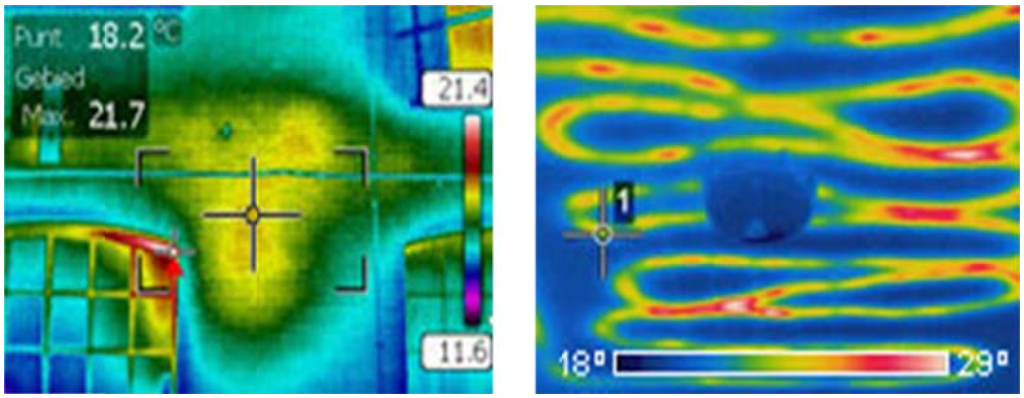

Figure 1.5: Thermography of water pipeline.

[Picture fromhttp://www.leakdetectionspecialists.co.uk/thermography-leak-detection.htm]

Ground-penetrating radar: - According to Hunaidi and Wang [12], radar can be used to locate leaks in buried water pipes. This is done either by detecting voids in the soil created by leaking water as it circulates near the pipe or by detecting sections of pipe which appear deeper than they truly are because of the increase in the dielectric constant of water-saturated adjacent soil. Bimpas et al. [15] developed a technique to detect water leaks in supply

pipes, such as PVC pipelines and minor leaks. The operation of the technique was founded on the echo signal reception by using ground penetrating radar which has electromagnetic waves in the propagation media; the system was tested in various test sites in order to assess the performance. The results found were considered satisfactory and promising especially concerning the ability to detect and locate accurately leakage points. The system was recommended for efficient detection in plastic pipelines (PVC) to complement the deficiency of the acoustic method of leak detection.

Figure 1.6: Ground Penetrating Radar (GPR).

[Picture from http://www.directindustry.com/prod/radiodetection/gas-leak-detectors-23416-351890.html]

Non-acoustic measurement based methods.

Apart from the non-acoustic methods which are based on enhancement of the expected properties of the soil surrounding pipelines for leak detection, there are other

methods based on flow characteristics. These methods utilize the properties exhibited by flow in pipelines both at steady and unsteady states. One of such method is the ***inverse transient analysis (ITA).*** According to Karney et al. [16], the method was introduced in 1994 and has since then been promising leak detection technique having well demonstrated it power in laboratory and numerical settings. The method involves introduction of hydraulic transient into the pipe network by opening and closing of fire hydrant valve. The signal is then recorded at predefined locations within the network. The signals recorded are then correlated against a similar computer simulated scenario or pre-acquired experimental data at another point in time. Offsets between the recorded and validating signals at location are then used to track existence of leaks within the network. Karney et al. [16] undertook a simulation study using inverse transient analysis for leak detection in water distribution network. The study was carried out in an area in city of Regina as the field testing where the night supply and consumption of the district metering area (DMA) were monitored to serve as the experimental validation of the simulation for the scenario. The main factors affecting the effectiveness of this method were analyzed and they found that effectiveness and accuracy of the method relies on availability of reliable and calibrated transient model for the system. Also that ITA method may be an effective tool for determining leaks of intermediate to large size as it may not be able to detect small leaks within the acceptable levels of induced transient pressure. Similarly Covas and Ramos [17] undertook a study using ITA for effectiveness and factor studies; they found out that the success of ITA does not depend on the steady and unsteady friction likewise not on the accurate estimation of wave speed or pipe viscoelasticity. ITA method can locate leaks with accuracy of 24m which is

corresponding to 2% of the total pipe length used by Covas and Ramos [17] in their study. They also found out that inverse transient solvers gave unsuccessful results in leak location and sizing in plastic pipe. This is as a result of the method not taking into account the frictional, mechanical losses and the valve closure time. It is very imprecise in the description of transient event in polyethylene pipes which hinders the correct location of leaks. However, their finding was in line with that of Karney et al. [16] that, ITA can locate leaks of reasonable sizes.

Shinozuka [18] developed *a non-destructive monitoring* of a pipe network using MEMS-based wireless network, the design incorporated the accelerometer as the means of monitoring signals from the pipes. The MEMS sensor network monitors the pipe surface acceleration at each network joints. For the development, a small scaled symmetry water network consisting of 40PVC pipes of 1-in diameter with seven valves was set up and leakages were introduced in between some junctions that differ from the outlet valves. Based on the analysis of the acceleration data measured, the pipe damage/detection can be tracked in between two end joints where the acceleration gradient values are local maxima. The developed system made use of a program based *pipeTECT* sensing system which collect the data from the joints of the network and analysis it. The results of the development showed that leaks and damages can be located in pipes by contour maps, time correlated acceleration data analysis and frequency domain analysis.

Also reported in some literatures are the non-acoustic based flow parameter for leak detecting among which are the flow rate monitoring, PH monitoring and the pressure monitoring. For the flow rate monitoring, flow meters are installed along the length of the water distribution pipes. These flow meters are monitored for discrepancies of

measurement. Any discrepancy in the measurements between any two adjacent flow meters indicates leakages between the two points. The operation is generally carried out at night when the flow rate in pipe is relatively constant due to the low supply to user ends. The constraint of this method is the inability to detect very small leak size which characterizes early leakages in pipe because study has revealed that small leak takes an order of 0.001 of the nominal pipe flow rate.

1.3.3 Pressure Based Detection Techniques

Pressure monitoring on the other hand has been a promising tool in the leak detection in pipe, the early stage monitoring of pipe health has always been with pressure correlation of points. A study carried out by Mashford et al. [19] in which the pressure at different nodes in a pipe model were measured and processed using support vector machine. In the work, EPANET software was used to predict the pressure in a pipe network. One of the nodes was assigned as an emitter with coefficient varied from 0 to 0.0025 at a step size of 0.0001. The upper limit is equivalent to emitter flow rate of about 90L/hr. He found out that the accuracy of the method depends on the amount of information available from the distribution and resolution. The method predicted the exact location of leak at 35% accuracy while the exact location of leak lays 500m range from prediction. Thus, the method is only applicable for initial isolation of leaks.

Also Wu et al. [10] developed a leak detection model based on the pressure dependent of leaks. The model is formulated to optimize the leakage node location and their associated emitter coefficients. This is done either as an independent task to locate the leak hotspot in a network or combined with hydraulic calibrations. Greyvenstien and Van Zyl [20]

had an experimental investigation of pressure leakage relationship of some failed pipe. The study involved the data collection of from pipes of different materials and attached to some portions of these pipes are calibrated pressure transducers. The pipes used were new with artificially induced failure. It was found that both pressure and flow measurements included short terms fluctuation as this was related to the transient behavior of city water distribution system used in the experiment. The results of the experiment showed that leakages exponents found is significantly higher than the theoretical value of 0.5 except for that in the plastic pipes which is close to the value for circular leakages and that the highest exponent occurred in the corroded steel which was associated with the reduction in the strength. The study provided a realistic data for leakage exponent for several pipe materials so as to have a good account of leakage when designing models.

In the recent research Ben-Mansour et al. [21], CFD simulations of leak in a typical water pipeline were carried out. The steady state simulations in the work highlighted the parameters of great influence in the vicinities of leak. It was shown that the pressure gradients around the leaks are high. Also the result shows that vorticity within the vicinity of leak is quite high which is a possible mechanism for generation of noise by leaks. The steady state results of the work serves as basis initiating the present study. The results showed clear influence of the leak on the pressure gradient along the different paths of the flow inside the pipe. It was found out that for very small leaks (below 1 liter/min), the influence is not strong in the static pressure distribution, but very clear in the pressure gradient distribution. The study indicates that signal due to pressure changes in the vicinity of a leak reduces as the leak flow rate reduces and could barely be noticed

at the centerline of the 4 inch pipe with 1mm x 1mm opening at the wall. However, the study found a good signature of pressure gradient in the vicinity of simulated quadrilateral leaks. Based on the study, in-pipe mobility device was designed for water pipe leak detection. The device is designed to drive sensors closed to the pipe walls for detecting behaviors signifying leaks. Thus, optimization of this system requires consideration of other flow characteristics which give clear definitions in leaks vicinities.

Based on the highly localized pressure gradient around the vicinity of the leak, Chatzigeorgiou et al. [31] designed and evaluated an in-pipe leak detection based on force transduction. The mechanism is designed in such a way that the pressure difference between the pressurized pipe and atmosphere (opening on pipe) is transformed to suction force. This force pulls the sticky membrane attached on a drum being driven by a mobility module. The correlation of readings on the sensor adapted on the drum is then used in defining the position of the leak.

Many other leak detection methods are being developed with all methods having different places of relevance and limitation, a full evaluation of all leak detection methods with their merits and demerits can be found in the review of Ben-Mansour et al. [21] and Khulief et al. [22]. Some of these other methods are pre-developed commercial leak codes like that of Bentley, use of Pressure values by support vector machines etc.

In summary, it has been shown from the review that many methods have been developed overtime for leak detection in pipeline. The reviews of literatures for this study have particularly highlighted the shortcomings and failures of most of the previous methods. These ranges from the high tendency to false alarm of some of the methods due to environmental activities to the cost and non robustness of some of these methods when

applied to plastic water pipeline leak detection. Another is the inapplicability of most developed technique to pipeline under operational conditions.

1.3.4 Overview of In-pipe leak detection techniques

Most of the leak detection techniques discussed above operates outside the pipe. This approach has many limitations has identified. Accuracy post a major challenge as the mechanisms could only be used to isolate areas in pipe network suspected of leakages. In addition, loss of signal due to attenuation into soil surrounding the pipeline limits the effectiveness of the acoustic related methods. In order to detect leakage effectively, in-pipe leak detection techniques approach are recently being adopted. The components of in-pipe leak detection mechanism are two. One is the sensing module while the other is the mobility module.

A smartball according to Fletcher and Chandrasekaran [29] was a new approach which combines the sensitivity of acoustic leak detection in the sensing module with the full coverage of floating hydraulic ball as the mobility module. The device only requires a single acoustic sensor. This gives it cost advantage over the permanent monitoring sensors based on acoustics. A major problem with this device is size; it was developed for larger pipes compared with the size found in the majority of water distributions. Another problem arises when the intended pipe is under operation. Turbulence interferes a lot with the leak noise signal while the pipe is under operation. Thus, the method is being used for large petroleum pipelines with no flow. In the work of Chatzigeorgiou et al. [30], he examined sensing capabilities and evaluation of in-pipe leak detection sensor with acoustic sensing components. He evaluated the quality of signal received against loading

conditions, leak size and surrounding media. The results showed that the leak signals are clearly distinguished from any background noise for no flow conditions. Also the sand medium intensifies the leak signal the more thus, giving an advantage while detecting leaks in buried pipe.

Another in-pipe based leak detection which incorporates a non-acoustic sensor in its sensing module is the force transduction. In the development by Chatzigeorgiou et al. [31], the system combines in-pipe mobility with a fluid pressure generated force within the vicinities of the leak. The advantage of this over the acoustic based sensing is its ability to work under operational condition like fluid flow.

In summary, the advantage of in-pipe leak detection approach over the outside pipe approach includes;

- Efficiency and Accuracy
- Cost effectiveness with respect to coverage area
- Ease of usage for non-routine checks
- User friendliness of the approach

Figure 1.7: Smartball being deployed into gas pipeline.

[Picture from: http://www.puretechltd.com/products/smartball/smartball_oil_gas.shtml]

1.4 Research Motivations

Larger percentage of countries of the world depends on water distribution networks as means of getting potable water to the populace. Leaks account for, on average, 10,000 gallons of water wasted in a typical home in the USA every year, which is enough to fill a backyard swimming pool according to Environmental Protection Agency, EPA [2]. According to Urban Water Resources Management UWRM [4], up to 30% of the fresh water distributed in major cities in the world is lost through leaks. Owing to the

geographical location of Saudi Arabia, water management remains a priority to prevent the possibilities of water scarcity. Many of the discussed mechanism of leaks detection in pipelines have been explored. The limitations of these methods are high cost of implementation and maintenance, difficulties in actual location of leaks, ineffectiveness for buried plastic pipes, and false alarms amongst others. Visual inspection based mechanisms are not cost effectives because damages are always evidently pronounced prior to detection. Non-acoustics based mechanisms described above are both expensive and have limited coverage. Acoustic based mechanism is widely accepted for pipeline monitoring. This mechanism remains tricky in buried plastic pipe distribution network owing to interference of ambient noise from human/environmental activities with the leak acoustic signal. Furthermore, like some other leak detection techniques encountered in the literature survey, the acoustic technique fails while pipe is in flow condition. This makes it inefficient for pipelines under operation. Therefore a more reliable method is sought.

In the recent study of Ben-Mansour et al. [21], CFD simulations of very small leaks for pressure transduction were carried out. It was reported there in that the static pressure signal around leaks greater than 1litre/min is appreciable for leak detection while at lower flow rates the pressure gradient remained the possible leak indicator. The plot shown in figure 1.8 below represents the static pressure close to the wall for a single circular leak in a water pipeline from the study of Ben-Mansour et al. [21]. The result indicates clear distinction of pressure in the vicinity of the leak, despite the low flow rate within the pipe. Similarly, the pressure gradient along the centerline of the pipe was found to have appreciable signal despite the low leak flow rate. The plot shown in Figure 1.9 represents

the plot of the pressure gradient along the centerline of the pipe. With these clear definitions provided in this previous study, the present work undertook a preliminary study. In the preliminary work, determination of important flow characteristics for leak detection in water pipes was carried out. The study was based on multi-leaks located along pipes and eventually motivated further studies both experimental and numerical approaches. Also, the thesis solves some problem on the in-pipe mobility module designed in the research group to drive sensing modules.

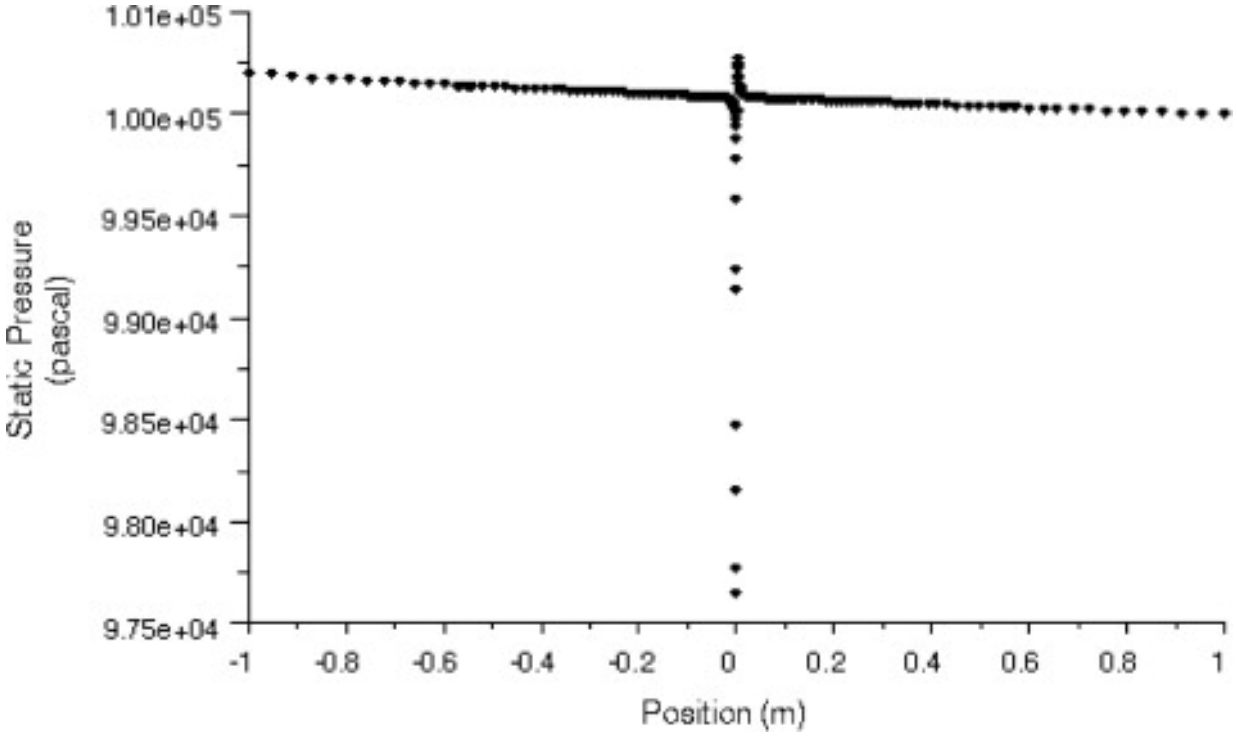

Fig.1.8: Pressure variation 1mm below a leak in a pipe Pline = 1 bar, V = 1 m/s, leak: 1 mm x 1 mm. Ben-Mansour et al. [21]

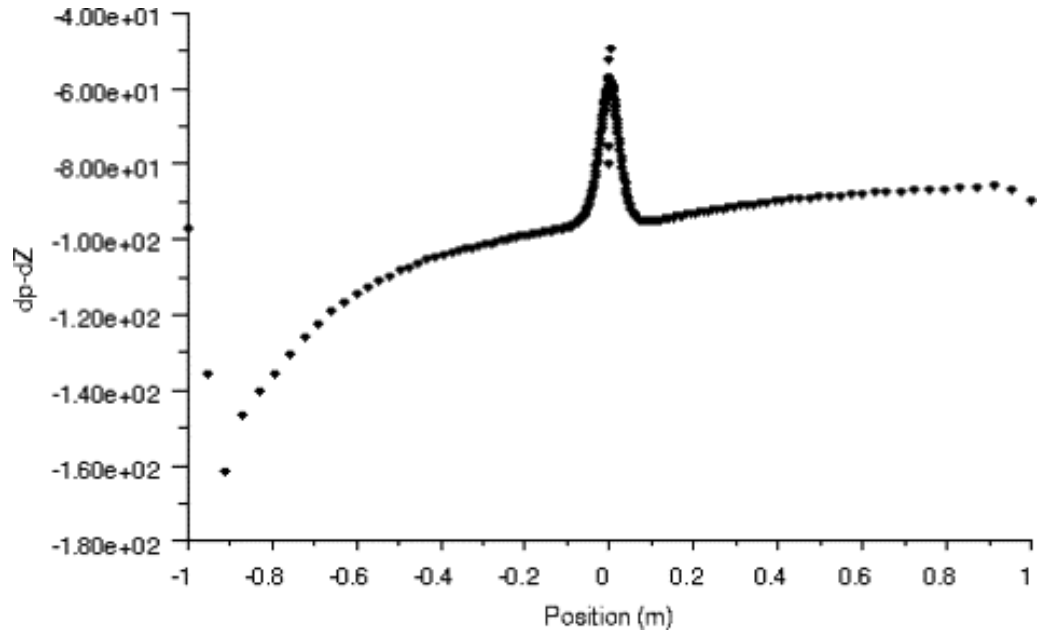

Figure 1.9: Pressure gradient variation along the centerline in a pipe Pline = 1 bar, V = 1 m/s, leak: 1 mm x 1 mm. Ben-Mansour et al. [21]

1.5 Analysis of Proposed Method

In a fluid pipeline network, contents are supplied to delivery units by pressurizing the pipe. The pressure within a standard potable water distribution pipe ranges 30Psi and 80Psi for municipal water distribution. It is expected that this pressure remain fairly constant within the pipe with the negative gradient of magnitude less than 1Psi as can be deduced from the static pressure plot through the center of the pipe shown in Figure 6.

The surface of the leak exhibits a pressure condition lower than that of the line pressure of the pipe, e.g 0 Psi for leaks exposed to the atmosphere pressure. Thus, this negative gradient favors flow through the leak. A differential pressure sensor is a transducer that compares pressures of two points in a system. In this application, the sensor is expected to measure the difference in pressures at within the vicinity of leaks where pressure gradient is highly localized.

The numerical simulations allow evaluating the magnitude of these differential pressures at various sensor heights. In the CFD, taken to consideration are the sensor interference with the leak flow, effects of line pressure and fluid flow velocity. The experimental study allows validation of the CFD results. Both the experimental and numerical results will be used to evaluate the effect of like size, leak geometry and sensor heights on the workability of the method for water pipeline leak detection.

1.6 Objectives and Methodology of Study

The present work investigates the prospect of using differential pressure as parameter for in-pipe sensing module. The specific objectives of this work entails; *to make experimental and numerical studies of differential pressure around leaks in typical water filled pipe section to compare the experimental and computational results*. The following shows the outlines of how the study addresses the aim of the work;

- Preliminary parametric study was carried out to identify the parameters that can possibly indicate leaks at their vicinities for typical water pipeline. The preliminary study involved numerical calculations. The target was to ensure that the proposed method is feasible. Some of the points that were investigated in the study include, parameters indicating leaks in pipe and the effect of line pressures
- Test sections were designed and constructed for experimental investigation of differential pressure for leak detection. In this, leaks are simulated as cylindrical holes of three different diameters (2.2mm, 4mm and 6mm) and as a crack type leak is approximated as longitudinal in the pipe wall.

- Experimental data collation of differential pressure measurements within the vicinities of simulated cylindrical leaks. The pipe sections were pressurized at a typical pressure of 30 Psi. The differential pressures were noted at various heights (0.5mm, 1mm, 1.5mm and 2mm) from the holes using Omega differential pressure transducers of various sensitivities. Similar measurements were done on the slot in water loop. The results were to be taken at heights (0.5mm and 1mm) away from the slot
- Full three dimensional CFD simulations were carried out with the conditions related to those of the experimental study. The numerical work involves, geometry creation using GAMBIT and solving the discrete equations using ANSYS FLUENT 12.1 commercial software. Mesh independence study was done to ensure that the numerical solutions are optimized in terms of resources and results.
- The Computation results are compared with the experimental results. Based on both numerical and experimental results, inferences are made as regards the trend of results with the sensor locations (distances and heights).
- Modifications are made to the designed mobility module. The modification involves incorporation of propeller propulsion unit and sealing under pressurized condition.

CHAPTER TWO

EXPERIMENTAL SETUPS

2.1 Introduction

This chapter presents the description of components of the experimental setup and the description of the simulated leaks. It also presents the results of calibration of the components.

2.2 Description of Test Loop

Two test sections were constructed for experimentation of differential pressure within vicinities of simulated leaks. Figure 2.1 shows the picture of the test section with cylindrical holes. The section consists of a 4-inch straight pipe segment with a T-pipe section. The T-section connected along the pipe serves as access for components insertion and retrieval. On one part of the pipe, 2.2mm, 4mm and 6mm holes are made. Also the part accommodates a relieve valve for line pressure regulation. On the other part, pressure gage is mounted closed to the pipe inlet to monitor the line pressure in the test section. During tests on each of the holes, the others are sealed using the pipe clamps with rubber paddings so as to avoid interference with the pressure values being measured and to reduce pressure loss within the section.

The second section is created to experiment leakage a typical crack within a pipe. Crack in pipe is an opening propagated from inside the pipe as results of aging, corrosion, and

other phenomena related to such a pipeline transport system. Crack has no definite geometry. Experience has shown that it starts its propagation from the most vulnerable part of the pipe and extents along the pipe where the material strength can no longer hold the stress being induced within the pipe. First initiation of a crack in a pipe occurs as a thin opening which expands due to stress induced by the line pressure. This opening later expands either radially or longitudinally depending on the mode of failure. The opening is closest to slot in geometry. Thus, the experimented crack is approximated as a thin slot. This section has the same length with the test section with simulated cylindrical leaks. The crack was made by sliding knife into 4 inches plexiglass pipe. Figure 2.3 below presents the close view of the 0.6mm X 12mm slot generated.

Water from the municipal line is connected to one end of the test section while a the other end is connected to a drainage. During the tests, the inlet valve is kept open to allow water into the system while the outlet valve is closed. The relieve valve keeps air out the system while the loop is being filled up and being used to regulate the pressure at instances of high pressure within test section.

The following are the components attached to the test section:

- Pressure gage
- Inlet and outlet ports
- Inlet and outlet control valves
- Pressure relieve valve

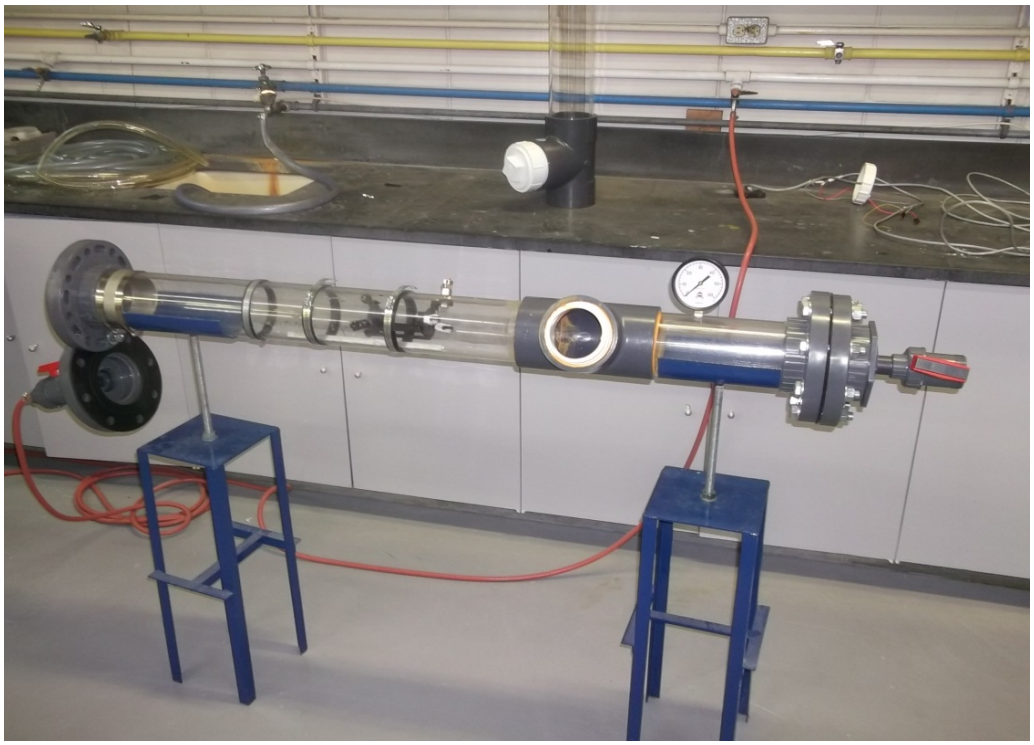

Figure 2.1: Test section with cylindrical holes covered with pipe clamps

Figure 2.2: Test section with crack approximated as slot

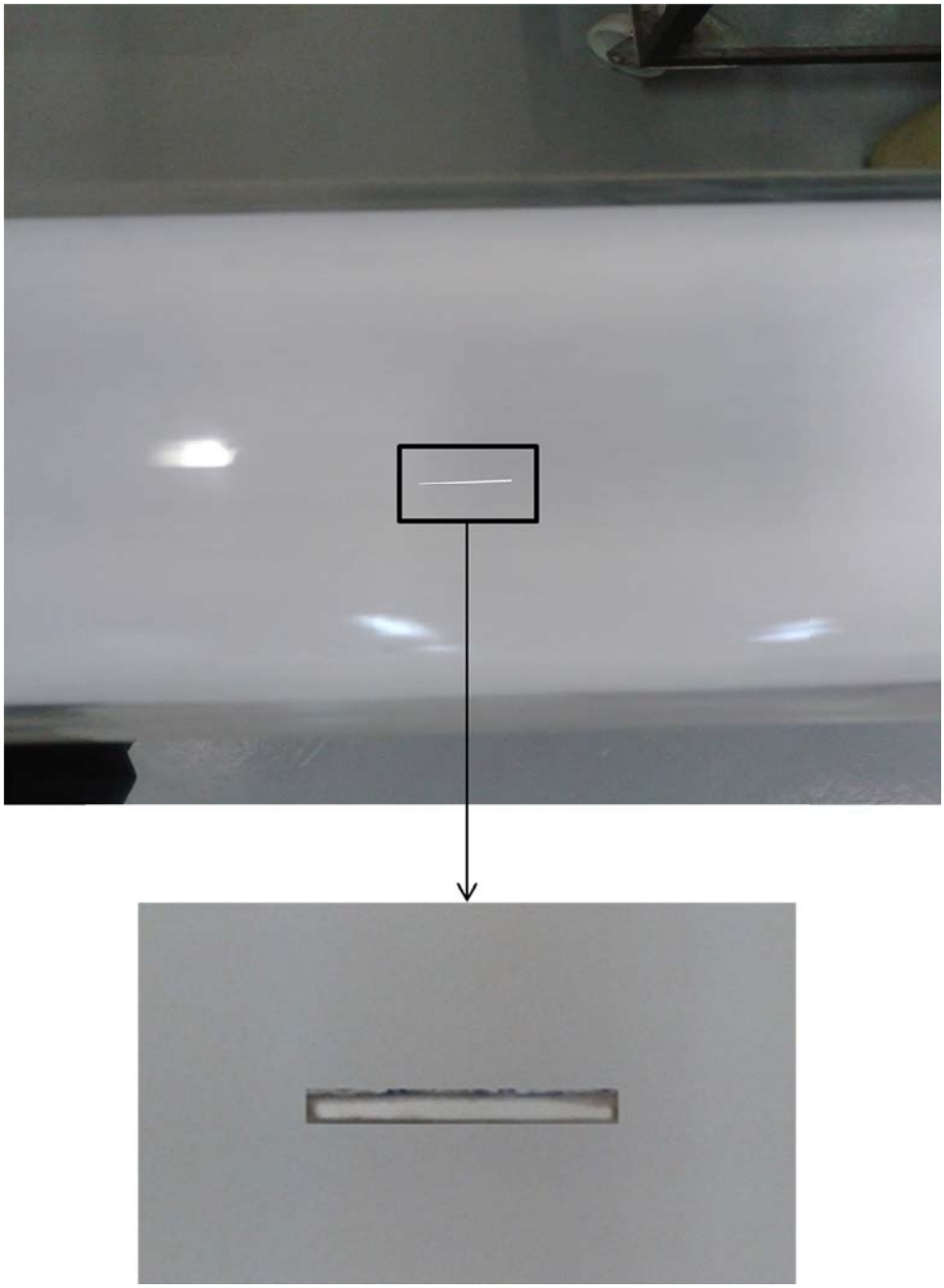

Figure 2.3: Close up view of experimented slot (0.6mm X 12mm)

2.3 Simulated leaks

For purpose of the experiments, leaks are simulated both cylindrical holes and slot. The cylindrical holes are created using drill bits of 2mm, 4mm and 6mm. The 2mm drill bit eventually resulted into a 2.2mm hole from measurement taken after drilling while the other two bits resulted into holes having the same dimension as the bits. The crack is created as a slot by slicing a side of the section with a knife of 0.6mm thick. This resulted into a 0.6mm thick gap of 12mm long. Under a pressure of 30psi within the section, figures 2.4 and 2.4 compare the water jets from the 4mm holes with that from the slot. Although, the flow rate out the 4mm holes is more than that of the slot, yet the spread of water jet from the slot looks more like ones from real pipelines.

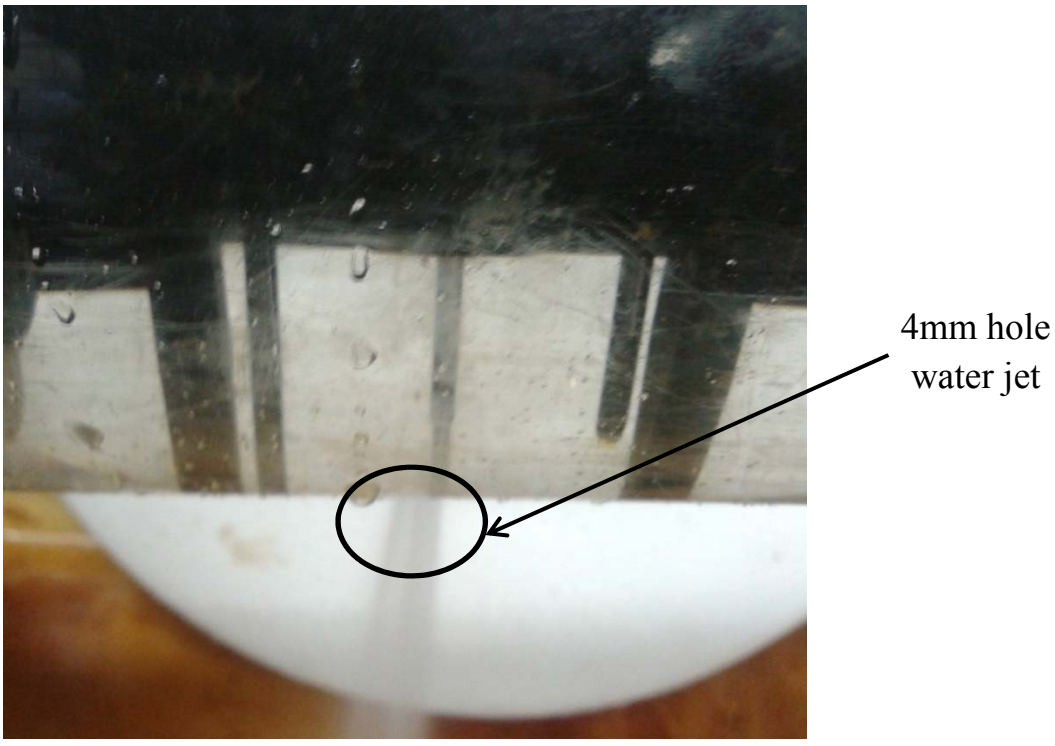

Figure 2.4: Water jet from 4mm cylindrical hole along a test section

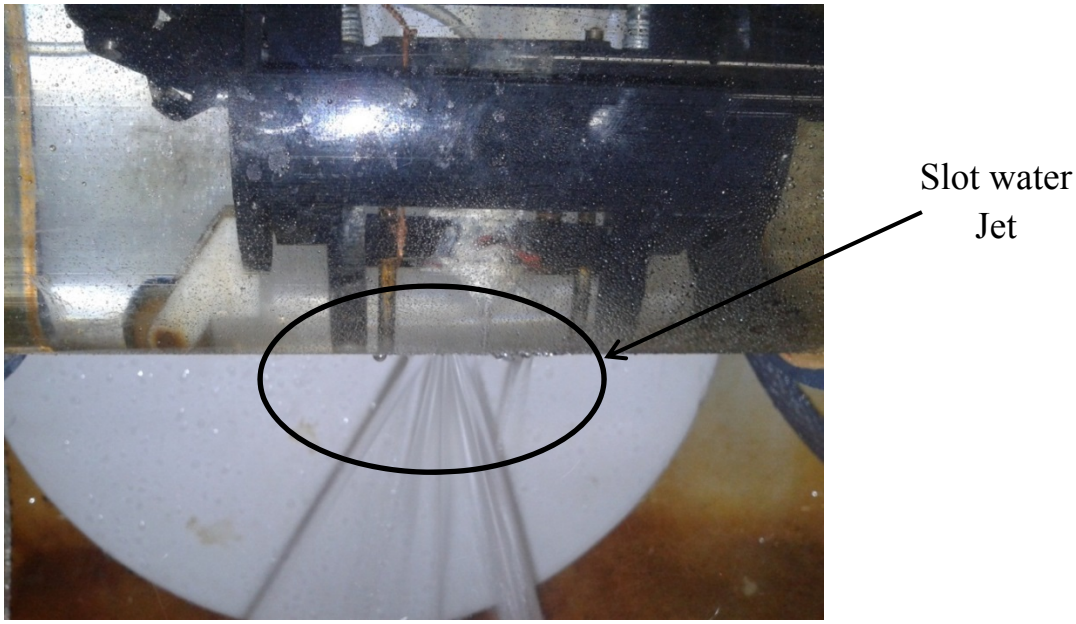

Figure 2.5: Water jet from 0.6mm X 12mm slot along a test section

2.4 Mobility Module

The mobility module is skeletal system with the purpose of holding the transducer in place. It is made up of plastic cylindrical plates jointed together by movable rectangular structure. The structure is flexible enough to make a radial movement of about 360^{o}. Attached to the flat plates are 3 legs each. A spacing of 120^{o} is kept between adjacent legs to ensure stability during axial movement of the module. As shown the picture below, the legs carry rollers for easy maneuvering. Attached to one of the legs is a magnet with which the body is controlled from outside using an opposite pole magnet. This plastic structure has a grove, springs and guides through which the sensor tap distance from the pipe wall could be adjusted. The tap is held in place by a plastic bar. The part holding sensor through the groove is made detachable from the model for

heights' adjustment. The solid work model shown in 2.6 is the mobility module that was previously in use to explore differential pressure within the vicinities of leaks. The prototype has no problem while the fluid in the section is water as the sensor pins get short-circuited. Therefore, alterations were made to make the prototype useable in water. The sensor is replaced with a pressure tap attached to the holder and a capillary tube connected to the tap runs through the pipe wall to outside the test sections. The amended sensor holder and the carriage are shown in figure 2.7.

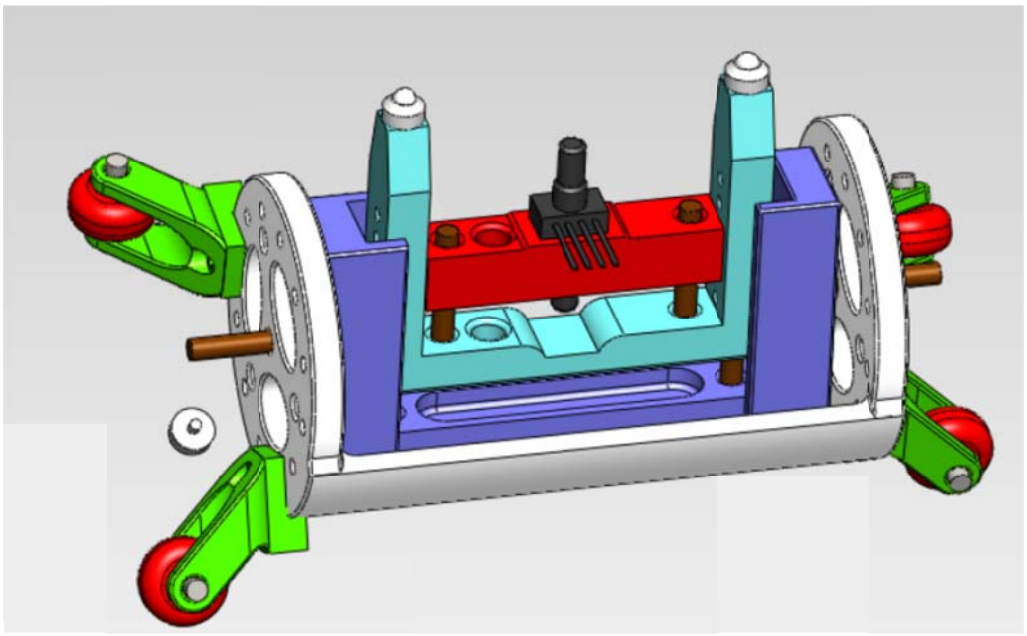

Figure 2.6: Solid work model of the mobility module

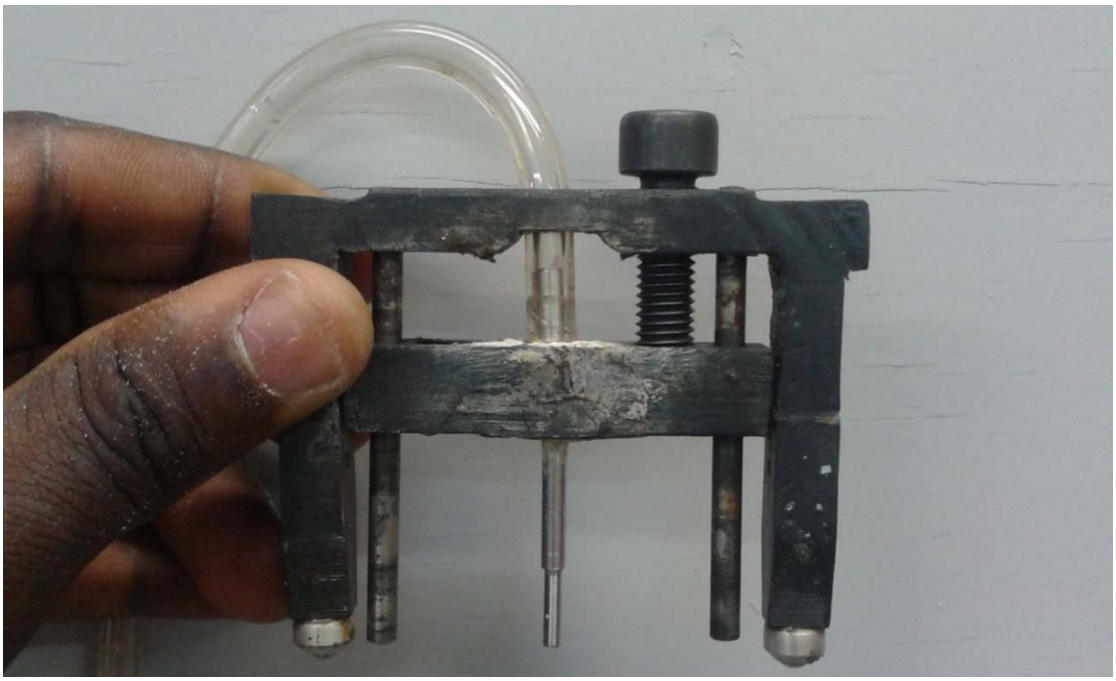

(a)

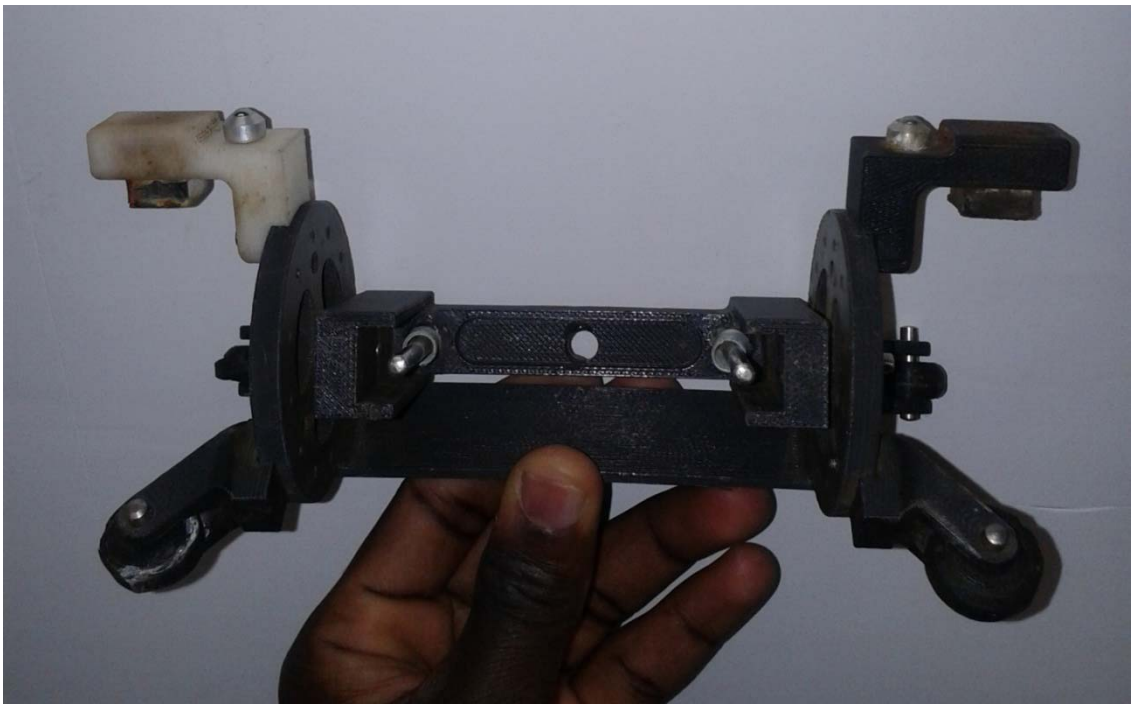

(b)

Figure 2.7 Amended sensor holder and the carriage.

2.5 Differential Pressure Sensor and other electronics

The differential pressure transducer used in experimentation of the proposed method is the Omega PX26 series. These pressure sensors feature state-of-the-art silicon technology which permits both sides of the diaphragm to handle liquids. According to the sensors' manual, they are characterized with unique conductive seal between the silicon diaphragm and the plastic housing allows for wet/wet applications and lower production costs than typical gold wire silicon sensors. As shown in picture below, the ends of the sensor detect different pressure signal, line pressure at one end and the pressure in the vicinities of the leak at the other end. The MEM based sensor then compares the difference in these pressure value to indicate an output. With the arrangement that places the sensor outside the pipe, the ends are connected to capillary tubes which pick up pressures at the desired locations. On the underside of the sensor are 4 pins. Two of these pins are connected to the power source while the other two are connected to the voltmeter to read sensor output mV. The sensor is excited with 10 VDC using power supply shown in Figure 2.9. The manufacturer's specifications of the sensors used are as given below;

Sensors' specifications

- Excitation: 10 Vdc, 16 Vdc max @ 2 mA
- Output (@ 10 Vdc): 1 psi = 16.7 mV; 5 psi = 50 mV; >5 psi = 100 mV; 250 psi = 150 mV
- Linearity: ±0.25% FS BFSL typical (±1% maximum) P2 > P1
- Hysteresis and Repeatability: 0.2% FS
- Zero Balance: ±1.5 mV; Span Tolerance: ±3.0 mV

- 1-Year Stability: 0.5% FS
- Operating Temperature: -40 to 85°C (-40 to 185°F)
- Compensated Temperature: 0 to 50°C (32 to 122°F)
- Input Resistance: 7.5 kΩ; Output Resistance: 2.5 kΩ; Response Time: 1 ms

Two sensors with maximum output of 30 psi and 5 psi are used for the holes and slot respectively after considering the maximum differential pressure measurable within the vicinities of these simulated leaks.

Through a flexible electric cable, the output pins are connected to the multi-meter. Figure 2.9 shows the photo of the variable output power supply (EZ Digital GP-1303DU) and multi-meter (Omega HHM 31) used in the study. The maximum output of PX26-030GV sensor is 100 mV and this corresponds to the highest pressure of the sensor while PX26-005GV has its highest output voltage as 50 mV. Thus, the meter is set to the measurement range of 0-200 mV in order to capture these readings and ensure good resolution in the output measurements.

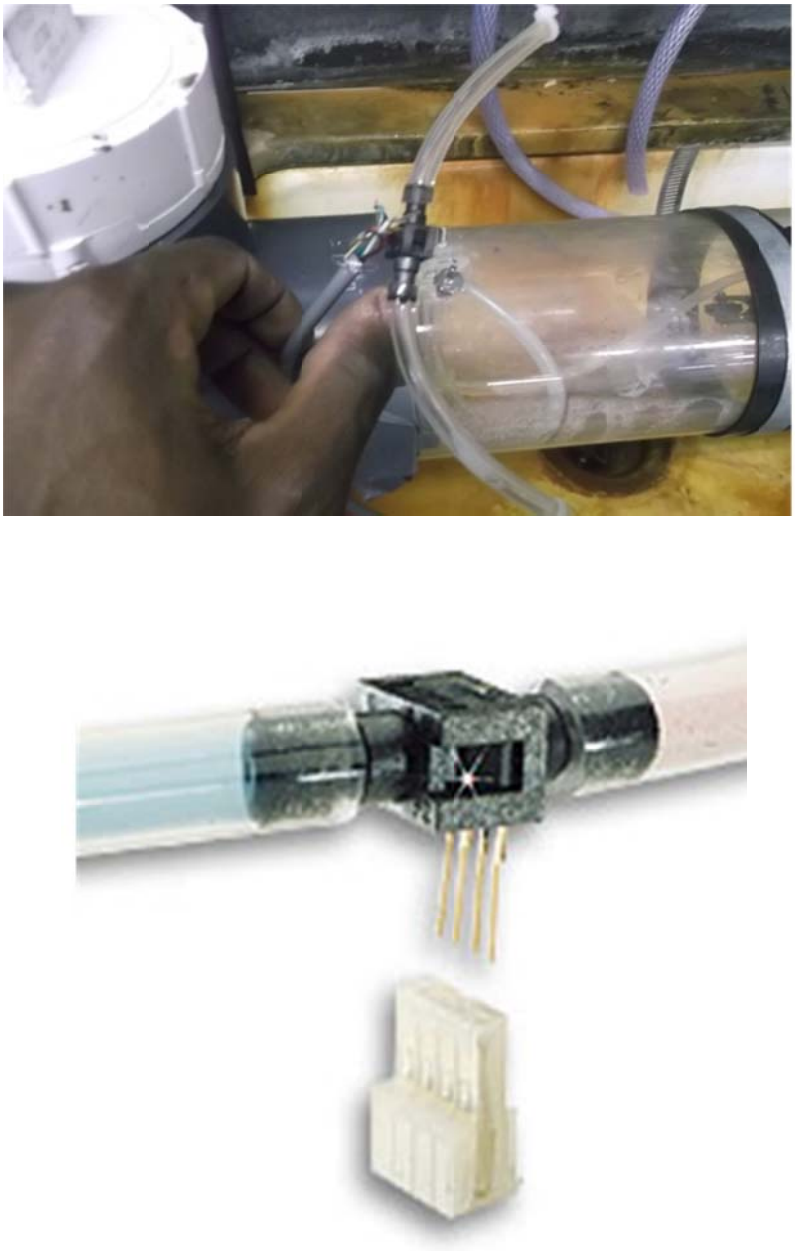

Figure 2.8: Pictures showing connections on the transducer

Figure 2.9 Picture of the power supply and the multimeter

2.6 Calibration of Components and Precautions

As a standard procedure, calibrations of the components were done prior to experimental implementation.

The pressure gage was calibrated using a dead weight tester shown in the figure 2.10 below. The pressure gage measures pressure between 0 and 60Psi. Dead loads of assigned values in the KN/m^2 are added to the tester while the corresponding pressure reading on the pressure gauge is read. Taking a load between 50 and $400KN/m^2$ with an interval of $50KN/m^2$, the plot shown in Figure 2.11 shows the pressure gauge response to loading with a slope of 1. Therefore, no correction is required to the pressure measured with this gage.

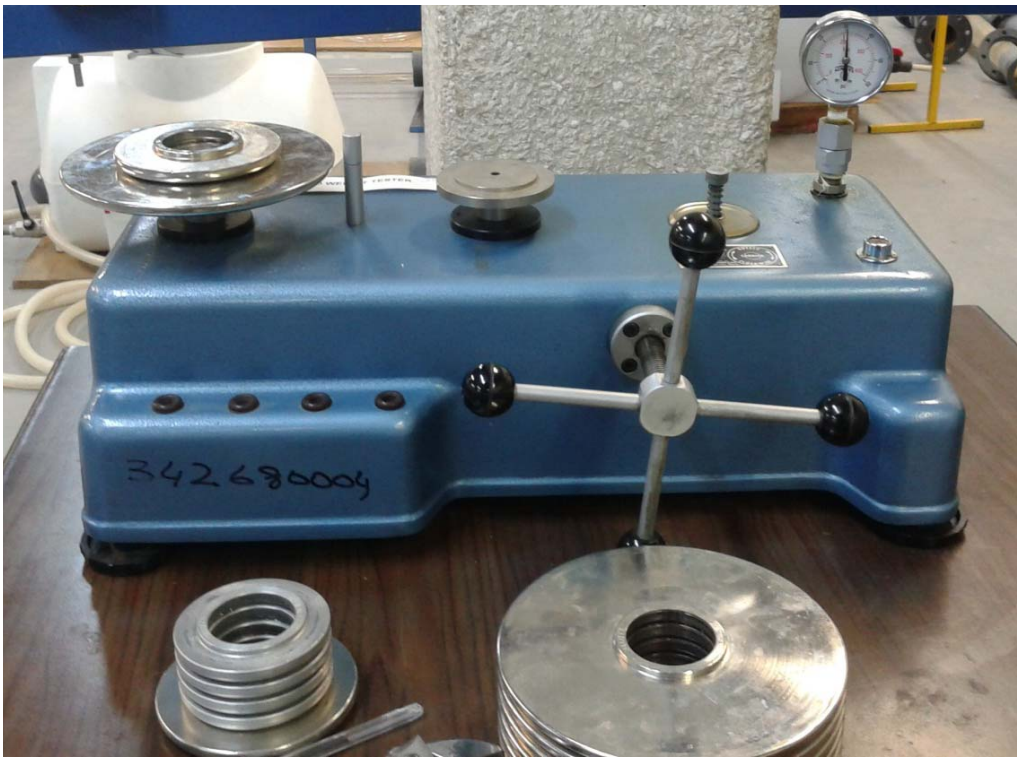

Figure 2.10: Dead Weight Pressure tester.

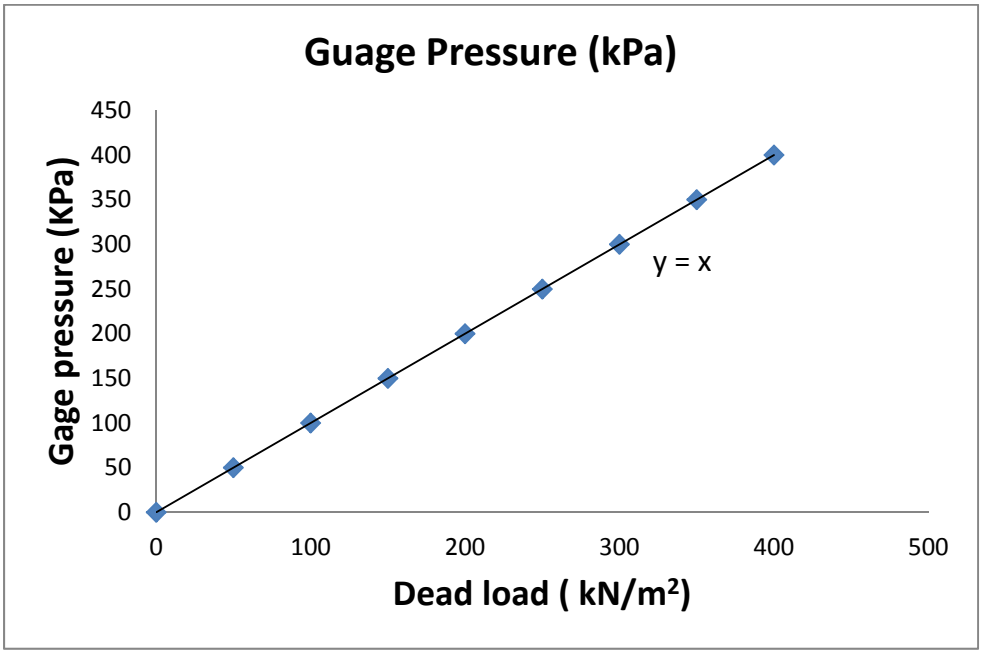

Figure 2.11: Response of the pressure gauge to dead load calibration

Figure 2.12: Filler gage for height sensor height settings

The axial distances away from the leaks are calibrated using a meter rule. During the experiments, steel rule is attached to the pipe. For the holes, the point with maximum output is taken as the 0 points while the axial distance is taken relative to this point in an interval of 1mm. For the slot, a calibrated meter rule graded in interval of 2mm is permanently attached to the length of the slot. Heights of the pressure tap (amended sensor) from the wall are ensured with the use of precision filler gage shown in figure 2.12.

To ensure accuracy of the reading, the sensors were re-calibrated using the experimentation test loops. To measure the actual sensitivity of the sensors, they were excited while the test loop is pressurized. The sensor tap is set up in the pipe in a way that the differential pressure is measured as difference between the pipe line pressures and the atmospheric pressure i.e. one end reads the atmospheric pressure while the other end

reads the pipeline pressure The plot shown in Figures 2.13 and 2.14 show the sensors' responses to different pressure line pressures. The best lines of fit are added to the plot by indicating a zero intercept. The slopes of the curves generated represent the actual sensitivities of the sensors. These values are used in converting the read voltage to psi equivalent.

From the calibrations done on the sensors, the sensitivities of the sensors are adjusted. The voltage readings from the sensors are divided by the new sensitivities, i.e. the slope of the lines of best fit. The zero reading on the sensors are noted for all experimental data deduced and are used in correcting the measured voltage readings. Also, all readings are taken at times beyond the response time of the sensors.

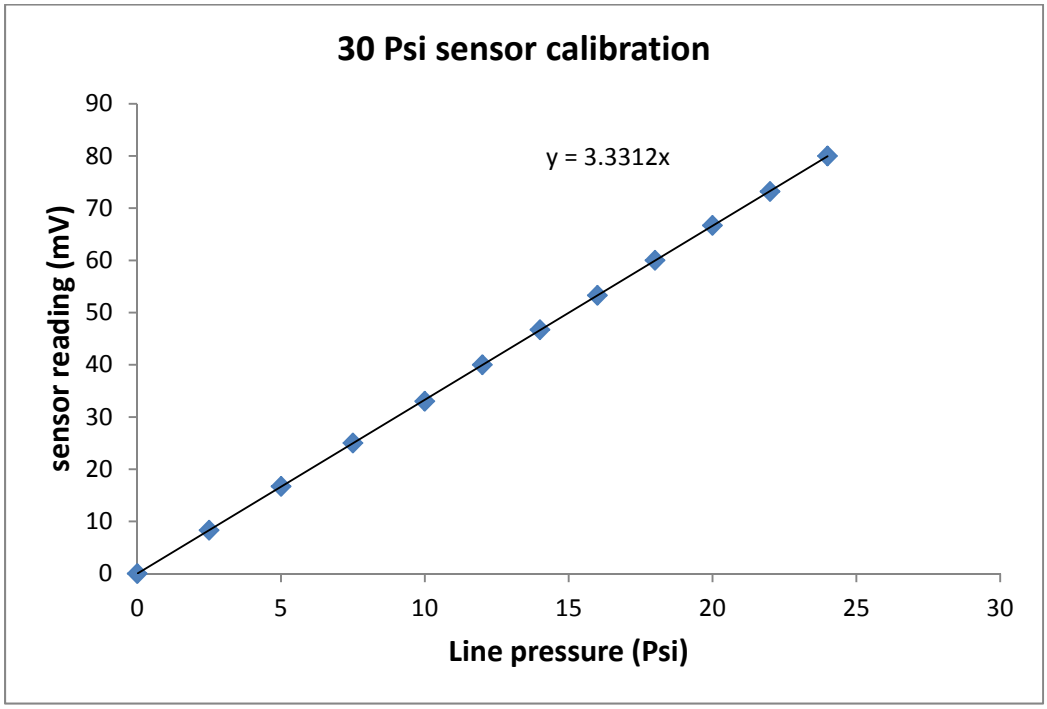

Figure 2.13: Response of 30 psi sensor to line pressure

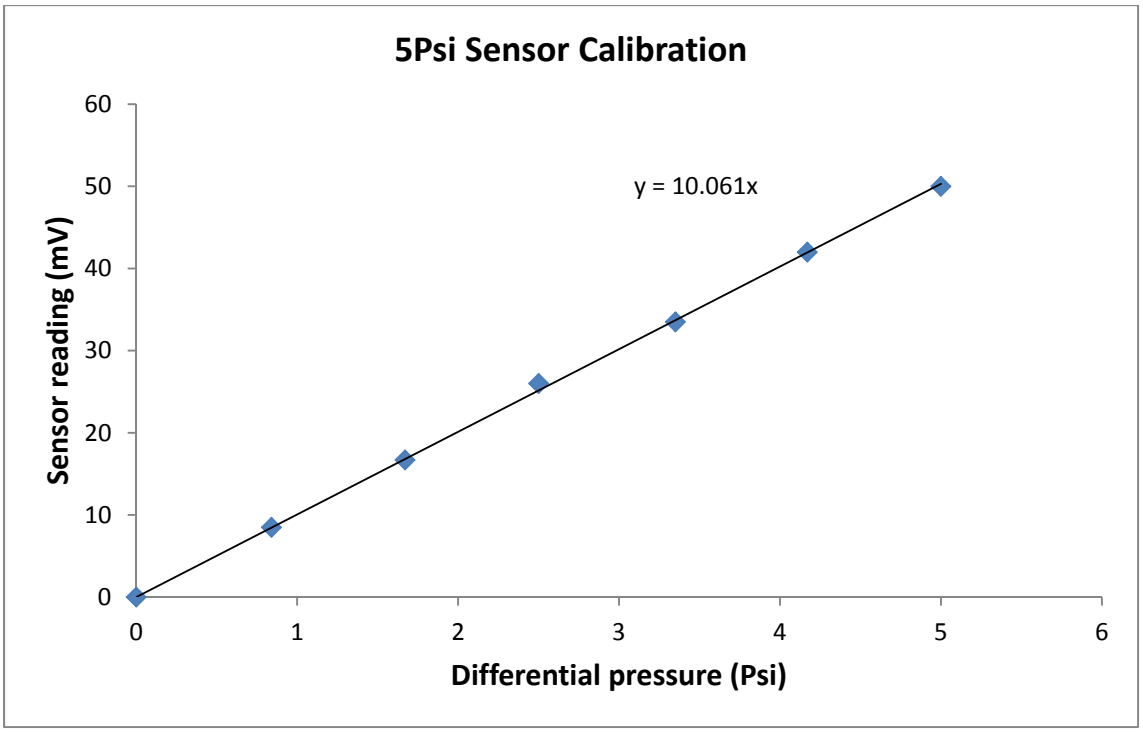

Figure 2.14: Response of 5 psi sensor to line pressure

2.7 Experimental Measurements

On each of the simulated leaks, the measurements of the differential pressure around the leak and leak flow rates are the goals of these experiments. The differential pressures are measured at various locations within the vicinities of the leaks. A sensor tap of 2.2mm diameter is used for the cylindrical holes while a sensor tap of 0.5mm diameter is used for the slot. The effects of the sensor tap intrusion on the simulated leaks are observed through the flow rate of the leak.

2.7.1 Differential Pressure Measurement

With the set up as described above, magnet is used to move the mobility module to location where the measurements are to be taken. The test section is pressurized at 30 psi

line pressure. These readings are taken at height of 0.5mm, 1mm, 1.5mm and 2mm above the leak. At these heights for each of the simulated cylindrical leaks, readings at least four locations along the axial direction of the pipe are recorded with interval of 1mm from the center of each of the holes. Previous and preliminary studies have shown that the differential pressure around a leak is radially symmetrical. Thus, readings are taking only from on direction of the pipe. For the simulated crack, readings are taken at 0.5mm and 1mm above the crack. Also readings are taken along the length of the crack in an interval of 2mm with other two points lying 2mm away from the either sides of the slot.

2.7.2 Flow Rates Measurements

Flow rate measurements are targeted to measure level of sensor tap intrusion on the simulated leaks. These measurements are taken at various heights of the tap from the leaks and without the tap. At the working pipe inline pressure, leak outflow volumes were noted against the time of flow. To achieve these, leak outflows were collected in an open bath at 30 psi test section pressure while stop watch records the time taken. The outflows are measured with the calibrated beaker. The leak outflows are then calculated from the expression given in equation 1.

$$Q = V/t \qquad 2.1$$

Where Q = Leak volumetric flow rate (L/min),

V = Leak outflow volume (liters) and

t = time taken (min)

2.8 Experimental Results Presentation

All the experimental measurements are repeated at least three times in order to ascertain the quantity being measured. Thus, the results are reported in the form of the mean reading and the standard deviation of the set of readings taken.

$$x = \breve{x} \mp H \qquad 2.2$$

Where x is the measured quantity (e.g. Differential pressure)

$\breve{x}$ is the mean of all values for a measurement,

H is the standard deviation

$$\breve{x} = \frac{1}{N}\sum_{i=1}^{N} x_i \qquad 2.3$$

H is plotted as the vertical error bar in results presented for the experiment. Similarly, the human error due to wrong location could not be totally ruled out since the readings are done through media of different densities. Thus, apparent images cannot be corrected by mere statistical analysis. The results are presented with a typical error bar of 0.1mm on either side of axial distances. For instance, a reading at 1mm could be tracked within 0.9mm and 1.1mm in the axial direction.

CHAPTER 3

MATHEMATICAL MODELING

3.1 Introduction

In this section, the details of the mathematical modeling of flows within pipes are presented. The domains under study are described; the governing equations are highlighted; the discretization using control volume approach is summarized; mesh generation in the geometry are explained and finally the mesh independence study are presented.

Flow in water pipelines is turbulent in nature. Computational fluid dynamics, CFD, in the study is concerned with numerical solutions of complex differential equations associated with the turbulent flow in the media. Recent developments in the CFD have drastically reduced the reliance on experimental studies for research purposes. Owing to high cost of experimental setups, difficulties of experimenting some phenomenon (e.g unsteadiness and turbulence), and complexities involved in some experiments.

To study the fluid flow interaction in the vicinities of leaks, the present study undertook full three dimensional simulations. In the study, CFD was used for preliminary parametric studies, comparison of results of flow analogous to the experimental conditions and to study the effect of pressure and flow on the differential pressure around the leaks.

3.2 Descriptions of Computational Domains

Three different categories of domain were used, these are;

- Two cylindrical leaks in a straight pipe wall are used for preliminary parametric studies
- Simulated leaks through holes on straight pipes similar to those on the experimental test section.
- Simulated leaks through crack approximated as slots similar to that experimented.

3.2.1 Leaks along Straight Pipe

For the preliminary parametric study, a pipe of 100mm diameter is taken as it represents the mostly used pipe in distribution networks with a length of 4m. Two cylindrical leaks are located at position 1m and 3m from inlet, along the pipe. Figure 3.1 shows the 2D representation of the domain. The leaks are approximated as a cylinder with height indicating the thickness of the pipe. As informed from literatures, the major challenge of most methods of leak detection that have been developed is ability to detect a small leak in water networks. This was a limitation of the ITA method studied by (Didia & Helena, 2010), therefore the preliminary study assumed small leaks of 2mm diameter (<1% of the total flow).

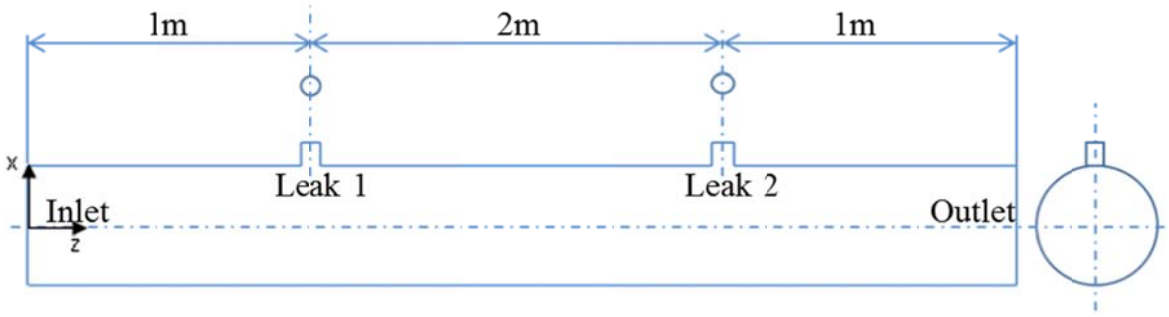

Figure 3.1: Two dimensional representation of the straight pipe

3.2.2 Simulated Leaks with Sensor Taps

The geometry for simulated leaks through holes around a straight pipe is similar to that of the straight pipe used for parametric studies. To approximate the experimental set up, sensor taps are modeled into the geometries. This would allow us to identify the effect of pressure tap in the leaks' vicinities. The cylindrical holes are of 2.2mm and 4mm diameters. As shown in the Figure 3.2, the solution domain is simply the flow domain inside the pipe and through the leak. The leak is placed mid-length of the pipe.

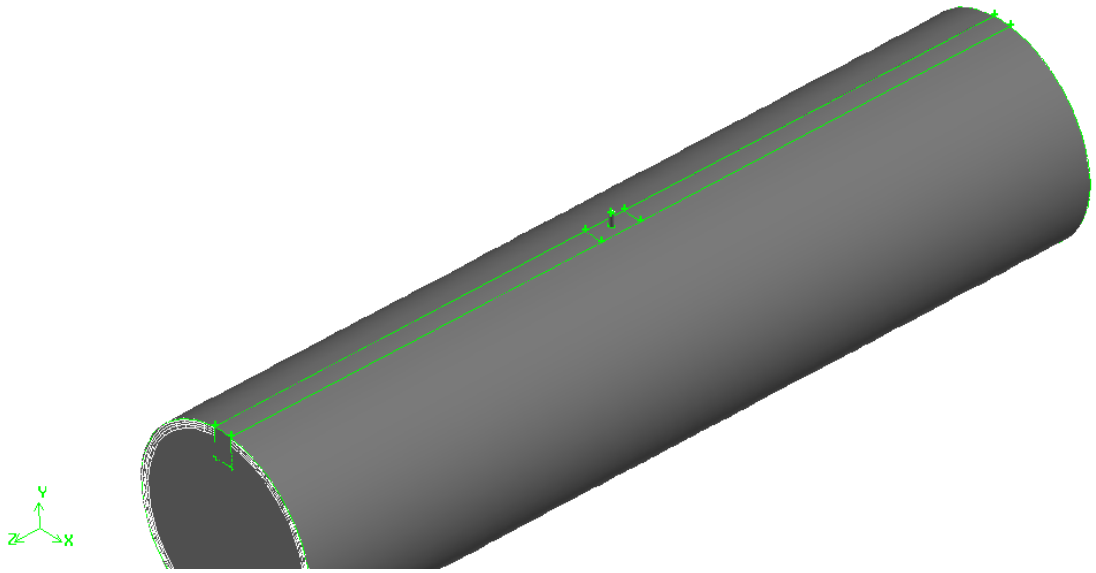

Figure 3.2: three dimensional geometry of pipe showing cylindrical hole

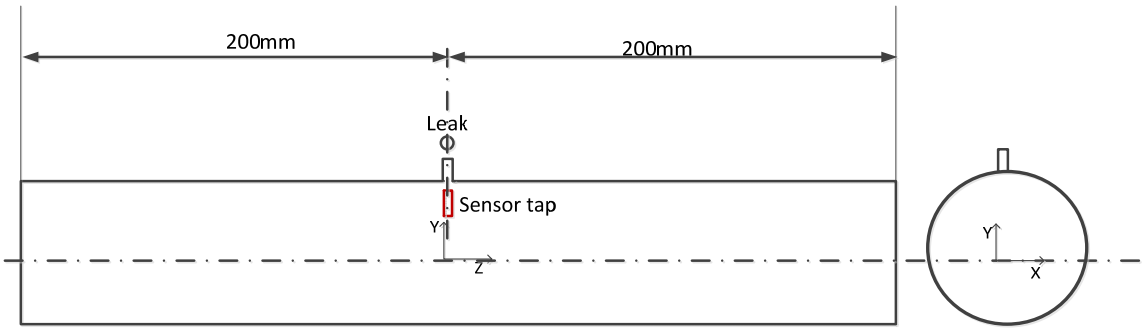

Figure 3.3: Domain of computation for cylindrical leaks showing inner detail of the pipe with sensor tap incorporated

To the inner part of the domain, a cylindrical (2.2mm diameter and 15mm long) geometry is made as shown in Figure 3.3 above. This represents the sensor tap which to capture the differential pressure in the experimental set up. This models the disturbance created by the sensor stem as water flows out of the leaks. The tap geometry is imposed with a wall boundary condition similar to the experiment.

Owing to the complexities involved in meshing domain with small details (leaks) attached to bigger domain (pipe), domain decomposition was adopted. The geometry was first constructed as a whole; bricks were used to decompose the domain along the axis containing the leak. These bricks were then splitted using faces in order to isolate the leaks for mesh refinement. Decomposition allows controlled meshing on the edges and allows mesh independence study viable. Also this allows mesh refinement within the vicinities of the leaks to capture the highly localized gradients of flow parameters. Boundary layer types of mesh are attached to walls to capture the sharp gradients and correctly modeling turbulence close the walls.

3.2.3 Simulated crack along Straight Pipe

The simulated crack is done by making a slot similar to that in created in the experimental test section. A slot is approximated as cuboid of surface area 0.6mm X 12mm and having a height of 5.6mm corresponding to the thickness of thickness of the pipe wall.

The slot is located at the center of the pipe (x=0 mm, y=5.56m, z=0mm). To the inner side of the pipe, a geometry representing the sensor tap is modeled. This sensors tap is placed on the locations corresponding to points where the experimental results are taken.

A 0.5mm diameter, 15mm long cylindrical tap is used in this case similar to the tap replacing the sensor in the crack test section. The study on the crack is extended further with addition slots 0.8mm and 1mm width having the same length with the one in the experiment. These are simply done by increasing the width of the previously made slot and increasing the number of mesh nodes along the edges.

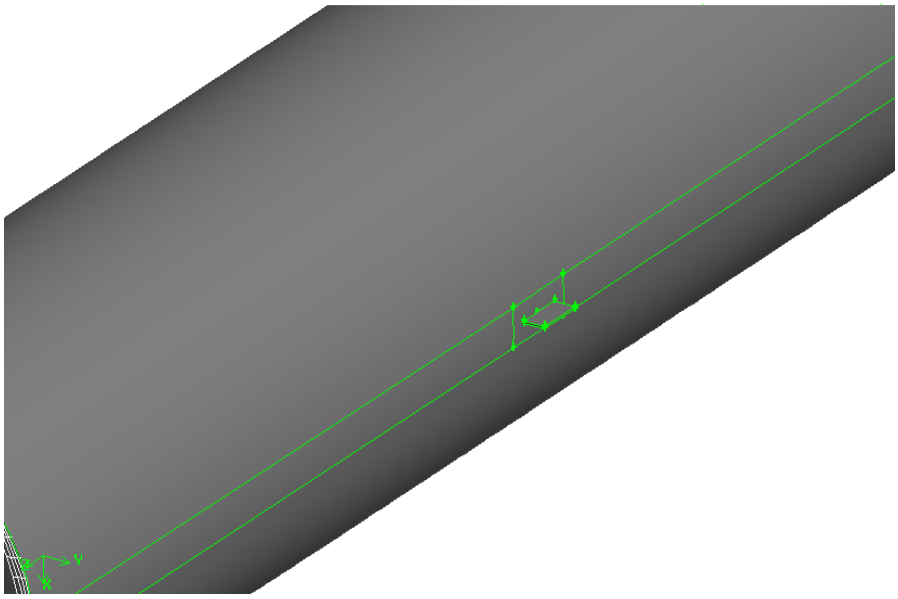

Figure 3.4: three dimensional geometry of pipe with a slot

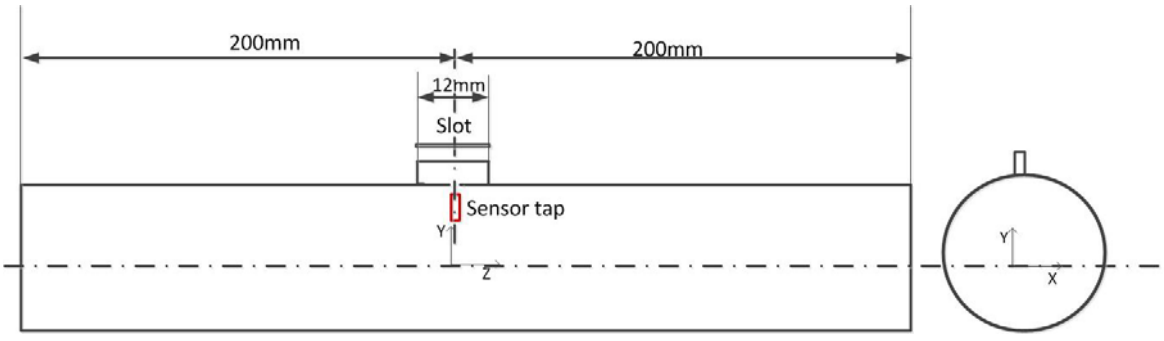

Figure 3.5: Domain of computation for crack showing inner detail of the pipe with sensor tap incorporated

3.3 Numerical Procedures

This section presents the formulation of governing equation and the boundary conditions

3.3.1 Formulation of Governing Equations

In practical water flow in pipeline, the major driven force is pressure. It is also characterized with turbulent mixing based on the flow velocities. Therefore a full three dimensional representation of water in a pipe would consist of the mass continuity equation, the momentum conservation equation and the equations for evaluation of the turbulence within the system.

Flow modeling

$$\frac{\partial u_j}{\partial x_j} = 0 \tag{3.1}$$

$$\rho \frac{\partial (u_i u_j)}{\partial x_j} = \frac{\partial p}{\partial x_i} + \frac{\partial}{\partial x_j}\left[\mu\left(\frac{\partial u_i}{\partial x_j} + \frac{\partial u_j}{\partial x_i}\right)\right] + \frac{\partial}{\partial x_j}(-\rho R_{ij}) \tag{3.2}$$

Where $-\rho R_{ij} = \mu_t\left(\frac{\partial u_i}{\partial x_j} + \frac{\partial u_j}{\partial x_i}\right) - \frac{2}{3}\rho k \delta_{ij}$ term describing turbulence.

The above equations are known as Reynolds Averaged Navier Stoke Equation. The simulations were carried out at constant density with the assumption that water is an incompressible fluid and flowing with Mach number of less than 0.25. Also steady state situation was taken with the assumption that flow in a pipe is relatively undisturbed during smooth operation. The choice of evaluation of the last term of equation 2 brought about turbulence model equations. Equation 2, if written in a full format contains the x, y and z directions momentum conservation equations.

Turbulence modeling

To handle the last term in the momentum transport equations, many models had been develop. One equation, two equations and five equation models are well established to handle turbulence terms. The Standard k-ε model is in the category of two equation model that has proven to be accurate to many engineering applications. This semi-empirical model gives the solution to the turbulent kinetics energy（k） and the rate of dissipation of turbulent kinetic energy（ε）based on separate transport equations. The standard k-ε model and others of its kind, the RNG k-ε and the realizable k-ε model, are the simplest complete empirical models for turbulence.The Standard k-ε Model_focuses on the mechanisms that affect turbulence kinetic energy, Shuja et al. [33]

For the preliminary studies, alongside with continuity equations and three momentum equations (3D), the two equations in standard k-ε model are adopted. The two transport equations solve for the turbulence kinetic energy and dissipation rate and are described below;

$$\rho \frac{\partial}{\partial x_i}(u_i k) = \frac{\partial}{\partial x_j}\left[\left(\mu + \frac{\mu_t}{\sigma_k}\right)\frac{\partial k}{\partial x_j}\right] + P_k - \rho\varepsilon \tag{3.3}$$

$$\rho \frac{\partial}{\partial x_i}(u_i \varepsilon) = \frac{\partial}{\partial x_i}\left[\left(\mu + \frac{\mu_t}{\sigma_\varepsilon}\right)\frac{\partial \varepsilon}{\partial x_i}\right] + P_\omega - Y_\omega + (1-F)D_\omega \tag{3.4}$$

P_k describes the turbulence production term. Turbulence due to buoyancy effect and source are negligible in this problem, thus they are equated to zero.

$$P_k = -\rho R_{ij}\frac{\partial u_j}{\partial x_i}; \qquad \mu_t = \rho C_\mu \frac{k^2}{\varepsilon},$$

Where the constant employed are

C_1=1.44;

C_2=1.92;

σ_k=1;

σ_ε=1.3;

C_μ=0.0845;

According to the work of Ben-Mansour et al. [21] this value, C_μ=0.0845 was derived using the mathematical model RNG "renormalization group" Choudhury [24]. This accurately describes the variation of turbulent transport with effective Reynolds number for better near wall treatments.

The choice of turbulence model for the cases similar to the experiments is done by comparing the results of five turbulent models with experimental result at 1mm above 2.2mm hole. The models are realizable k-epsilon, standard k-epsilon, RNG k-epsilon, standard k-omega, shear stress transport (SST) k-omega and transitional k-kl models. The SST k-omega predicted the closest result to the experiment and therefore is used to evaluate turbulence for the rest of the study. In the case, the second transport equation described before is replaced by specific dissipation (omega) described in equation 3.5 below.

$$\rho \frac{\partial}{\partial x_i}(u_i \omega) = \frac{\partial}{\partial x_i}\left[\left(\mu + \frac{\mu_t}{\sigma_\omega}\right)\frac{\partial \omega}{\partial x_i}\right] + \rho \frac{\alpha}{\mu_t} P_k - Y_\omega \qquad (3.5)$$

Detail on evaluation of the Y_w (dissipation of omega) is found in the FLUENT 12.1 user manual. The preset constants in 12.1 version of the software are used for the simulations. Six equations comprising of mass continuity, X Y Z momentum conservation, two turbulence transport variables are solved in each case to establish all the parameters

required in the study. These governing equations were discretized by a numerical scheme employing a control volume method and finite volume set of algebraic equations were obtained. These equations were solved with a commercial CFD package, employing the SIMPLE algorithm for handling pressure linkages with details in Patankar [32].

3.3.2 Boundary Conditions

To assume a real flow situation the following boundary conditions are taken with their corresponding justifications.

Inlet Boundary Condition: Two types of inlet boundary conditions were utilized in the cause of the study. First is the velocity inlet boundary condition. This is imposed so has to comply with the direction of flow of supply through a pipe from a source. We assumed a water flow velocity of 1m/s. This corresponds to a flow rate of 7.85L/s which agrees with the international standard of 2.5m/s maximum velocity in water pipe distribution. To simulate a scenario similar to experiments, the pressure inlet condition is imposed on both ends of the pipe. This is to represent a segment of a pressure pipe. Finally to observe the effect of flow on the differential pressure with the vicinities of leaks, the inlet velocity (0.5m/s to 2m/s) is imposed.

Outlet Boundary Condition: the pressure outlet condition is imposed so as to mimic the real condition of flows in pressurized pipes. This condition is imposed on the exit of the pipe for the preliminary study.

Leak Outlet condition: the pressure outlet conditions are imposed on these boundaries as the leaks hole exits. Leaks are modeled as exposed to atmospheric pressure. This is similar to the condition experienced with the experiments.

Pipe walls: the pipe wall was treated with the standard wall condition of no slip as it is conventional for flows through a stationary pipe with a predefined roughness parameter of 0.5 by the solver.

3.4 Mesh Independence Studies

Mesh independence studies are carried out on the domains.

3.4.1 Mesh Independence for Preliminary Study

Here three meshes (M1, M2 and M3) are tested and simulations are done using the above boundary conditions with the outlet gauge pressure of 2bars. The properties of the mesh and the corresponding leak flow rates are given in Table 3.1. By refining the mesh from M1 to M2, an improvement of ~7% in the leaks flow rate was obtained. However, further refinement in mesh M3 did not significantly improve our results. The static pressure along a line 10mm (Figure 3.5) close to the leak shows no significant difference for both meshes M2 and M3. By considering these results and assuming mesh independency with less than 2% in the predicted leak flow rates, the solution obtained using mesh M2 is mesh independent and hence selected for the rest of the computation.

Table 3.1: Mesh Independence study (Line pressure = 2bars, average velocity =1m/s)

Mesh	Number of Cells	Leak 1 flow rate (kg/s)	Leak 2 flow rate (kg/s)	Percentage increment in Leak 1 flow rate	Percentage increment in Leak 2 flow rate
M1	586,944	0.0411	0.0410	-	-
M2	1,646,202	0.0440	0.0440	7.06	7.32
M3	2,633,578	0.0448	0.0448	1.82	1.82

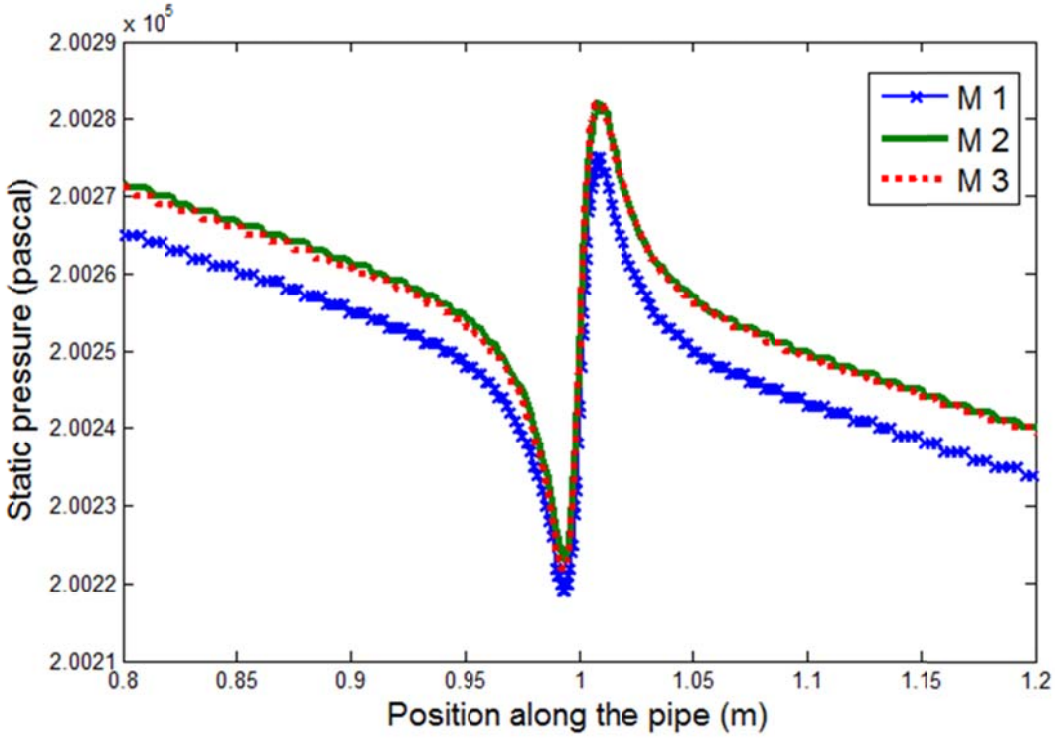

Figure 3.6: Static pressure along a line 10mm below the leaks (V=1m/s P=2bars)

3.4.2 Mesh Independence for cylindrical leaks in a Pipe

To study the effect of mesh of the geometry with simulated holes around pipe, a straight pipe with 2.2mm cylindrical hole at the middle of its length was used. The geometry representing the sensor is also modeled into the domain with at least 12 nodes of meshes in all the cases. The sensor is placed at a height of 0.5mm away from the leak. Three meshes are made by varying the numbers of nodes on the decomposed domain edges. Overall increment on the total cells approximately 60% of previous cases. Table 3.2 below shows the summary of the study.

Considering the results in the Table 3.2 and assuming mesh independency with less that 2.5% in the predicted leak flow rate, therefore the solutions obtained using mesh two are mesh independent and hence this mesh sufficed for the rest of the computation. The meshing scheme was extended to other geometries by increasing the numbers of nodes on edges by the length incremental factors.

Table 3.2: Mesh Independence study (Line pressure = 2bars, 2.2mm hole, Tap at 0.5mm above leak)

Mesh name	Number of cells	leak flow rate (kg/s)	Percentage increment in leak flow rate
M1	112,638	0.0385	-
M2	183,607	0.0397	3.12
M3	263,672	0.0407	2.26

3.4.3 Mesh Independence for slot in a Pipe

The mesh independence studies on the previous domain aid choice of mesh for the case of the slot. The nodes are meshed similar to the mesh independent domain for the simulated hole. However, the number of cells required is larger because of larger area refined around the slot. The sensor is placed at a height of 0.5mm away from the slot, directly above the center. Three meshes are made by varying the numbers of nodes on the edges. Table 3.3 below shows the summary of the study.

Considering the results in the Table 3.3 the solutions obtained using any of the meshes are mesh independent as observed with the flow rate out of the slot. Owing to the large aspect ratio of the slot and need to capture the variation close to the slot, mesh M1 was dropped. Computational time for achieving solution with mesh M3 made the choice to be left out. Mesh M2 has good aspect ratio to capture the gradient within slot and relatively low number cells thus, saving computational time. The rest of the computations on the slot are done using mesh 2.

Table 3.3: Mesh Independence study (Line pressure = 2bars, 0.6mm x 12mm slot, 0.5mm Tap at 0.5mm above leak)

Mesh name	Number of cells	Slot outflow rate (kg/s)	Percentage increment in leak flow rate
M1	304,401	0.1054	-
M2	655,905	0.1099	4.27
M3	954,403	0.1108	0.82

3.5 Parameters for Simulations

The following are the parameters used in the models for all the simulation work carried out.

- Models

Space: 3D

Time: Steady state

Viscous model: Standard k-epsilon turbulence model and Shear stress transport k-omega

Wall treatment: Wall Treatment Standard Wall Functions

- Boundary Conditions

Inlet condition: Velocity inlets (0.5 -1.5m/s) and pressure inlets

Outlet condition for inline pressure: Pressure Outlet (1bar - 5bar for preliminary study) and (5psi -30psi)

Leak outlets: Pressure outlet (0 gage pressure)

- Pipe content

Water-liquid (Density= 998 kg/m^3, μ = 0.001003kg/m-s)

Walls: 0.5 roughness parameter and 0mm roughness height

- Discretization Scheme

Pressure Standard

Momentum: First Order Upwind

Turbulence Kinetic Energy: First Order Upwind

Turbulence Dissipation Rate: First Order Upwind

CHAPTER 4

RESULTS AND DISCUSSIONS

4.1 Introduction

This section discusses all the findings of the work. It is divided into two subsections. The first subsection presents the results of the preliminary studies which could be summarized as a parametric study undertook in order to determine the important flow parameters that give indication of leaks in its vicinities. The other subsection gives a detailed discussion on the experimental and computational study of differential pressure in vicinities of simulated leaks.

4.2 Results and Discussions on Preliminary Study

The results of preliminary study on a straight pipe with two cylindrical leaks are presented. First the simulations are validated against the theoretical orifice equation by varying the line pressure from 1 bar to 5 bar and correlating the pressures with leaks flow rates. The static pressure and the pressure gradient within the vicinities of the leaks are observed at normal distances to the wall likewise at the center. Effect of the line pressure on the pressure gradient is also observed with line pressure varied from 1 to 5 bar. In addition to the pressure related parameters, convective accelerations are also observed to explain their prospect to leak detection.

4.2.1 Validation for Preliminary Study

The preliminary study was carried out with different working pressures so as to validate the result with the theoretical calculations of flow through an orifice. it was found that the rate of flow from a water distribution depends on the working pressure contrary to the past view given in the orifice equation represented as in the equation below.

$$Q = C_d A\sqrt{2gh} \quad 4.1$$

In a broader view of the equation, the flow rate, Q can be represented in terms of the working as pressure with equation 4.2 as given in most of the literature cited in this study:

$$Q = CP^{\alpha} \quad 4.2$$

Where the C is the leakage coefficient of discharge and P is the working pressure in the pipe while α is the leak exponent. Theoretical value of α for round holes (orifice) was found to be 0.5. In the experiment carried out by Greyvenstien and Van Zyl [20], the leakage exponential for steel and uPVC pipes with round hole was found to be 0.52. Similarly, in the work of Mashford et al. [19], he described modeling of leak in EPANET with the above equation, and that the pressure exponent is assigned to be 0.5. The CFD predicted flow rates through the leaks for different line pressure values are presented in Table 4.1 below. For comparison with theoretical prediction, these results are shown in Figures 4.1 and 4.2. The best line of fit is given by equation (4.3).

$$Q = 1.867P^{0.5026} \quad 4.3$$

This CFD result is in agreement with the experimental value as described. In addition, the leakage coefficient is of the order represented by Torricelli's equation of orifice

Table 4.1: Leak flow rate for different line pressure at velocity 1m/s through a straight pipe

Pressure (bars)	Leak1 flow rate (L/min)	Leak 2 flow rate (L/min)
1	1.8680	1.8667
2	2.6471	2.6458
3	3.2453	3.2437
4	3.7497	3.7477
5	4.1941	4.1919

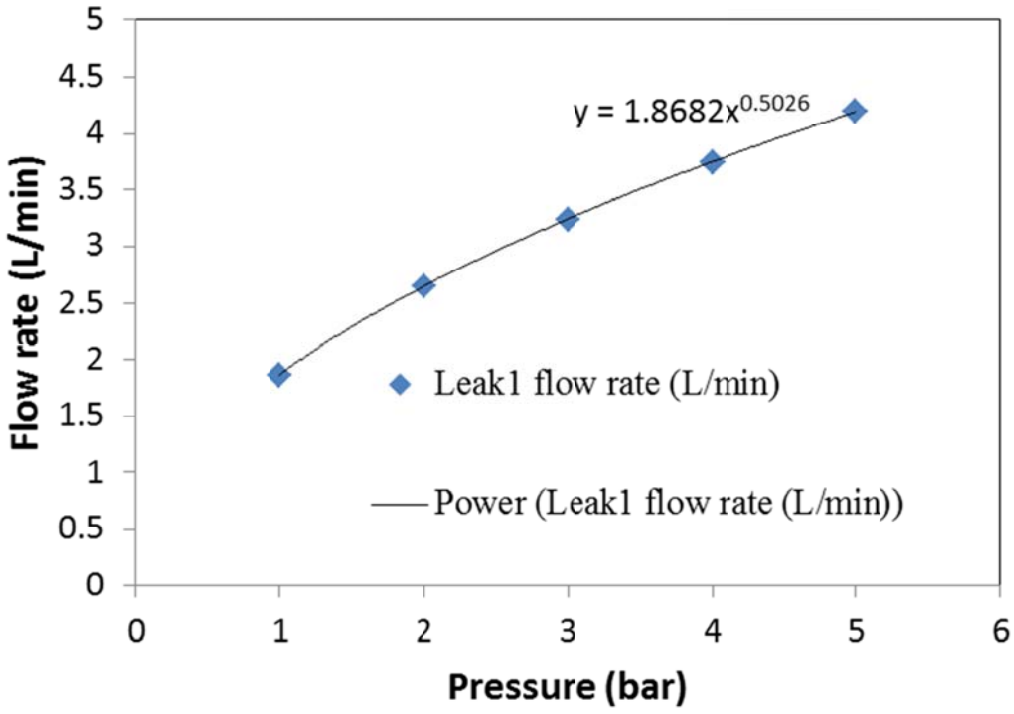

Figure 4.1: Plot of flow rate through leak 1 against line pressures

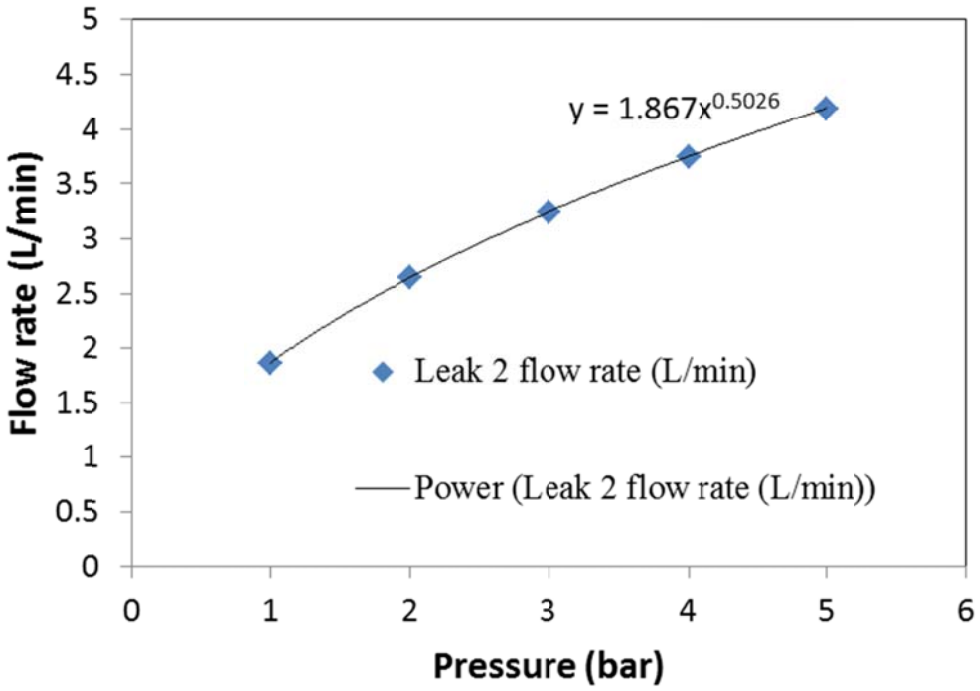

Figure 4.2: Plot of flow rate through leak 2 against line pressures

4.2.2 Pressure Behavior within the vicinity of leaks

This section presents the behaviour of pressure within the vicinities of the leak. To study the behaviour of pressure within the vicinity of the leaks, a straight pipe with a 2 bar pressure line was considered. On a plane across the leak 1, a faraway observation of the contour plot depicts that the pressure is constant in the pipe and hardly noticeable on the plane across a leak (Figure 4.3). A close up look in the vicinity of the leaks reveals a localized gradient toward the leak (Figure 4.4).

For better understanding of the pressure variation along the pipe, plots of pressures along some lines through the length of the pipe were made. A plot of the pressure along the a line 2mm below the leaks in Figure 5 shows that the pressure is fairly constant with

variation predominantly between 2.0 and 2.005 bars. However, there are clear distinctions a few millimeters before the leaks with a sudden great reduction and recovery to fairly constant state. This is caused by the fact that the pressure changes from the line pressure of 200,000 Pas (gage) to 0 gage in a space of 2 mm. This indicates that a static pressure close to the leak deviates greatly with magnitudes detectable by pressure sensors. At a distance of 10mm below the leak, the effect of the pressure change in the vicinity of the leaks becomes slightly dispersed (Figure 4.6). This implies that the effect of a leak on pressure variation will become disperse as the transducers move away from the walls of the pipe. A plot of the pressure along the centerline of the pipe shows a fairly noticeable kink in the leaks vicinities (Figure 4.7). The sharp change comes as a result of the velocity increment towards the leaks. At 10mm from the wall, the magnitude of pressure drop has drastically reduced to approximately 60 Pa which is quite difficult to be detected by available pressure sensors.

To better appreciate the causes of the sharp pressure change at the vicinity of the leaks, the vector of velocity around one of the leaks was observed. As shown in Figure 4.8, the velocity magnitude increases relatively towards the leaks and dies further down the pipe. The increase in static pressure after the center point of the leaks is as a result of reversed direction flow around the vicinities of the leaks as observed with the velocity vector. Effectiveness of a pressure transducer in leak monitoring is the detection ability irrespective of leaks position. Thus, it is required to get a parameter that gives higher magnitude of distinction in the vicinities of the leaks especially along the centerline. This gives better resolution when close to walls of the pipe. Despite the two leaks having the same size, it can be observed that the magnitudes of static pressure due to the two leaks

are different. There is a negative pressure gradient along the axial direction of the pipe. The centerline pressure measured at leak 1 is expected to be higher than that of leak 2. This amounts into higher differential pressure between the centerline pressure and the atmospheric pressure around leak 1. Also, application of mass conservation equation to the pipe indicates a higher mass flow rate before leak 1 compares to leak 2.

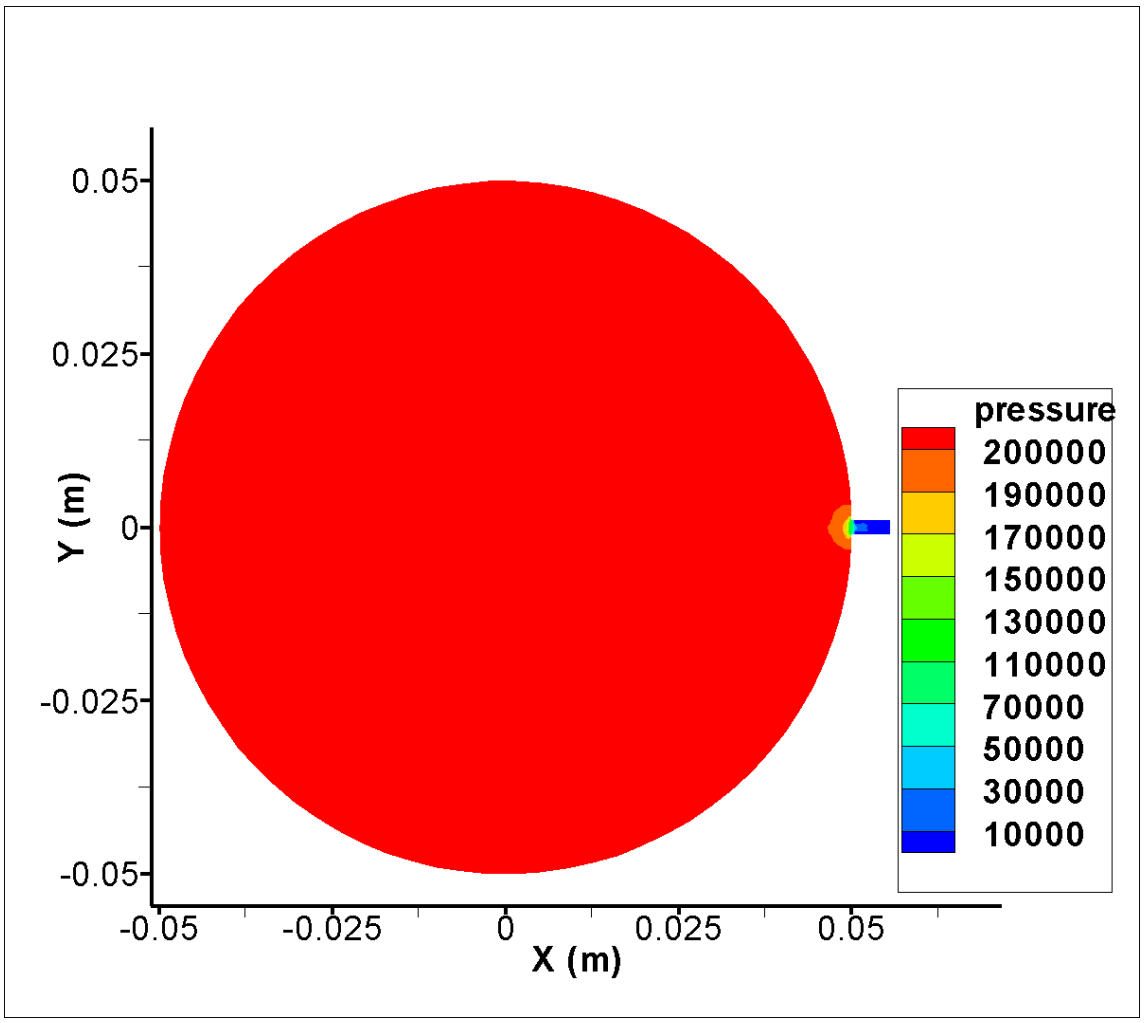

Figure 4.3: Faraway view of contour of pressure, Pa, on plane across leak1 (V=1m/s P=2bars), leak size = 2 mm ϕ

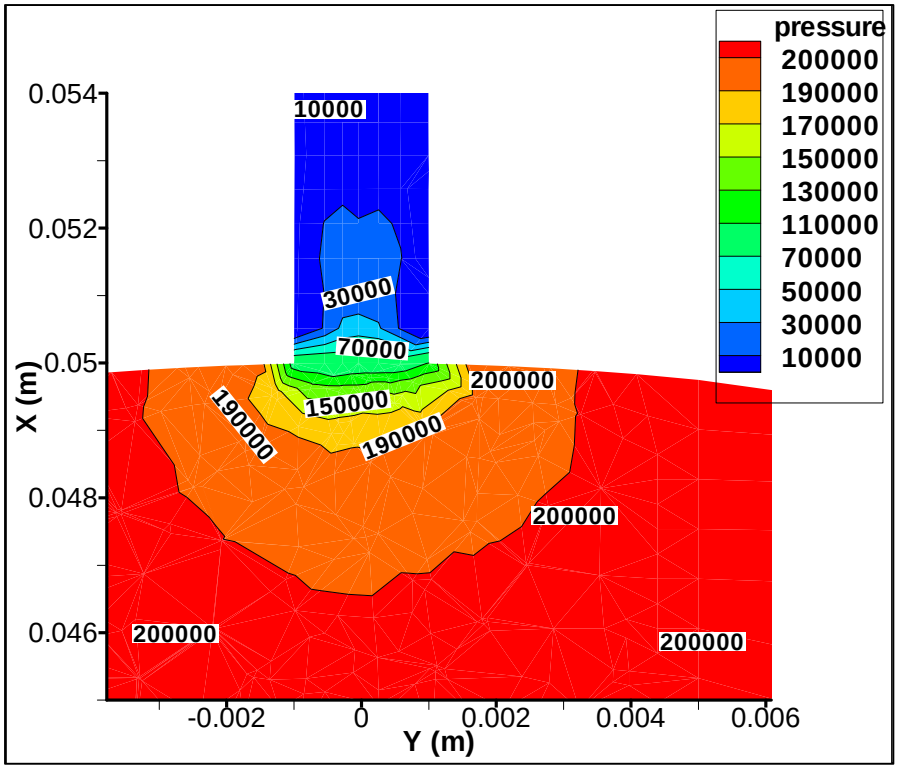

Figure 4.4: Close up view of contour of static pressure, Pa, in vicinity of leak 1 (V=1m/s P=2bars) leak size = 2 mm ϕ

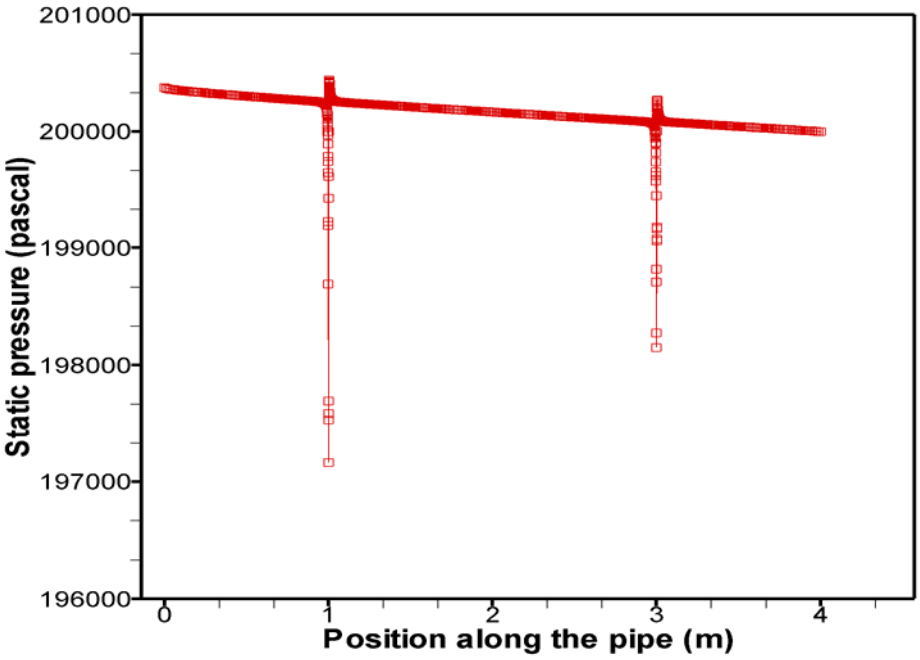

Figure 4.5: Static pressure along line 2 mm below the leaks (v=1m/s P=2bars)

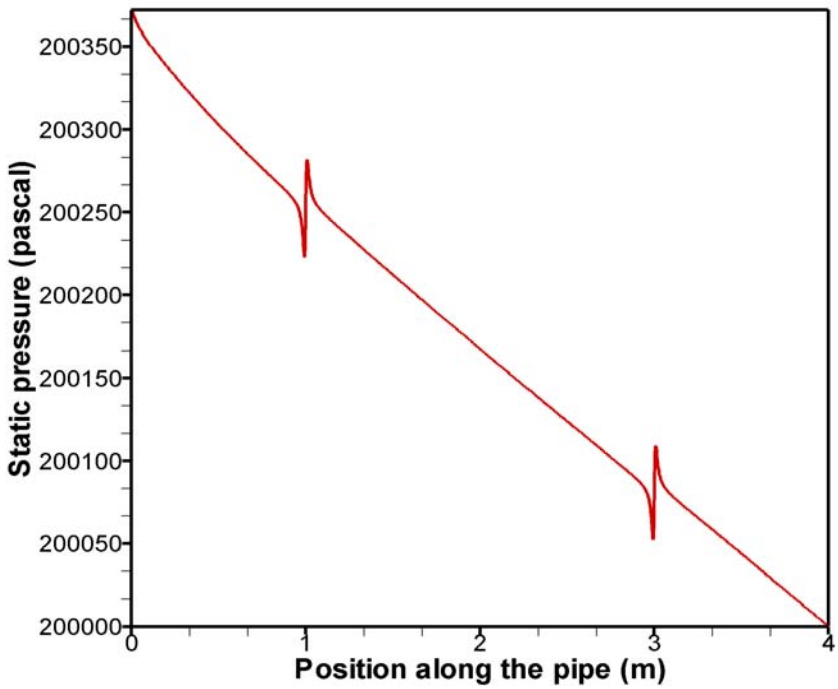

Figure 4.6: Static pressure along line 10 mm below the leaks (v=1m/s P=2bars)

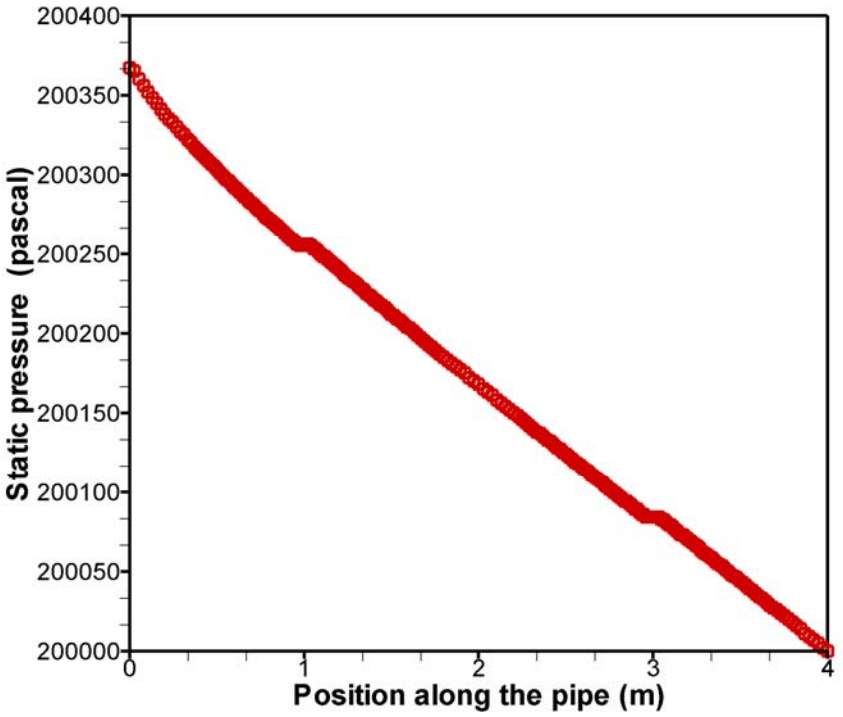

Figure 4.7: Static pressure along the centerline of pipe (V=1m/s P=2bars)

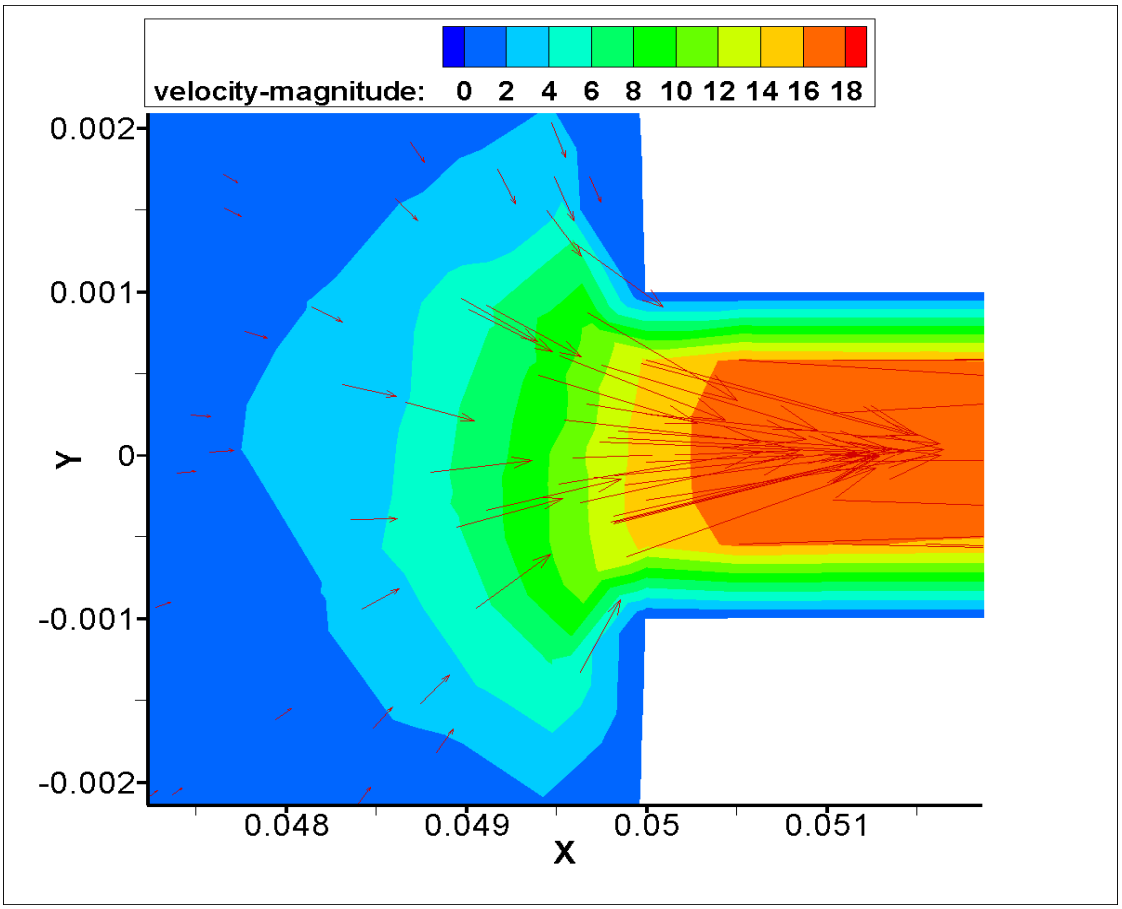

Figure 4.8: Close up view of velocity vector coloured by velocity magnitude, m/s in vicinity of leak1 (V=1m/s P=2bars)

4.2.3 Effect of Pressure gradient

Measurement of pressure gradient in a pipe is amounting to either having two pressure transducers taking measurement along the pipe simultaneously or a single transducer taking two different readings sequentially along the pipe while studying the difference in the measurements. Considering the pressure gradient across the pipe cross-section, there appears to be a wider localization of the pressure values coupled with higher ranges of values compared to that of the pressure. The trend of the pressure gradient at the inlet of

the pipe shows the developing region of flow characterized with higher acceleration and turbulence. Thus, the solution within the entry region is applicable to supply inlets and junctions service junctions. The plot shown in Figure 4.9 represents the effect of the leaks on the pressure gradient along the pipe centerline. It can be observed that the maximum pressure gradient occurs across the leaks. Similar to what was observed with the pressure, the closer the line of measurement to the leak the stronger the distinction within the leaks vicinities. The pressure gradient 2mm below the leaks gives a clear distinction in the vicinity of the leaks with about 25KPa/m around the leaks. This magnitude is appreciable for monitoring despite the miniature size of the leak.

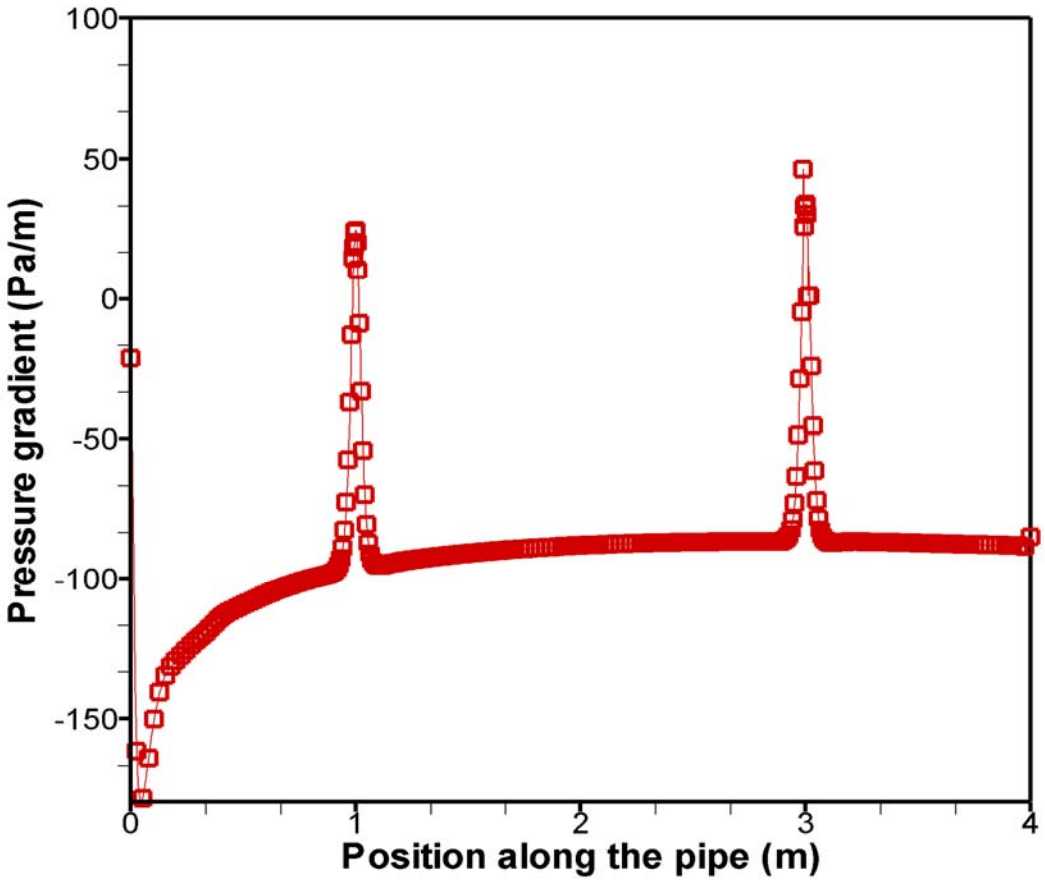

Figure 4.9: Pressure gradient along the centerline (v=1m/s P=2bars)

Along the centerline the pressure gradient has a wider distinction in the leaks vicinities with the gradient forming local maxima at the leak points with the values being limited to the range of -10 to 100Pa/m within the vicinities of the leaks. This gives higher advantage with magnitude over the pressure measurement. Also, well-defined changes are noticed in the leaks vicinity. This eliminates the inaccuracy that may set in as a result of sensor resolution and threshold value. The correlation of the results can be handled with the data acquisition setup.

We observed the effect of line pressure on the gradient of pressure within the vicinities of the leaks. As shown in figures 4.10 and 4.11, the pressure gradient along the centerlines increases with an increase in the line pressure. Thus, the gradient within the vicinities of leaks would be higher with pressure increment. *It is vital to identify that; increase of pressure within the pipe network would increase the chances of pinpointing leaks with parameters related to pressure.* This is why parameters related to pressure are highly recommended for non-acoustic based leak detection especially with the rising trend in developments of in-pipe mobility module that can drive sensors close to the walls of the pipe.

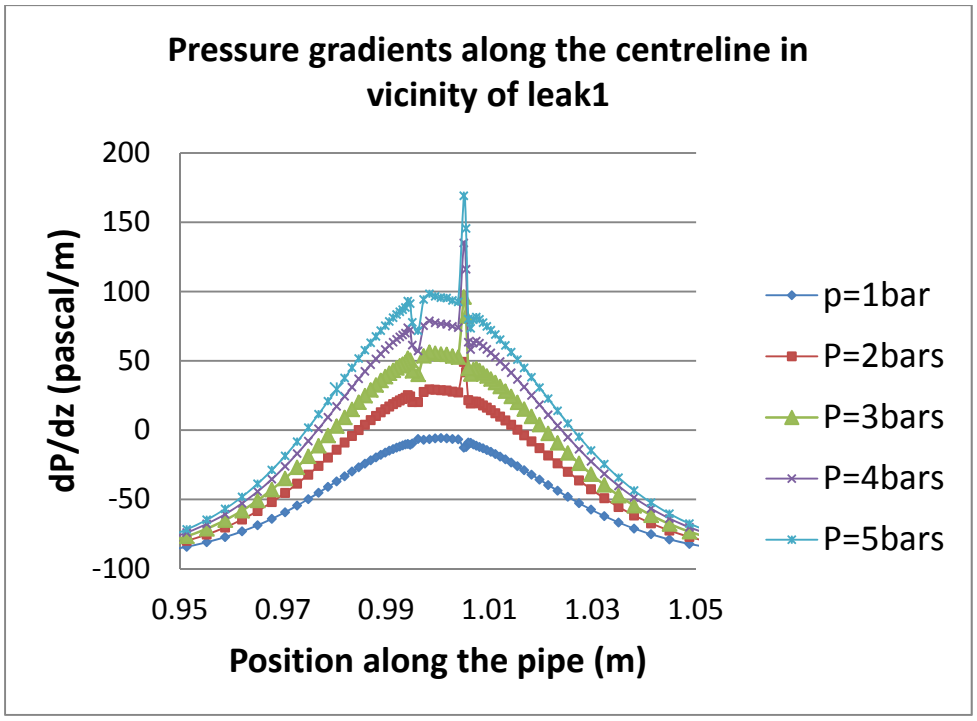

Figure 4.10: Pressure gradient along the centerline, within vicinity of leak 1 (v=1m/s);

2mm diameter leak at z=1m

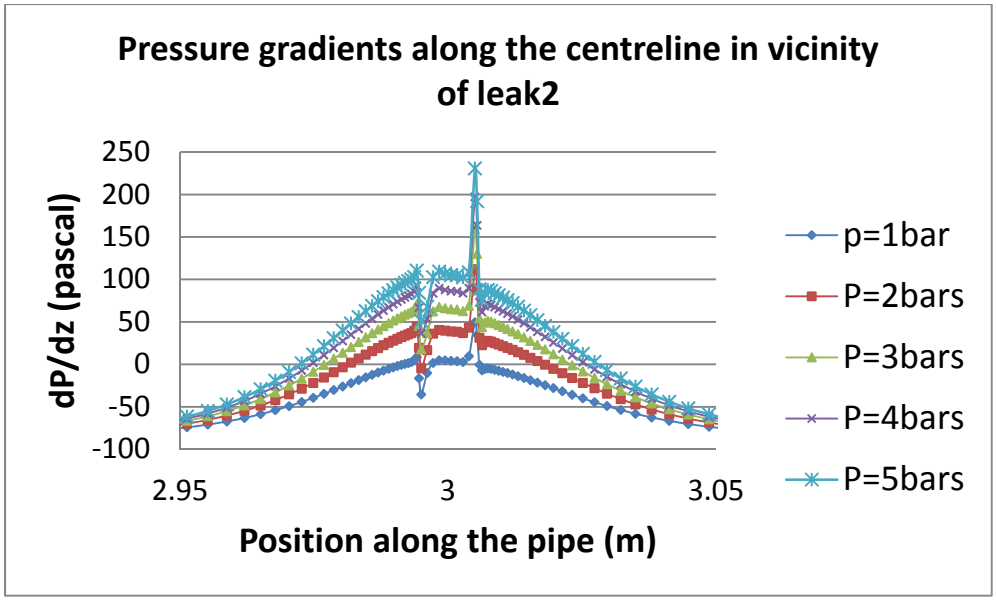

Figure 4.11: Pressure gradient along the centerline, within vicinity of leak 2 (v=1m/s);

2mm diameter leak at z=3m

4.2.4 Study of Acceleration around the leak

Another parameter studied for leaks detection is the acceleration. A study of flow acceleration in the pipe was carried out to evaluate the acceleration behavior within the leaks vicinity to evaluate the possibility of using an accelerometer as a transducer in water pipe leak detection. The following equations were modeled into the solver to define the convective acceleration components and the overall magnitude of acceleration.

$$a_x = u\frac{\partial u}{\partial x} + v\frac{\partial u}{\partial y} + w\frac{\partial u}{\partial z} \tag{4.3}$$

$$a_y = u\frac{\partial v}{\partial x} + v\frac{\partial v}{\partial y} + w\frac{\partial v}{\partial z} \tag{4.4}$$

$$a_z = u\frac{\partial w}{\partial x} + v\frac{\partial w}{\partial y} + w\frac{\partial w}{\partial z} \tag{4.5}$$

$$a = \sqrt{\left(a_x^2 + a_y^2 + a_z^2\right)} \tag{4.6}$$

At distance 2mm below the leak, the acceleration value from the inlet of the pipe remained fairly constant with magnitude of 0 due to non-disturbance relative to x-axis along the pipe. A sudden increment of about 9000m/s^2 is noted in vicinity of leak 1 and a quick recovery from it to fairly constant value till vicinity of leak 2 where a similar hike is experienced. *The velocity of flow toward the outlet of the leak is approximately 20 times the pipeline velocity, thus, resulting to higher values in convective acceleration in the leaks' vicinities*. These clear distinctions within the leaks' vicinities were noticed for the plots of the x-acceleration at other distances below the leaks. Similar to what was observed with the pressure, the magnitudes of the kinks reduce as the lines of examination move away from the leaks and a plot to evaluate the effect of the x-

acceleration along the center of the pipe shows a clears definition of 0.075m/s^2 and before the leaks and -0.075m/s^2 after the leaks to recovery as shown in Figure 12 below.

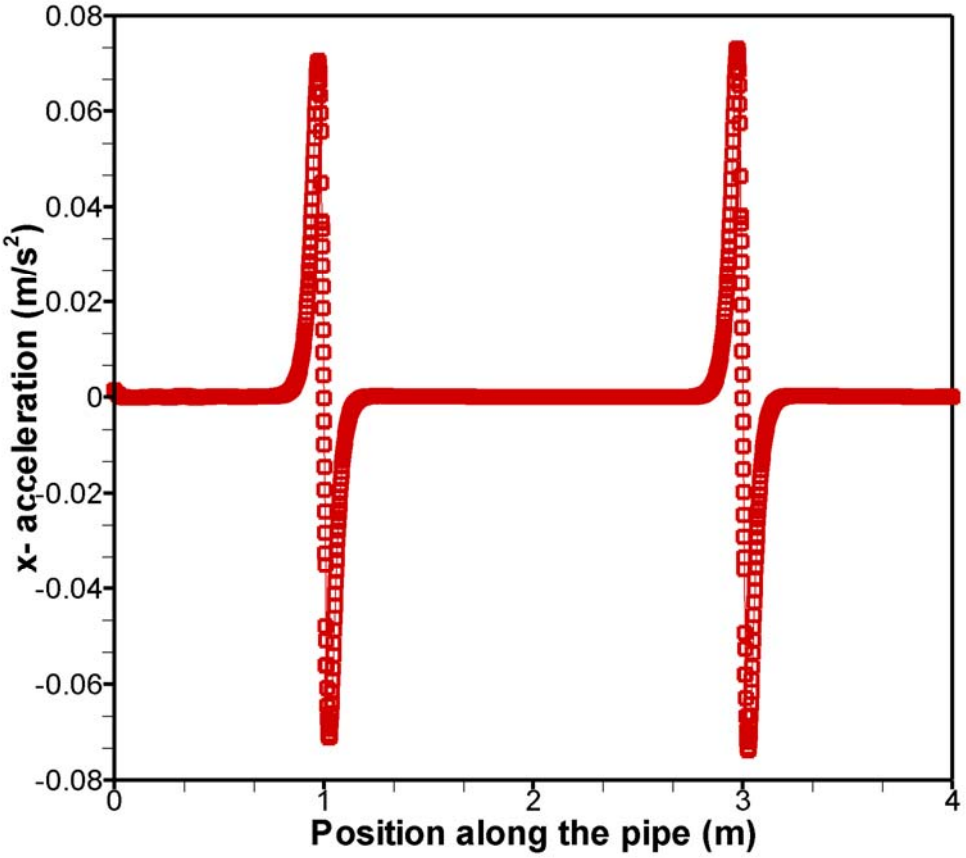

Figure 4.12: x-component of acceleration along the centerline (v=1m/s P=2bars)

A similar distinction is observed with the acceleration in y–direction with a wider evident of presence of the leaks as the definitions occur in wider vicinity but with a relatively lower magnitude. The lower magnitude in this coordinate is as a result of leaks' location. The leaks flow affects the x-acceleration more than the y-acceleration owing to the location of the leaks.

The plot in Figure 4.13 shows the y-acceleration along the center of the pipe. In z-direction a similar distinction is noticed and a wider displacement along the centerline

owing to disturbances along the center with respect to z-directions with relatively high magnitude of hike at the points of the leaks.

The study of the flow acceleration within the pipe shows that the largest acceleration occurs along the pipe (or flow direction). This is observed by comparing the three components of acceleration as shown in Figs 4.12, 4.13 and 4.14. In addition all the three components exhibit well-defined features seen as very clear peaks exactly in the cross sectional plane at the leak locations. Thus it can be deduced that accurate accelerometers can pick up the existence of a leak irrespective of their location and orientation. *This method can be reliable in early leak detection of unpredictable nature. However, this promising method for leak detection may face some technical challenges in its application even with the availability of miniature accelerometers, due to noise and interference problems.*

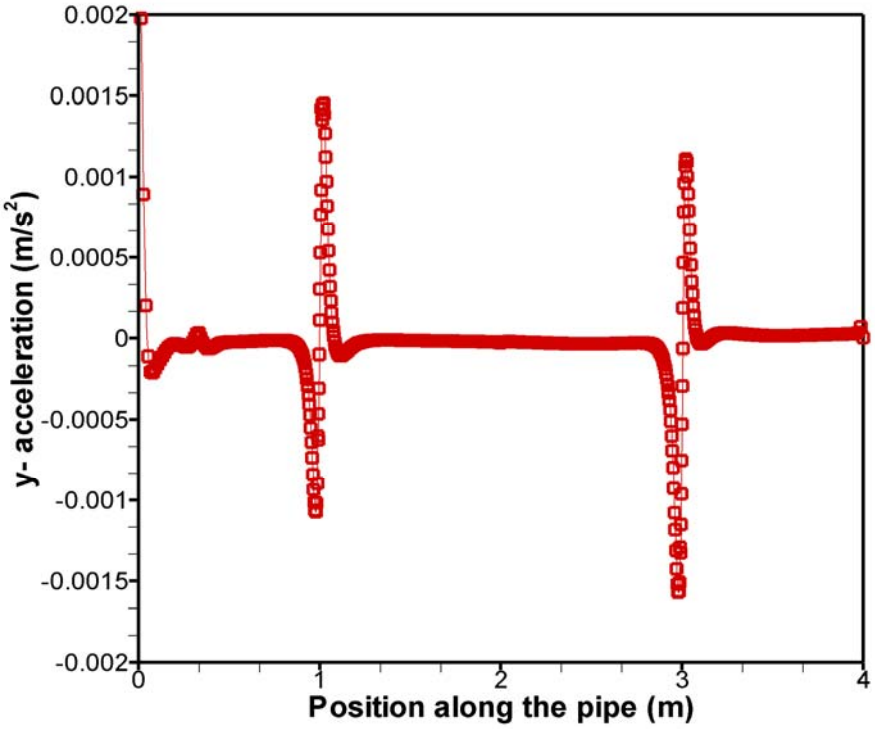

Figure 4.13: y-component of acceleration along the centerline (v=1m/s P=2bars)

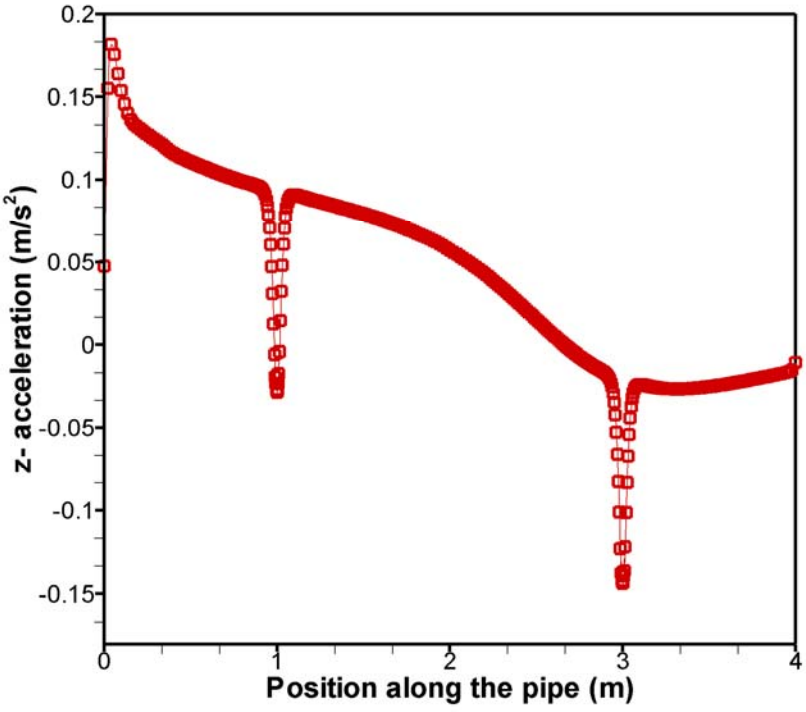

Figure 4.14: z-component of acceleration along the centerline (v=1m/s P=2bars)

4.3 Differential pressure within vicinities of leaks

From the just concluded subsection, it has been observed that there is highly localized pressure gradient within the vicinities of the leaks. Measuring the static pressure or the pressure gradient along a pipe could be quite challenging if these data are meant for leak detection but differential pressure transducers reduce such challenges. One end of the sensor could be placed at a point where pressure change is not pronounced while the other end is moved along the points of interest. This gives the sensor an advantage in the leak detection application. As we could see in the previous study, that the pressure change along the pipes' centerlines is not well pronounced while there is highly localized pressure gradient within the vicinities of the leaks. Thus, the following subsection discusses the use of differential pressure for leak detection.

4.4 Overview of Results of Differential Pressure around Leaks

The results of both experimental and numerical studies are presented. First the effect of the sensor tap in the pipe is presented on the 2.2mm and 4mm diameter leaks. The level of sensor intrusion is also discussed. Second, the results of both studies are compared; the effect of the size and geometry of leaks on the differential pressure measurable is also presented. Also, we present the variation of differential pressure with the normal height of sensor tap from the wall. Finally, effect of operational conditions (Line pressure and fluid flow) on the differential pressure is presented.

4.4.1 Effect of tap in pipe

The objective of this section is to present the effect of modeling the tap into the pipe. This is done by comparing the simulations done with sensor tap with the ones done without the sensor tap in place. A sensor tap of 2.2mm diameter, 15mm long was incorporated in-pipe above the holes to approximate the experimental scenario. At a height 1mm above the 4mm simulated leak, the computation predicted a maximum of 10 kPa pressure drop at the center of the hole without the sensor tap; when compared with a similar case where the sensor tap is incorporated, the computation resulted into about 200% increase in the differential pressure measurement. Figures 4.15, 4.16 and 4.17 show this comparison for 2.2mm hole at 1mm above leak, 4mm hole at 1mm above leak and 4mm hole at 2mm above leak respectively. *The plots indicate that the presence of the sensor tap increases the differential pressure around the leak.* The sensor tap creates a region of low pressure around the tips of the tap which spreads through the areas covered by the leak. The sensor tap creates a small aperture around the leaks which causes flow acceleration within that region. Thus, increases the differential pressure computed on the tap surface. With this significant effect of sensor tap, the rest of the computations were carried out with the sensor in place in order to have the simulations close to reality.

The plot of velocity vector (Figure 4.19) in the leak vicinities supports the fact the pressure gradient measured by the taps is predominantly leak induced. Apart from the intrusion caused by the sensor tap surface causing increase in flow acceleration around the surface, the velocity around the stem of the tap away from the surface does not significantly have effect on the values on the sensor tap surface. Similarly the plot of the

turbulent kinetic energy at the same location signifies an increase in turbulence as a result of leak pressure outlet rather than sensor tap.

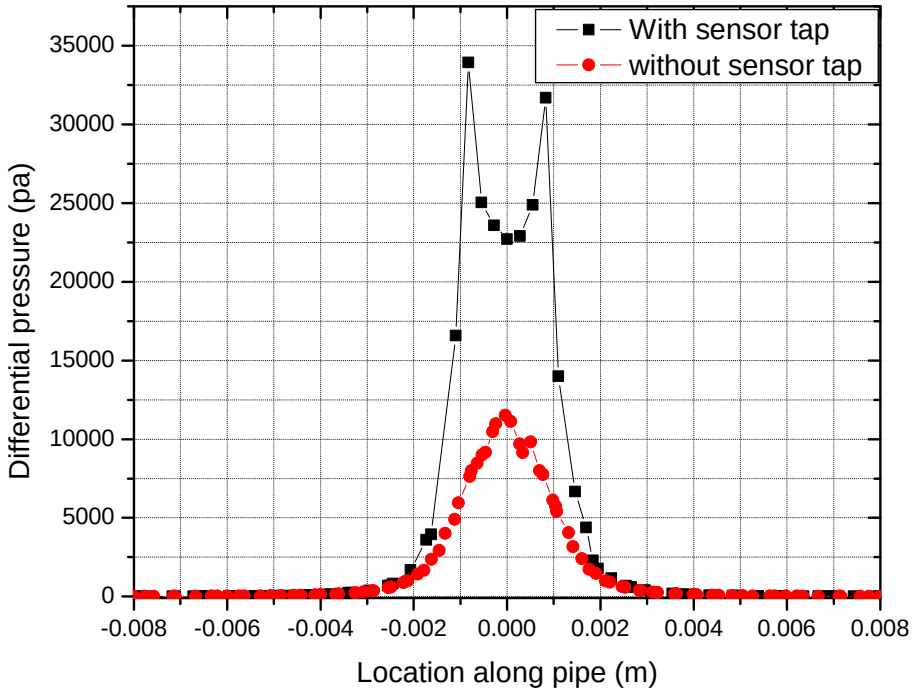

Figure 4.15: Effect of sensor tap on the differential pressure: 2.2mm hole; 1mm from the wall; 30 psi line pressure

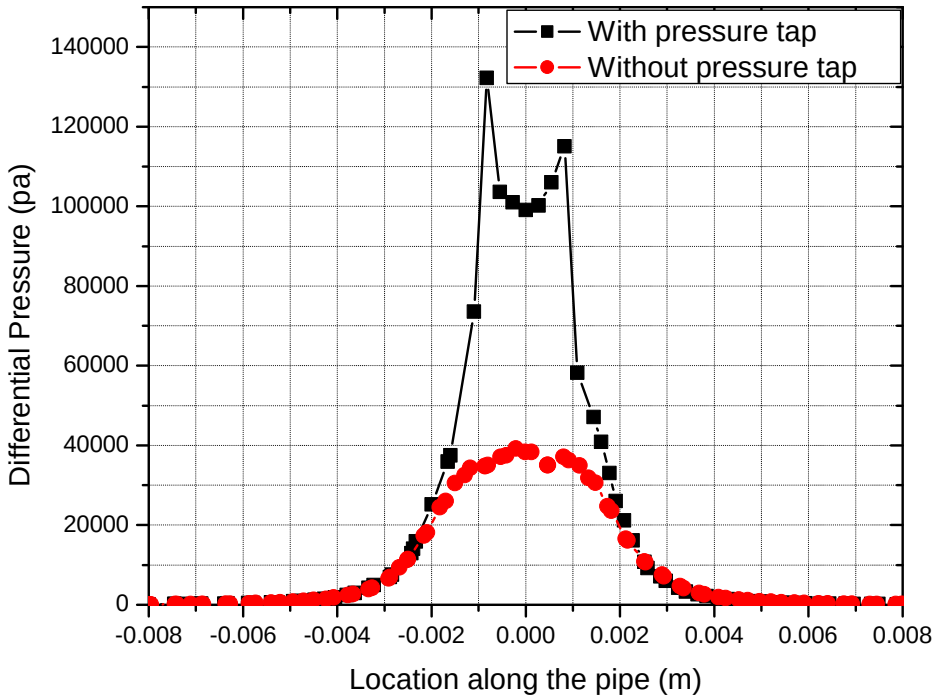

Figure 4.16: Effect of sensor tap on the differential pressure: 4mm hole; 0.5mm from the wall; 30 psi line pressure

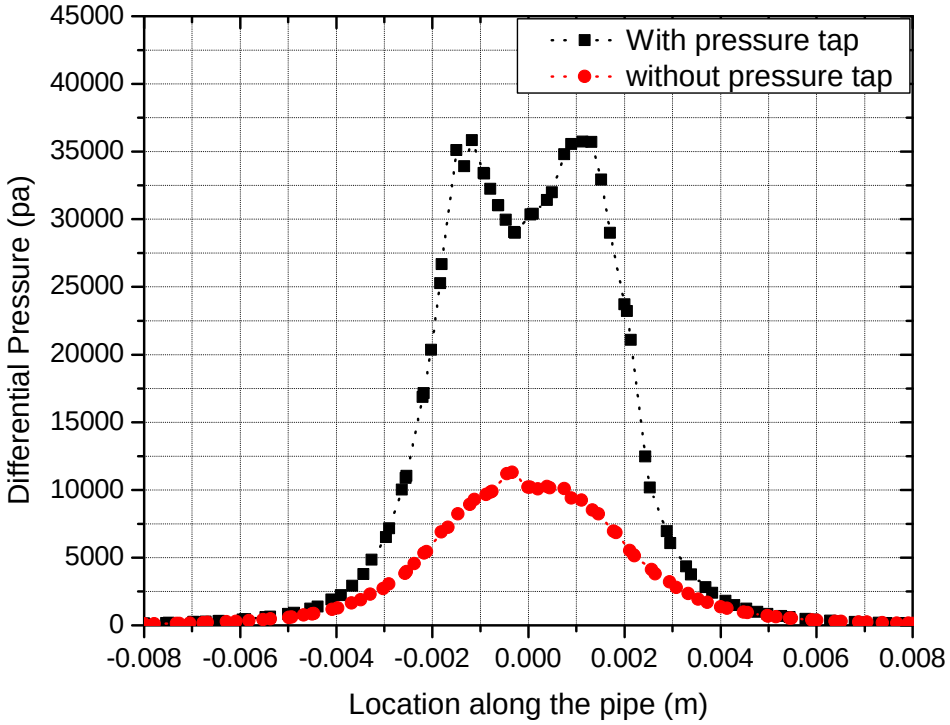

Figure 4.17: Effect of sensor tap on the differential pressure: 4mm hole; 1mm from the wall; 30 psi line pressure

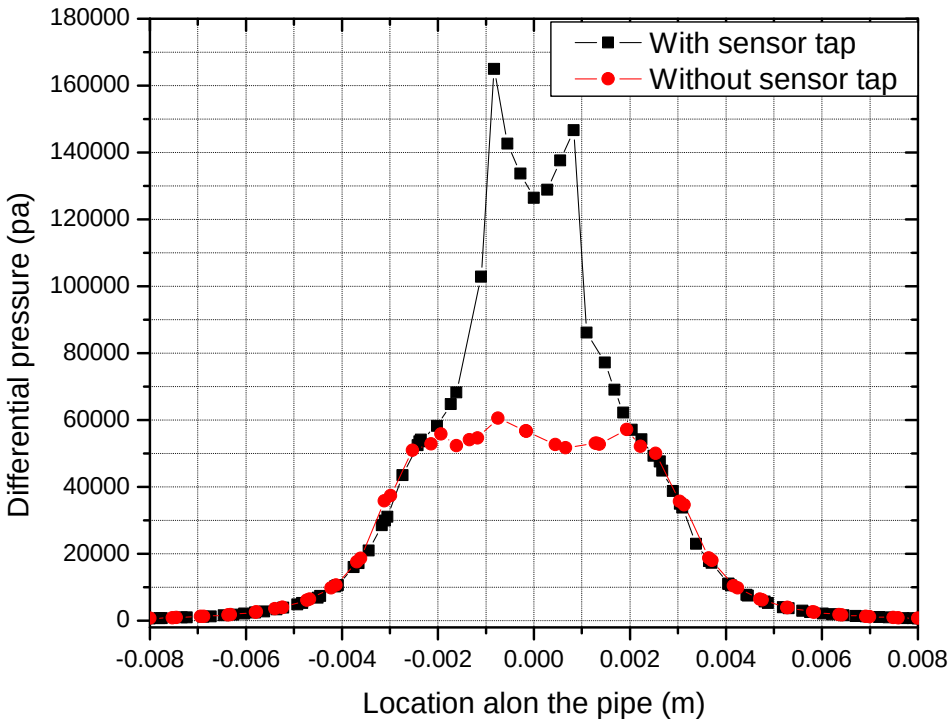

Figure 4.18: Effect of sensor tap on the differential pressure: 6mm hole; 1mm from the wall; 30 psi line pressure

From the plots, we could notice a parabolic profile signifying the surface of the tap. The maximum differential pressures occur at the either ends of the tap with the minimum values at the center. Experimentally, a sensor tap measure the average of the pressure on its surface rather than the point pressure. Thus, the computational results were post processed as the area weighted average on the surface of the slot. The differences between the range (difference between the minimum and maximum) of differential pressure is more in the 2.2mm hole than in 4mm hole. We can describe the alteration of the pressure values as a result of sensor tap as intrusion.

To experimentally measure the level of tap intrusion on the leaks flow properties, we chose flow rate as a parameter. The flow rates out of the each simulated leaks were collected at three different heights. In addition, base cases with no sensor tap were also

experimented for flow rates out of the simulated leaks. For each run, the test section was maintained at a pressure of 30psi with no flow other than induced by the leak flow outlet. Table 4.2 below summarizes the results at they are compared with the based case.

Table 4.2: Flow rates through simulated leaks for different sensor tap heights. (P=30 psi, no flow condition)

distance (mm)	2.2mm hole Flow rate (L/min)	% Intrusion	4mm hole Flow rate (L/min)	% Intrusion	6mm hole Flow rate (L/min)	% Intrusion
no tap	*4.4*	-	*12*	-	*27.2*	-
0.5	3.45	21.59	10.94	8.83	25.71	5.48
1	4.31	2.045	11.57	3.58	26.1	4.04
1.5	4.38	0.45	11.6	3.333	26.17	3.79

For 2.2mm hole, with the sensor tap at 0.5mm above the hole, we could notice about 22% reduction in the leak flow rate. This is owing to the size of the tap comparably to the leak size. At this height, the tap almost covers the leak thus, reducing the flow rate. In addition, the tap causes a strong jet as water forces its way through the narrow opening between the tap and the wall, creating a region of low pressure around the leak which consequently affects the pressure measure on the tap. The other two simulated holes at this height, experience a relatively lower level of intrusion. They have sizes larger than the size of the pressure sensor**.** *Thus, the smaller the sensor tap diameter compares with the leak diameter, the lower the level of intrusion and the more exact the differential pressure measureable.*

At height of 1mm above the walls, the intrusion of sensor tap is reduced with the minimum for 2.2mm hole at about 2% and maximum for 6mm hole at about 4%. At height of 1.5mm above the leaks, the level of intrusion further reduces with the effect barely noticeable for 2.2mm hole but still noticeable for hole 6mm hole at about 3.8% of the no tap leak flow rate.

In summary, the sensor tap presence in the flow significantly increases the differential pressure. The level of intrusion measured experimentally signifies higher values as the sensor tap moves close to the walls. These intrusions however, increase the magnitude of differential pressure measureable within the vicinity of leaks, thus can be used as additional advantage for effective leak detection. Also, *the closer the system is to the wall, the higher the intrusion and the higher the measureable values of differential pressure.*

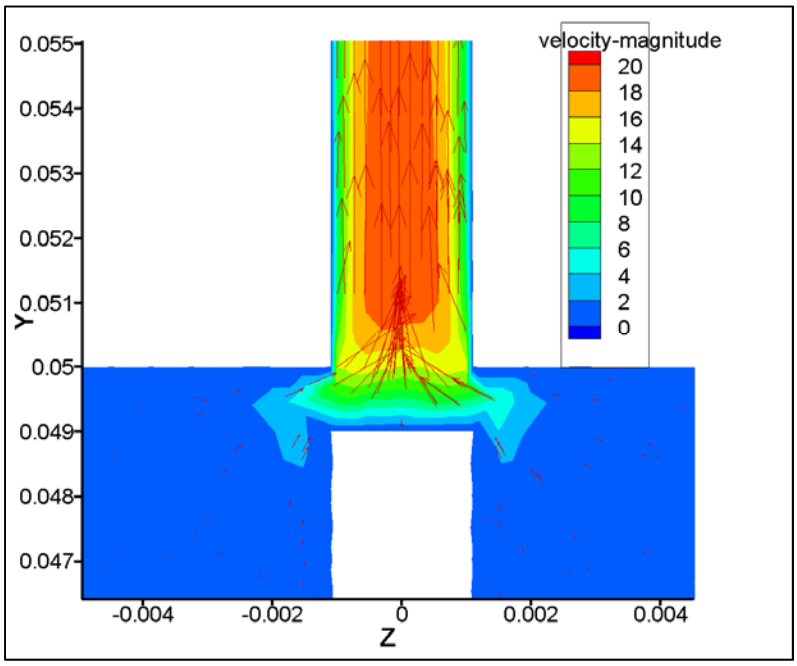

Figure 4.19: Velocity vector around the leak, colored by velocity magnitude, m/s: 2.2mm hole; sensor tap at 1mm from the wall; 30psi line pressure

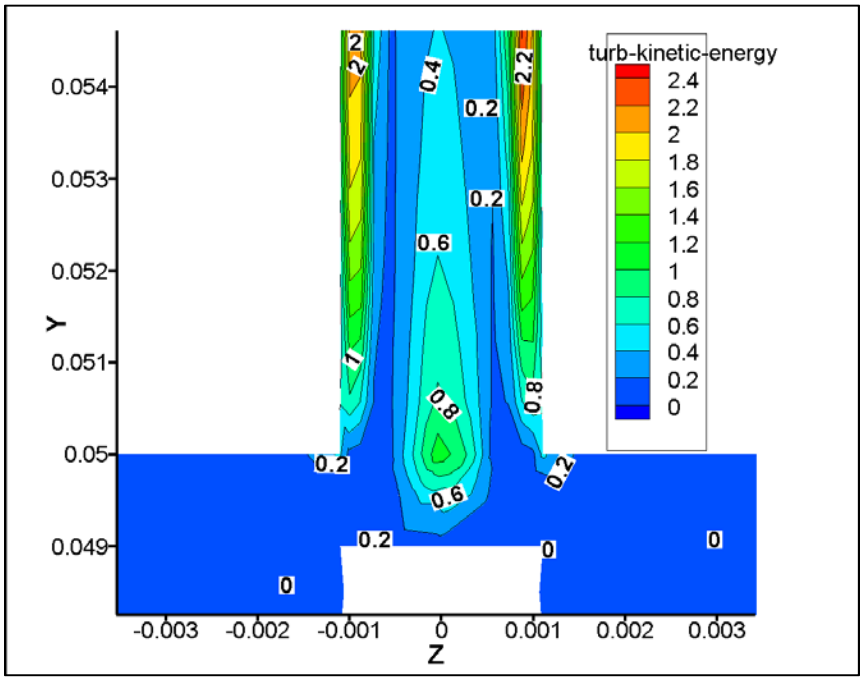

Figure 4.20: Turbulent kinetic energy round the leak: 2.2mm hole; sensor tap at 1mm from the wall; 30psi line pressure

4.4.2 Comparison of Experimental and Numerical Results

The objective of this section is to compare the results of the experimental work with those obtained using computational fluid dynamics. This would validate the preliminary study, identify the weakness of the research methods as applicable to the present research and provide inference for the discussion. To do this, we carried out systematic data deduction on the test sections described in the previous chapter, leaks studied for comparison are 2.2mm and 4mm simulated holes, and 0.6mm X 12mm simulated slot described before.

The experiments were carried out with approximately no flow except flow induced by the simulated leaks. The test sections were monitored and maintained at 30psi. The heights

of sensor tap from the wall were varied from 0.5mm to 2mm in an increment of 0.5mm for the simulated hole, and heights 0.5mm and 1mm for the simulated slot. The height limitation for the slot is as results of the slot dimension and characteristic of the available differential pressure sensor used for the experiments. Measurements were taken as distances varying from 0 to 5mm from the simulated holes in an increment of 1mm. Similarly, measurements were made along the length of the slot with two points lying on the either sides of the slot at 2mm away.

Tables below show details of the comparison with the deviation of the computational results from the experimental results.

Table 4.3: Differential pressure for 2.2mm simulated hole; tap at 0.5mm above wall

distance from leak (mm)	Experimental (pa)	Standard Deviation (%)	Computational (pa)	% Difference
0	96000	5.27	108500	13.02
1	53000	9.54	67000	26.42
2	9300	9.06	9900	6.45
3	4200	4.01	990	-76.35

Table 4.4: Differential pressure for 2.2mm simulated hole; tap at 1mm above wall

distance from leak (mm)	Experimental (pa)	Standard Deviation (%)	Computational (pa)	% Difference
0	34100	1.48	34000	-0.295
1	19000	3.59	22000	15.79
2	4200	2.32	4500	7.14
3	1300	7.46	950	-26.9
4	350	2.78	260	-25.7

Table 4.5: Differential pressure for 2.2mm simulated hole; tap at 1.5mm above wall

distance from leak (mm)	Experimental (pa)	Standard Deviation (%)	Computational (pa)	% Deviation
0	14000	7.26	17000	21.43
1	7800	1.25	7600	-2.56
2	2400	8.33	2700	12.5
3	900	11.11	680	-24.44
4	330	7.80	250	-24.24

Table 4.6: Differential pressure for 2.2mm simulated hole; tap at 2mm above wall

distance from leak (mm)	Experimental (pa)	Standard Deviation (%)	Computational (pa)	% Difference
0	4900	1.99	5000	2.04
1	3000	8.58	3600	20
2	1800	9.36	1500	-16.67
3	550	9.09	527	-4.18

Table 4.7: Differential pressure for 4mm simulated hole; tap at 0.5mm above wall

distance from leak (mm)	Experimental (pa)	Standard Deviation (%)	Computational (pa)	% Difference
0	144000	3.26	180100	25.1
1	120000	3.53	140000	16.67
2	86000	7.07	104714.88	21.76
3	18500	9.11	21281.773	15.04
4	3500	7.36	4100	17.14
5	1900	8.87	1550	-18.42

Table 4.8: Differential pressure for 4mm simulated hole; tap at 1mm above wall

distance from leak (mm)	Experimental (pa)	Standard Deviation (%)	Computational (pa)	% Difference
0	95000	1.02	110500	16.31
1	81000	2.08	98000	20.99
2	46000	3.66	47600	3.48
3	9900	4.28	12000	21.21
4	2800	7.14	3500	25
5	1600	6.08	1400	-12.5

Table 4.9: Differential pressure for 4mm simulated hole; tap at 1.5mm above wall

distance from leak (mm)	Experimental (pa)	Standard Deviation (%)	Computational (pa)	% Difference
0	54000	6.30	59000	9.26
1	43000	8.34	49000	13.95
2	23000	6.61	25500	10.87
3	7000	9.99	8600	22.86
4	2700	11.11	2900	7.41
5	1300	7.49	1250	-3.85

Table 4.10: Differential pressure for 4mm simulated hole; tap at 2.0mm above wall

distance from leak (mm)	Experimental (pa)	Standard Deviation (%)	Computational (pa)	% Difference
0	28500	1.18	31000	8.77
1	22000	2.76	25000	13.64
2	17000	2.29	15000	-11.76
3	5900	1.65	6000	1.69
4	2700	6.24	2400	-11.11
5	1100	9.09	1080	-1.82

Table 4.11: Differential pressure for 0.6mm X 12mm simulated slot; tap at 0.5mm above wall

Location along slot (mm)	0.6mm X12mm slot (Experimental.)	Standard Deviation (%)	0.6mm X12mm slot (computational.)	% Difference
-2	900	11.67	330	-63.33
0	15200	2.093	17000	11.84
2	29000	1.67	35000	20.69
4	29400	1.41	35400	20.41
6	30200	2.14	35500	17.55
8	29000	1.34	35400	22
10	28000	1.73	35000	25
12	14400	4.11	17000	18.06
14	700	11.71	298	-57.43

Table 4.12: Differential pressure for 0.6mm X 12mm simulated slot; tap at 1 mm above wall

Location along slot (mm)	0.6mm X12mm slot (Experimental.)	Standard Deviation (%)	0.6mm X12mm slot (computational.)	% Difference
-2	800	3.56	298	-62.75
0	4100	5.52	3915	-4.78
2	8086	5.40	7721	-4.52
4	8611	5.51	8384	-2.64
6	8954	4.21	8400	-6.18
8	8497	7.72	8384	-1.34
10	7903	5.59	7721	-2.31
12	4020	5.38	3915	-2.62
14	700	9.23	298	-57.43

For the simulated 2.2mm leak, deviation in the two results shows that the computationally predicted result is higher at tap height of 0.5mm except away from the center. This is similar to what is experienced with the 4mm hole at this location, particularly at the center of the leaks. This over-prediction could be related to the wall treatment of the model used, although, the model predicted to most proximal result to the experimental data as highlighted in the numerical formulation. The results still compare well with the experimental as it falls within the acceptable limits. Also, experimental error cannot be ruled out as the phenomenon under study has a very high gradient with a short span. The table in appendix 1 shows the standard deviations of the measurements.

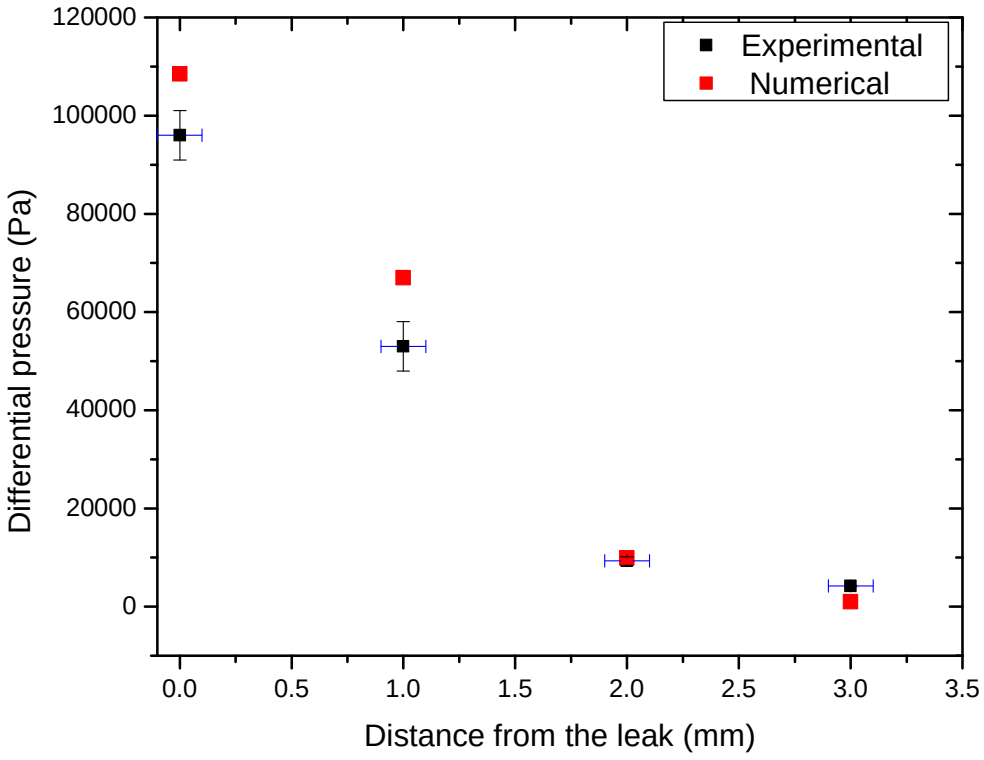

Figure 4.21: Differential pressure distribution away from leak: 2.2mm hole; 0.5mm above the wall; 30psi line pressure

For the simulated 2.2mm hole with sensor tap at 0.5mm, it could be noted from the table (not obvious on the plot) the computational results does not go in agreement with the experimental results as the distance approaches 3mm and beyond.

The problem lies with the experimental constraint. These over-predictions are traced to; (i) large gradient within the vicinity of the leaks which changes the result with slightest shift in actual location (Automated system is suggested for avoid this). (ii) Characteristic of the sensor which makes it difficult to measure low values of differential pressure accurately. At this tap height, a high level of tap intrusion into the flow was experienced. This creates regions of low pressure around the tips of the tap and thus, measuring a relatively higher value of differential pressure. The results have shown that characteristic of sensor is necessary to be taken into consideration while designing leak detection mechanism based on the method.

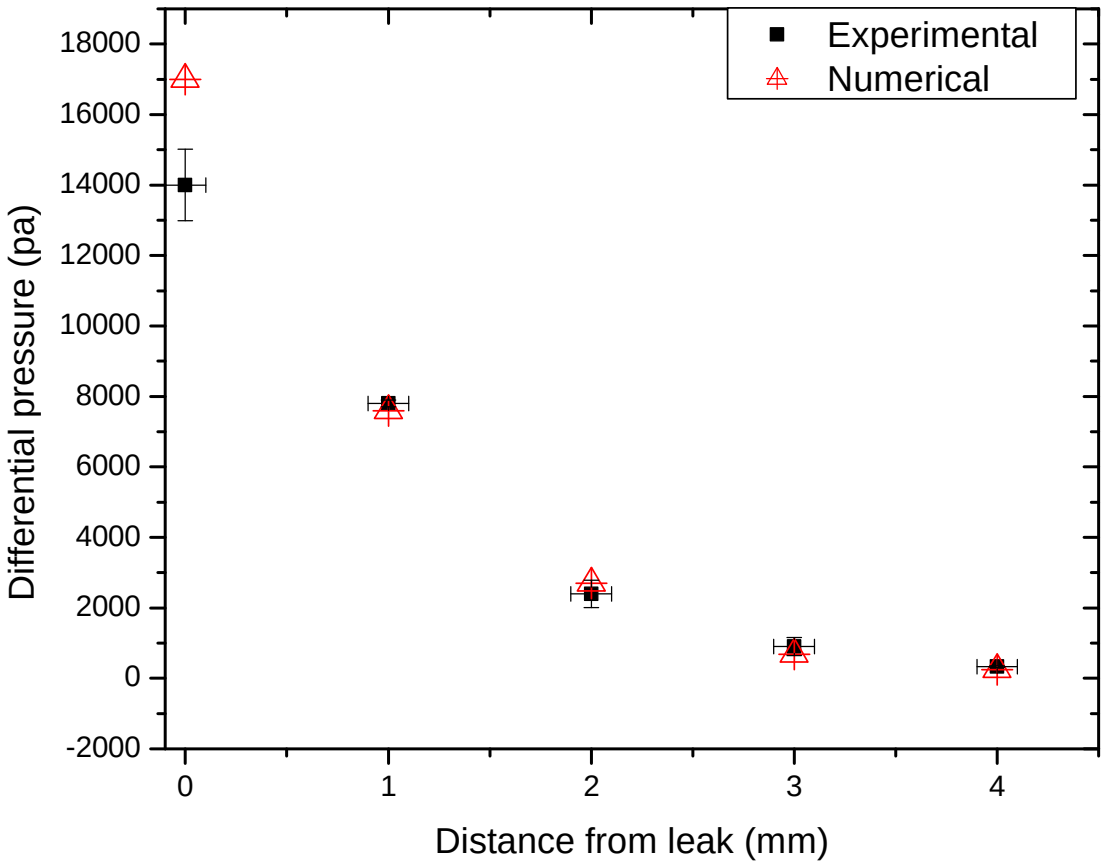

Figure 4.22: Differential pressure distribution away from leak: 2.2mm hole; 1.5mm above the wall; 30psi line pressure

The plot shown in figure 4.22 compares the experimental and computational results for 2.2mm hole at 1.5mm above the wall. The graph shows good agreement between the results. Similar to what was observed at 3mm away from the center of the leak at height 0.5mm, the computation predicts results higher than the experimental results. However,

the results show a better agreement as they are close to 70% of the experimental results. Thus, a reading taken at this height shows a higher level of confidence and viable of been used for pinpointing leaks. At higher heights, the gradient of pressure across the sensor tap reduces; this reduced the magnitude for 2.2mm simulated leak have good agreement with deviation limited to 30% of the experimental results except for few locations. Thus, further study on 2.2mm hole can be carried out computationally where necessary with trends not significantly affected by these deviations.

Comparing the computational and experimental results for 4mm simulated leak. Similar to what was observed with the 2.2mm hole, the deviation in these results reduces as the sensor tap is located farther away from the wall. As seen in the table, the results recorded for 0.5mm height of tap at the center assumed the most deviated at 29% of the experimental result. Deviation at corresponding location at height 1mm above the leak reduces to value of 19% and further to 9% and 8% at 1.5mm and 2mm respectively above the leak. Figures 4.23 and 4.24 show the comparison plots with good agreement along distances from the center of leak. We can associate the closeness of the results (computational and experimental) for the 4mm hole with the relative big size of the hole compared with the sensor tap. The effect of low pressure induced as a result of the tap is now comparably smaller to the actual pressure when compared with the 2.2mm hole.

The computational and experimental results are also compared for the slot with the sensor tap at 1mm above the wall (Figure 4.25). The results show good agreement with the computational results higher than experimental results at 0.5mm above the slot as observed with the holes. At height of 1mm above the slot both the experimental and computational results are the same along the slot with a deviation less than 3% of the

experimental results. For the slot, the thinner tap used in collecting the data improved the accuracy of the experimental result. For the slot, the level of intrusion due to tap presence for the slot is on the low side. *As the size of the sensor tap is reduced relative to the leak width, the deviation in the results reduces. This suggests a relative thin sensor tap for experimenting the pressure technique.*

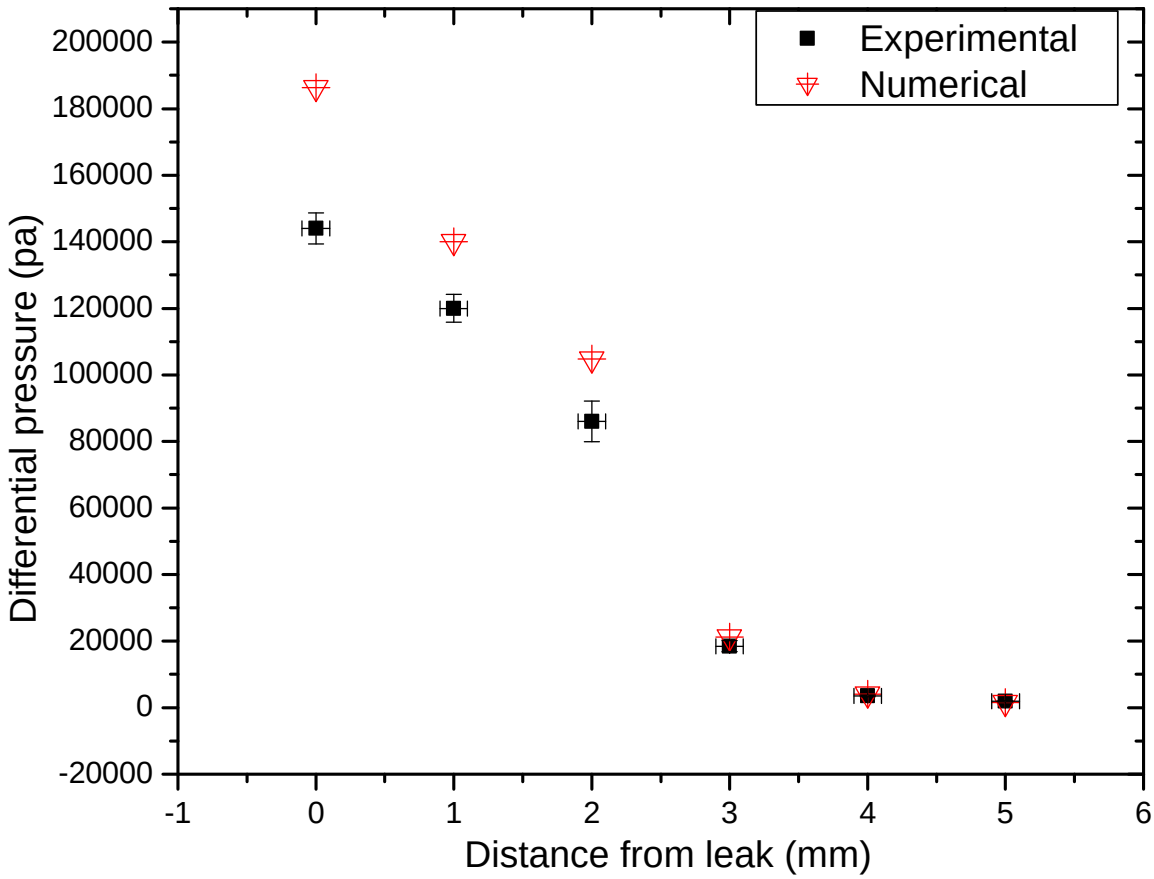

Figure 4.23: Differential pressure distribution away from leak: 4mm hole; 0.5mm above the wall; 30psi line pressure

In summary, results of both research methods gave a good agreement and thus, any of the research methods can be used for further study without significantly missing out required trends. A better agreement was achieved between the experimental and numerical results for 4mm holes as compared with the 2.2mm holes. Therefore, computational results using the same model on bigger sizes of leaks are valid. The standard deviations of all the experimental results lie below 10% of the average values (as presented in the appendix). This signifies high level of repeatability and consistency of the results. However, further experimentations might require setup with high level of precision in terms of location owing to the high pressure gradient experienced within the vicinities of the leak.

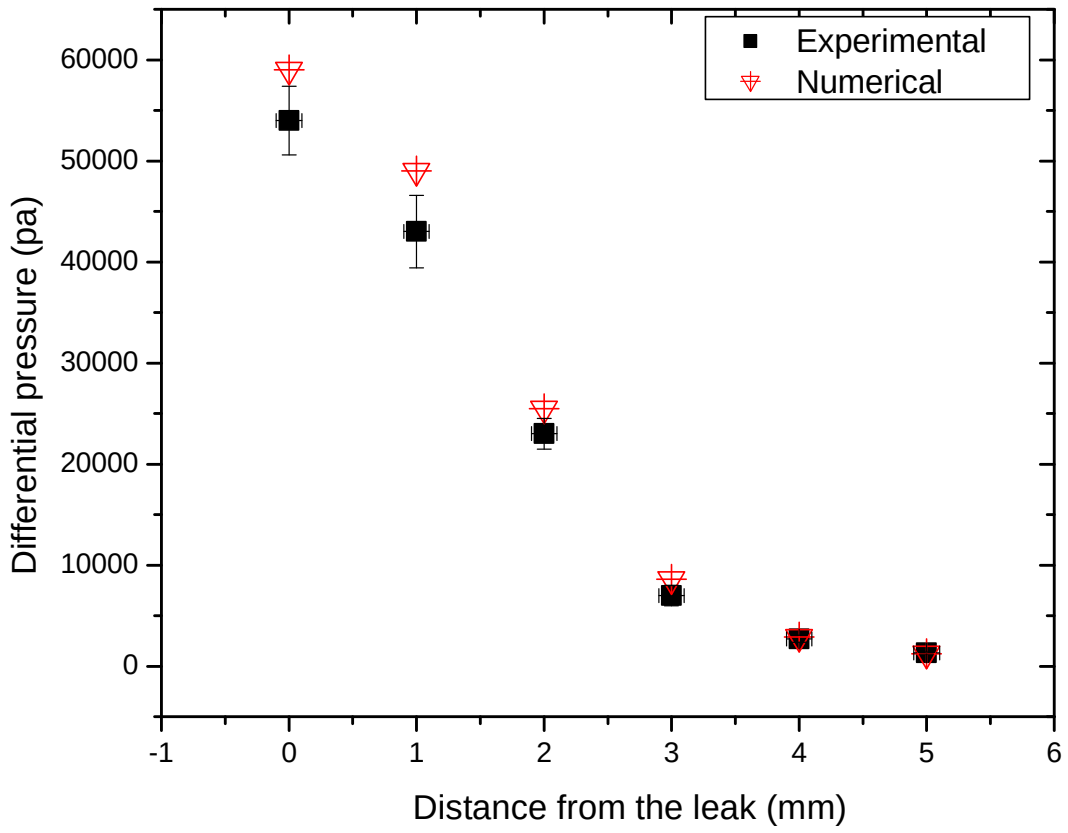

Figure 4.24: Differential pressure distribution away from leak: 4mm hole; 1.5mm above the wall; 30psi line pressure

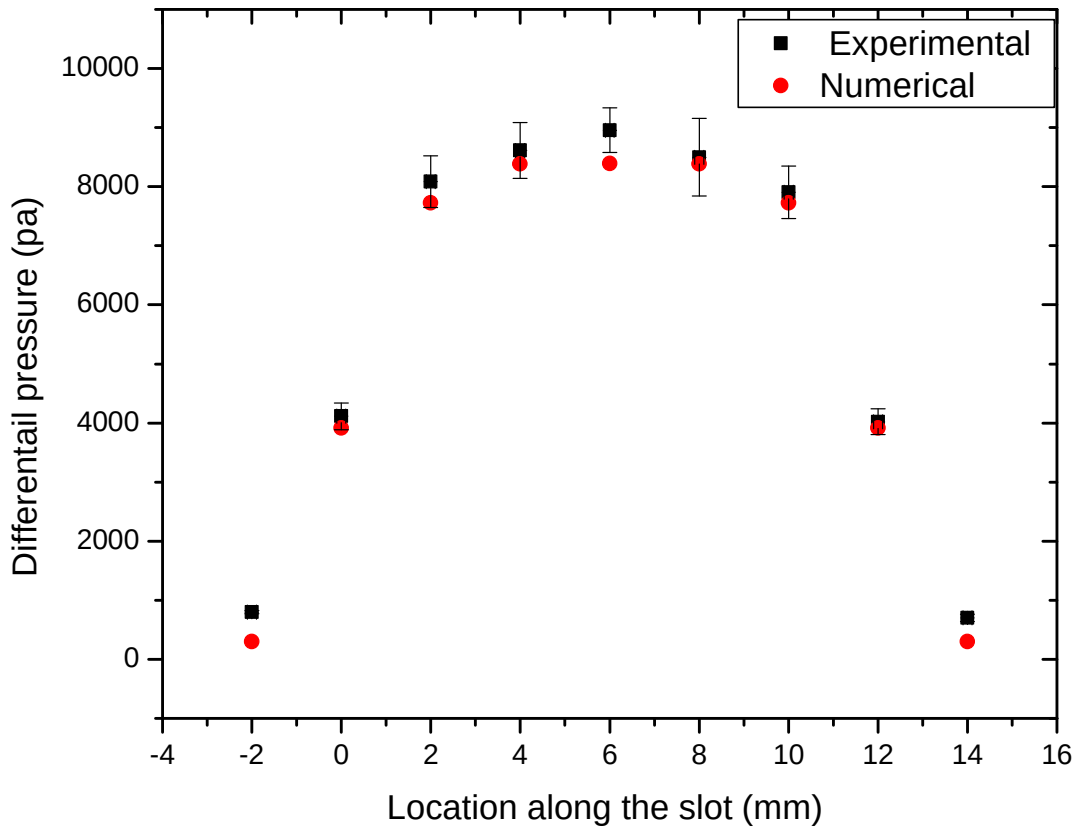

Figure 4.25: Differential pressure distribution along slot: 0.6mm X 12mm slot; 1 mm above the wall; 30psi line pressure

4.4.3 Effect of Leak Size and Geometry

The objective of this section is to present the effect of leak geometry and size on the pressure. The experimental results with the three simulated holes (2.2mm, 4mm and 6mm) are compared at a fixed condition. With no flow, the line pressure in the test section was kept at 30psi; readings were taken axially from the leak center at height of 1mm. Comparisons on the slots were done using computational results. In addition to the 0.6 x 12mm slot, two other slots of the same length with widths 0.8mm and 1mm were simulated.

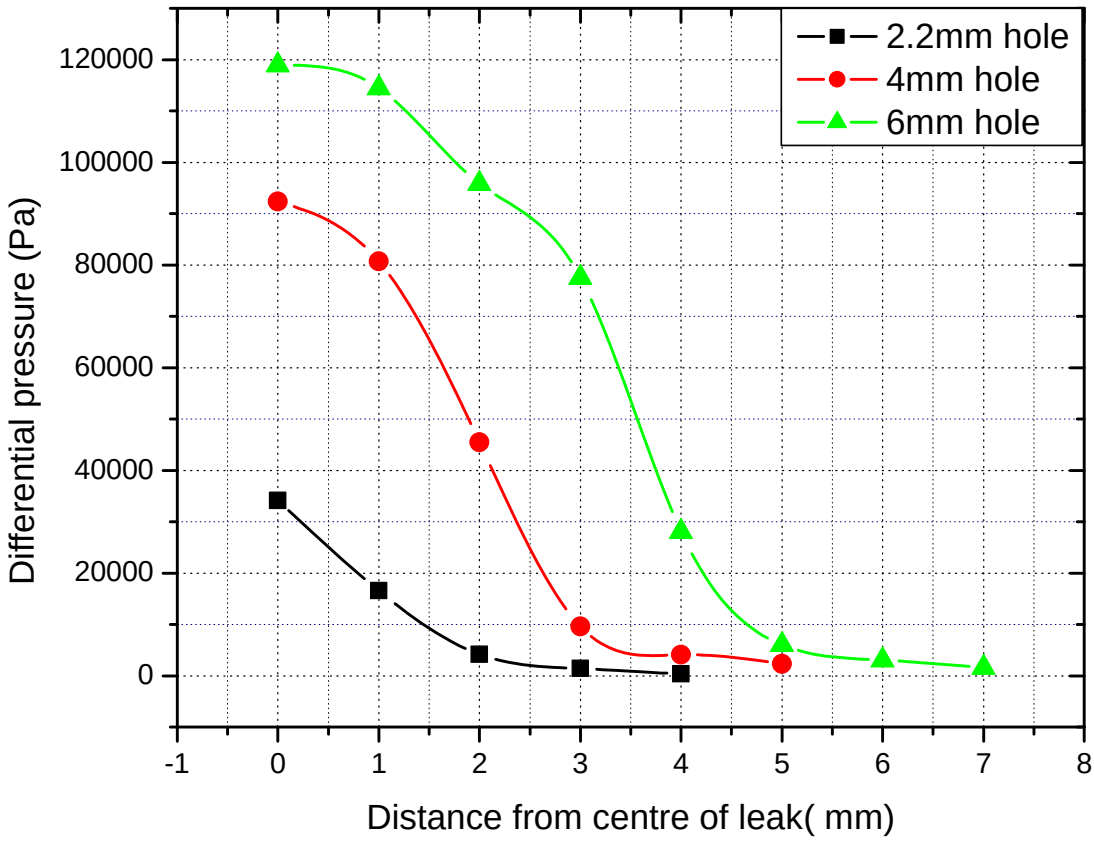

Figure 4.26: Effect of leak size: simulated holes; Experimental results; 1mm above the wall; 30psi line pressure

For the simulated holes, the flow rate increases with the increase in diameter which in turn increases the differential pressure between the vicinity of the leaks and the pipeline. From the plots in figures 4.25 and 4.25, *it is obvious that, the larger the leak size the larger the area covered by the leak signature*. For instance, a pressure difference of 4kpa approximately was measured at an axial distance of 3mm away (z = 6mm) from the leak circumference for 6mm leak diameter. However, the same magnitude of the pressure difference could only be felt at about 2mm (z = 4mm) and 1mm (z = 2mm) from the circumferences of leaks with 4mm and 2.2mm diameter respectively.

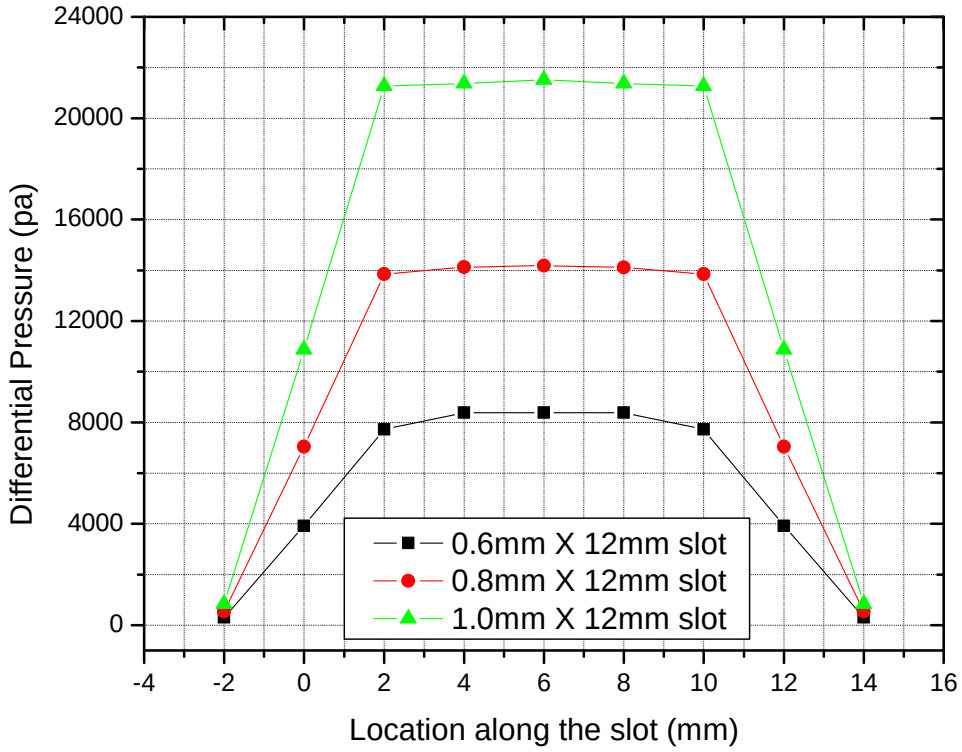

Figure 4.27: Effect of leak size: simulated slots; 1mm above the wall; 30psi line pressure

Maximum difference pressures occur at the center of the slots with an increase with increasing width of the slots. The differential pressure on the slots increases from the tips of the slot where highest gradient of pressure is observed to the centers. *Figures 4.27 supports the fact established before that the increase in the leak size increases the differential pressure measured in the leak vicinities.* The magnitude of the pressure difference for the 0.6mm thick slot at 1mm is less than 10kpa while it's three times that value for 1mm X 12mm slot.

This explains where the characteristics of the sensor come to play. At a fixed location above the wall, ability to pinpoint a leak depends on the sensitivity and measuring range

of the sensor. For instance, to accurately capture the pressure change in the vicinities of the slot, a more sensitive sensor was adopted.

Effect of the geometry on the obtainable pressure drop can be observed by comparing the peaks for all both the simulated holes and slots. *The width normal to the axial direction has significant effect on the magnitude rather than the overall surface area*. For instance, the 2.2mm diameter leak having a smallest surface area compared with the slots (0.6mm X 12mm, 0.8mm X 12mm and 1.0mm X 12mm) has a highest differential pressure. The length along the axial direction determines the range of signal detection along the pipe.

4.4.4 Sensor Tap's Normal Distance from Wall

This section presents the effect of the sensor tap height on the measureable pressure dfference. Figures 4.28 and 4.29 show the variation of height with differential pressure for the simulated holes (experimental results) and simulated slot (Computational results with a validation data) respectively. *In all the cases, the differential pressure reduces exponentially from the line pressure (30psi) at the wall (z=0mm) to 0psi (at different heights away from the wall).*

For the 2.2mm holes, the differential pressure started approaching zero at height beyond 2.0mm from the wall while the signal for 4mm and 6mm holes are still on higher slopes. Similar trend is observed with the slots. For the slots, it can be claimed from the trend of the results that the differential pressure would approach a magnitude not detectable by most commercially available sensors.

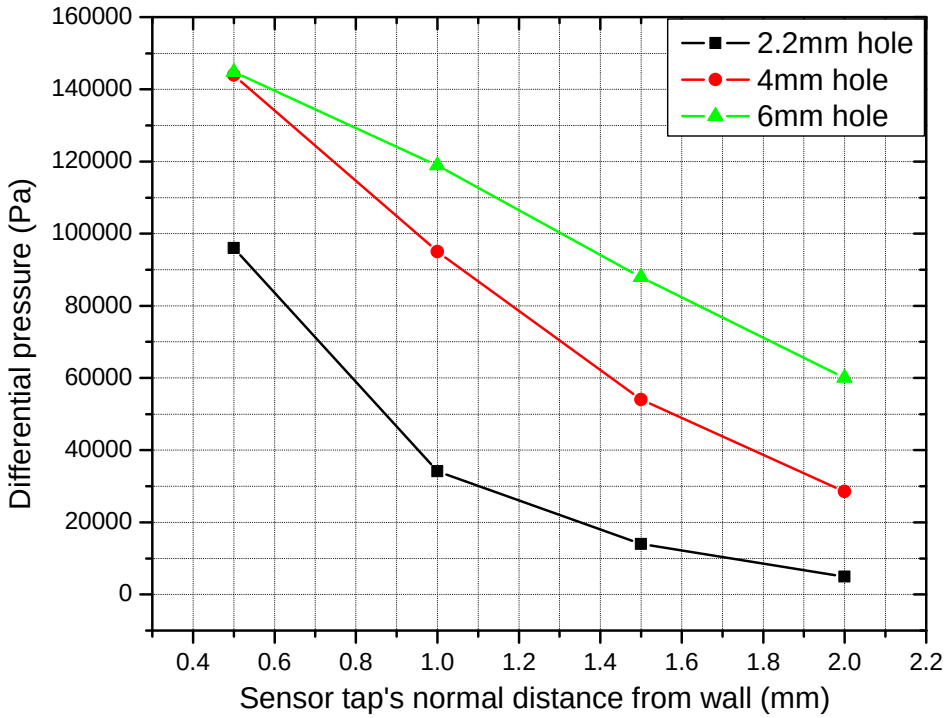

Figure 4.28: Effect of sensor tap's normal distance: simulated holes; Experimental results; 1mm above the wall; 30psi line pressure

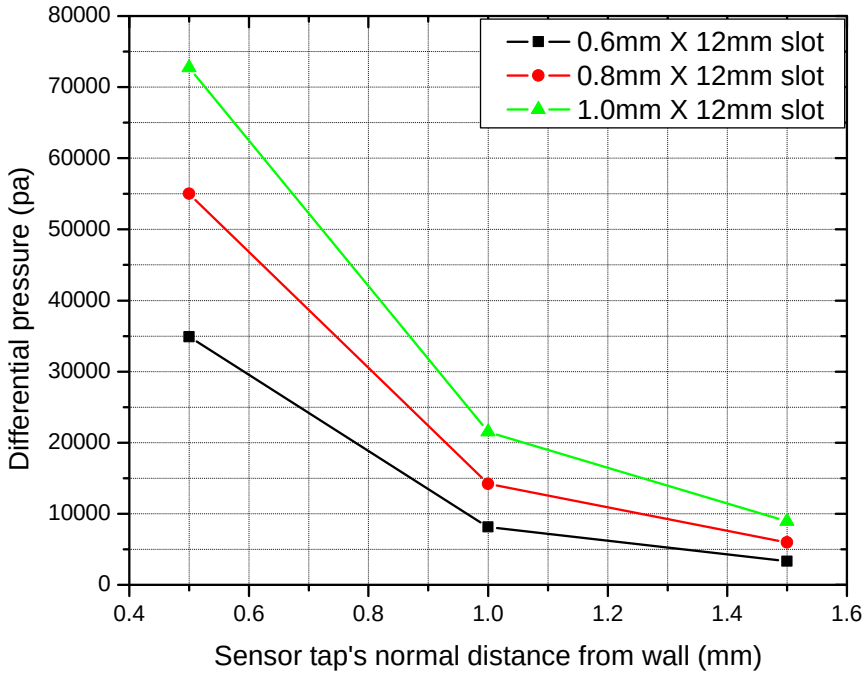

Figure 4.29: Effect of leak size: simulated slots; Numerical results; 1mm above the wall; 30psi line pressure

4.4.5 Effect of Line Pressure

In this section, we present the effect of pipeline pressure on the obtainable differential pressure. Using computational valid model, the differential pressure for each of the simulated leaks at height of 1mm above the wall was observed. The line pressure was varied by changing the pressure inlet boundary conditions from 10psi to 30psi in an increment of 5psi. The plots shown in figures 4.30 and 4.31 represent the trends for holes and slots respectively. *The differential pressure increases linearly with the pipeline pressure.* This relationship can be explained with Bernoulli's equation. Beyond the entrance region of a closed pressure driven pipe, the pressure distribution is a straight line function of the two boundary pressures. *The slope of the curves is a function of the leak geometry as it becomes steeper as the size of the leak increases. Thus, we could infer that the leak detection based on this technique works optimally at the peak line pressure.*

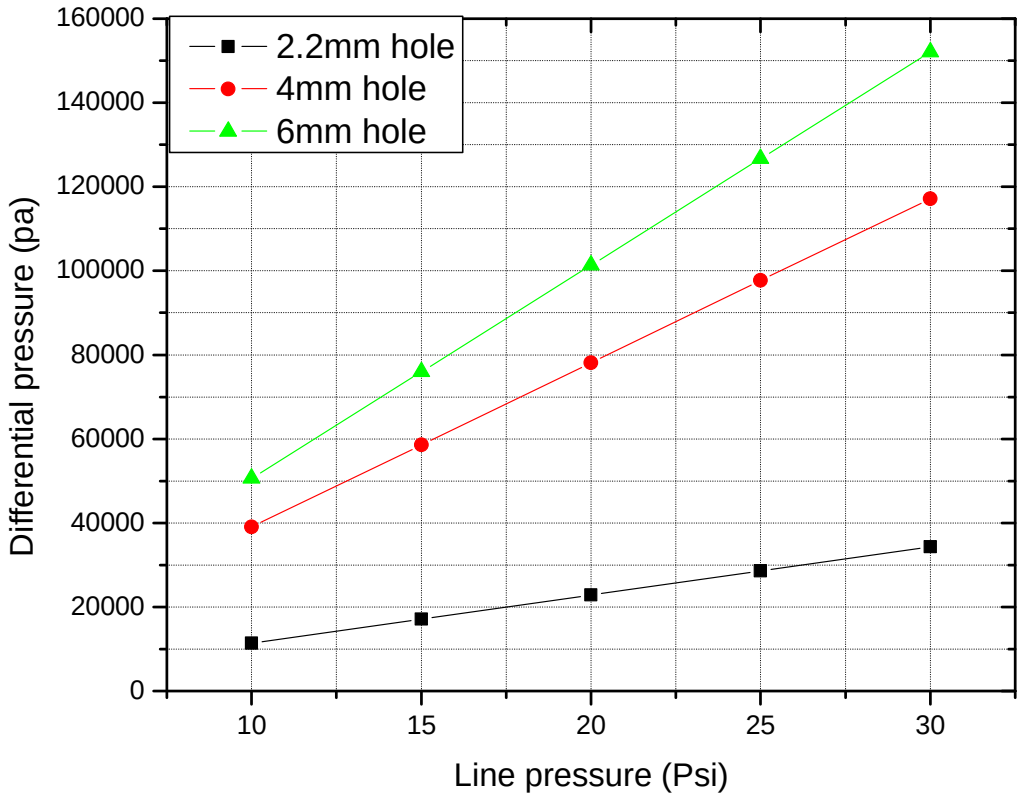

Figure 4.30: Effect of line pressure: simulated holes; Numerical results; 1mm above the wall;

z = 0 (center of the leaks)

In summary, the effect of the line pressure shows that pressure drop varies linearly and directly with the line pressure. This fact is supported by theoretical predictions using Bernoulli's equation. Thus, we suggest that the technique is best put into use at the off-demand-peaks where the maximum pressure in a typical water distribution network is achievable.

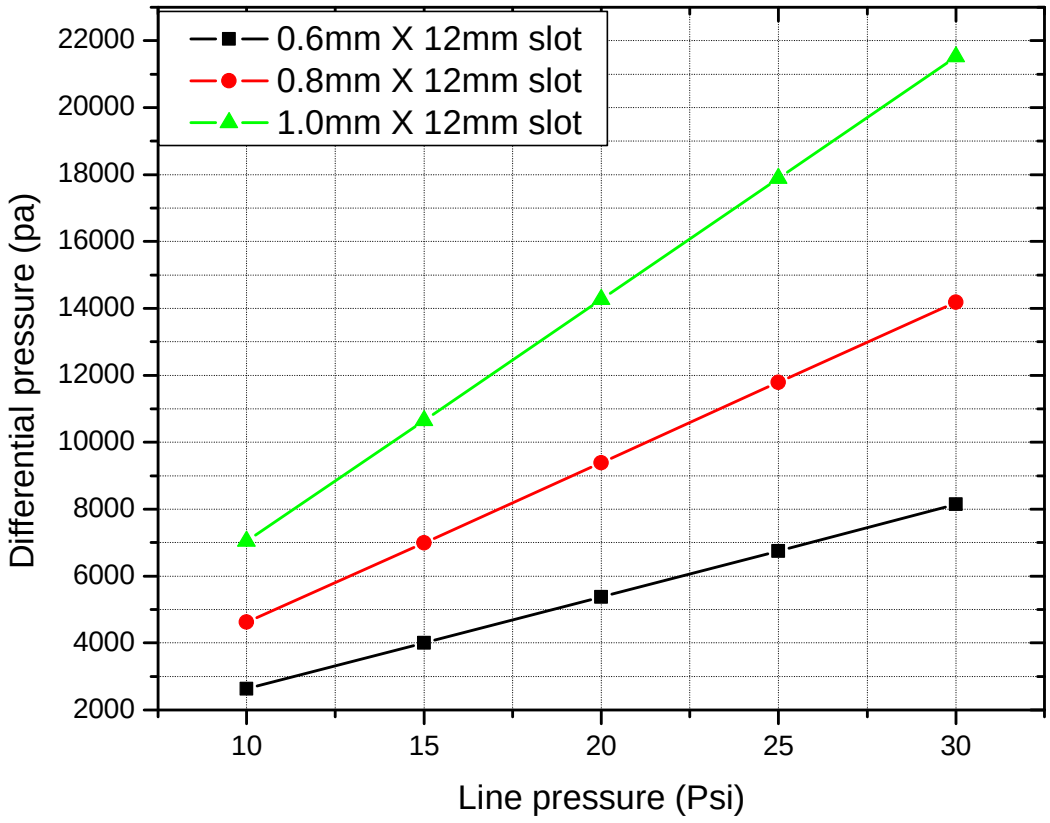

Figure 4.31: Effect of line pressure: simulated slots; Numerical results; 1mm above the wall;

z = 6mm (center of the slots)

4.4.6 Effect of Flow

A case of no pipe flow represents the best form of test for response of sensor to a quantity, thus the bulk of the study was carried out in a no flow condition. This allowed parameters like height, size of tap and pressure to be examined. A real pipe network however is characterized with flow; therefore a functional leak detection system is required to be tested against flow condition. Apart from the negative environmental

interference problem deterring the use of acoustic technique for leak detection, there is a big difficulty in using the technique under flow condition. We studied the prospect of differential pressure technique against this condition to identify the effect. From the first sight of Bernoulli's equation, one might say flow in the pipe will have an influence on the pressure distribution and thus having effect on the differential pressure in the vicinities of leaks.

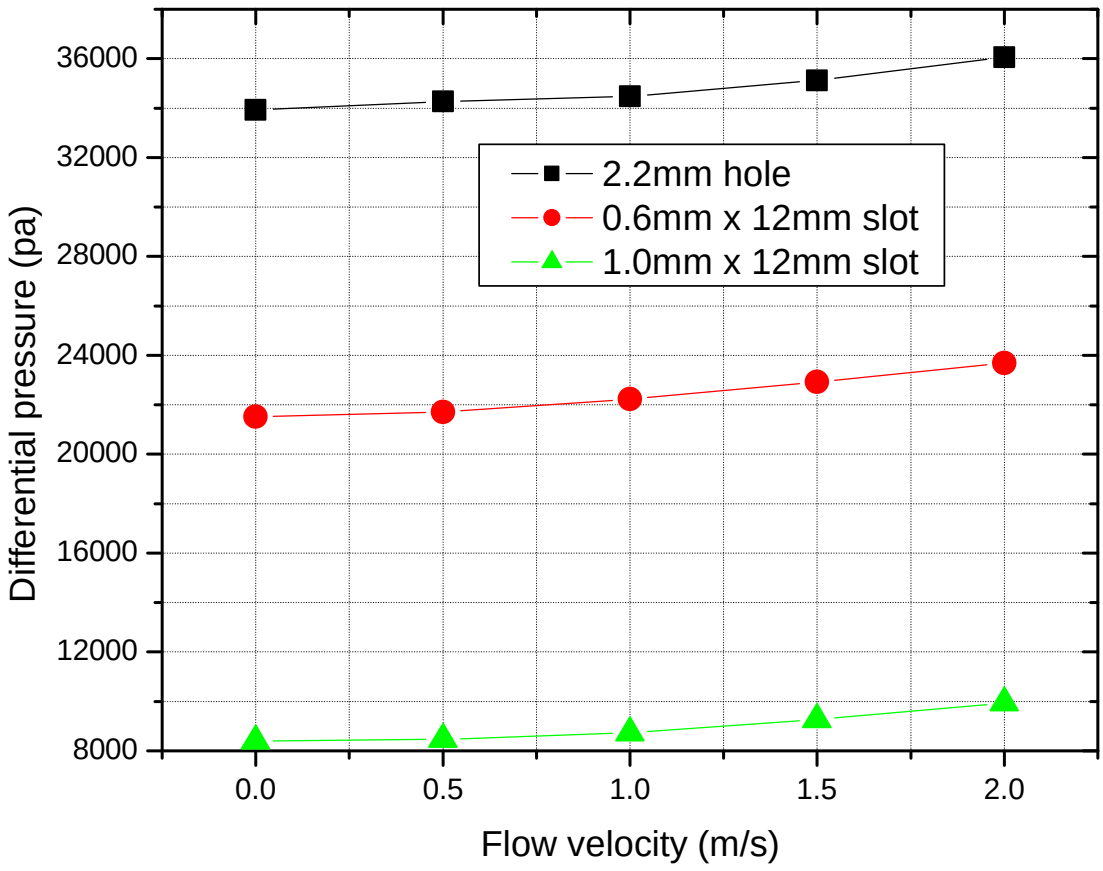

Figure 4.32: Effect of flow: simulated slots; Numerical results; 1mm above the wall; Center of the leaks

This effect was studied using CFD for the cases of 2.2mm hole, 0.6mm X 12mm slot and 1mm X 12mm slot. This was done by changing each of the pipe ends to velocity inlet (to control flow) and pressure outlet (to regulate pressure). The pressure at the end of the pipe was fixed at 30Psi for all the simulations while the velocity of flow was varied from 0.5m/s to 2m/s in an increment of 0.5m/s. Figure 4.32 shows the effect of velocity variation on the differential pressure. *For all the cases, the differential pressure did increase insignificantly with the increase in the velocity of flow.* At lower flow rate, the difference in the differential pressure as compared with the no flow condition is almost unnoticeable. Even at higher flow velocity (2m/s; close to maximum allowable in a typical water distribution network), the differential pressure has no remarkable increase. *We can therefore claim that the pipe flow increase has positive if any significant on the measurable value of differential pressure within the vicinities of the leaks.* This technique can therefore fill the gap for leak detection for operational pipe networks where most of the other leak detection methods fail.

CHAPTER 5

CONCLUSIONS AND RECOMMENDATIONS

5.1 Deductions from the Thesis

The thesis investigated the use of differential pressure as a parameter in-pipe leaks in the sensing module of an in-pipe leak mechanism.

The work used three-dimensional CFD turbulent flow calculations to investigate the flow characteristics close to simulated small cylindrical leaks in a typical water distribution pipelines. In which pressure related characteristics and acceleration were identified to change greatly in the vicinities of leak. The simulations results were validated against experimental and theoretical orifice equation; and an excellent agreement was found. In terms of reliable leak detection methods two variables were identified. The first variable that showed clear effect of the leak is the pressure gradient in the vicinity of leaks. The second clearly observable variable affected by the leaks is the flow acceleration.

Experiments were set up to investigate the behavior of differential pressure within vicinities of leak. Small leaks (starting with 2.2mm diameter hole) were simulated as cylindrical openings in the wall of the test section likewise crack approximated as slot was also studied. Also, 3D simulations were carried out to investigate the behavior of differential pressure within the leak vicinities. Results of both studies were compared at several locations and practical conditions of line pressure. In the experimental set up,

pressure sensor holder was adapted by incorporating a pressure sensor tap in order to isolate the sensor from the pipe.

Deductions were made by studying the field differential pressure field around the leaks for design recommendations. The effects of the pressure sensor tap on the differential pressure measurement are studied to identify the challenges that could be faced in full scale implementation of the method. In further extension to the experimental studies, the effect of fluid flow velocity on the differential pressure was studied numerically. This is done by addition simulations with the conditions (velocity inlet) which simulate pipe fluid flow condition. The velocities studied are within the range of specified in international standards. Also the effects of pipe inline pressure on the differential pressure measurements are studied by varying the pressure within the pipe.

Finally, in-pipe mobility module using propeller propulsion unit was designed, fabricated and tested for water-proof.

Based on the studies, the following conclusion are made

1 Static pressure close to leaks varies greatly in magnitudes as detected by pressure sensors. Also as we move away in normal distance from the wall, the magnitude of deviation reduces and the signature spreads out.

2 There is highly localized pressure gradient within leak vicinities. This pressure gradient increases with an increase in the pipeline pressure. Thus, increase of pressure within the pipe network would increase the chances of pinpointing leaks with parameters related to pressure

3 The velocity of flow toward the outlet of the leaks is approximately 20 times the fluid flow velocity in other parts of the pipe, thus, resulting into higher values in convective acceleration in the leaks' vicinities. Thus, we identified convective acceleration as another means of pinpointing leaks with the use of accelerometers.

4 The presence of the sensor tap and any other obstructions as result of the in-pipe mechanism would bring about an increase in the differential pressure around cracks and openings in pressurized pipes.

5 The result of intrusion at normal heights from wall indicates very high level at 0.5mm from wall, which results into higher differential pressure. Thus, the closer the sensor to the wall, the more efficient the method.

6 Both experimental and numerical results agreed well in both magnitude and trend.

7 The larger the leak size the larger the area covered by the leak signature indicated by the differential pressure.

8 Increase in the leak size increases the magnitude of differential pressure measurable in the leak vicinities. The width normal to the axial direction has significant effect on the magnitude rather than the overall surface.

9 The differential pressure reduces exponentially from the line pressure (30psi) at the wall (z=0mm) to 0psi (at different heights away from the wall).

10 The effect of the line pressure shows that pressure drop varies linearly and directly with the line pressure.

11 The fluid flow increase has positive if any significance on the measurable value of differential pressure within the vicinities of the leaks.

5.2 Recommendations for Future Work

The following are recommended as an extension for future work based on findings of the work;

1 Construction of robust experimental set ups (purposefully for in-pipe leak detection methods) which could easily be adapted to for quick investigation of numerical findings.

2 Further experimentation of the method on-site in operational pipeline in order to address other challenges.

3 Test sensor against movement

4 Optimal control of speed and thrust for the propeller propulsion unit of the fabricated mobility module.

Appendix

MOBILITY MODULE

The objective of this section is to redesign and incorporate a propulsion unit to mobility module previously designed by the research group. This is in line with the overall goal of a complete autonomous in-pipe leak detection technique. We present the general review of the previous contributions on the work. Also in this section, the overview of different propulsion units available to drive the mobility module is presented. The redesigns done on the work in terms of the body structure and sealing are also presented.

In the previous chapter, we have discussed on sensing module working on the principle of differential pressure within the vicinities of leak. We have shown that, this method works well as there are appreciable magnitudes of differential pressure in the leak vicinities. However, mobility of such sensing mechanism in water still presents a challenge involving isolation of the components (sensors and circuitries) in a pressurized water pipe.

There are previous mobility modules designed to move inside pipes. Figure 5.1 shows the assembled 3D printed mobility module designed by Chatzigeorgiou, [35]. Owing to the invasive nature of this particular of leak detection approach, the body was designed streamlined to minimize its effect of its presence in a pipe network. The prototype was

designed as two separate halves with hooks for attaching the legs. The six legs serve the functionality of support to the whole body and also act as means for applying brake on the system during slow down and stopping. The floating ability of the system was tested and it was found that the body floated well with minimal instability in the direction of flow. CFD simulation done the hull of the module revealed that, there are no flow separations at the trailing edge of the body; thus, sensing mechanism could be attached to the body without much disturbance.

In the work of Changrak [36] on an effort to design the propulsion unit for the design shown in figure 5.2, he identified four designs that could be incorporated. The first of which is the magneto-hydrodynamic propulsion (MHD), the disadvantages of this method as related to the present sensing is the possibility of the magnetic interference on the on-board circuitry and the overall low thrust and velocity achievable by this method. The second is the fishlike propulsion which has limitation on the length of the mobility module with an inability to actually control braking of the system. Another option he looked into is the synthetic jet propulsion. This could drive the sensing module within the constrained space at reasonable speed and thrust but has a limitation on the direction i.e. it can only move in one direction. The final option is the use of propeller propulsion unit. Although, the mechanism has a disadvantage of noise during operation and the risk of damaging the propeller in case of accident however, it has the capability to produce a thrust of up to 7.41N as against the 5N calculated for propulsion at the worst drag case in water-filled pipe. Also, a speed up to 2.3m/s could be reached as against 2m/s relative speed required as maximum for braking in free floating mode or accelerating in a no flow pipe condition.

Figure A.1 Assembly of the 3D printed mobility module by Chatzigeorgiou, (2010) [36]

Propeller propulsion units still stand the best chance to achieve the desired autonomy in the control of the mobility module for the in-pipe leak detection technique we are developing. In using this propulsion unit for back and forth movement, two problems are identified.

Casing leakage: In a design of an autonomous leak detection technique, all the components (sensing and communication circuitries) need to be on-board, isolated from moist. However, a propeller driven mobility module transfer torque through a shaft which passes through the casing. This hole creates a high risk of damaging the in-shell components. Therefore, proper sealing is required around the shaft to prevent water from entering into the casing.

Friction: There are sources of friction when a propeller propulsion unit is incorporated into the mobility module. First is as results of imbalance in the transmission. The major is as result of the surface between the shaft and seal.

The following section describes how the mobility module is redesigned to match the KFUPM workshop capability and the solution incorporated to the above highlighted problems.

The mobility module is described basically on four headings, these are; the capsule, the Legs and legs holder, cover seal, and the drive.

Capsule: The capsule of the present version has a total length of 130mm. It contains three parts connected together by threaded joints. The upper and lower parts are made as hemispheres of diameter 50mm. The middle part is made hollow with a thickness of 1mm through the length except at the ends with 2mm thickness to accommodate for the threads and grooves for sealing. The grooves on the ends are made to accommodate O-rings. This is designed to seal the joints under pressure. The body weight balances out floats well in pipe without other components attached. The capsule has enough space to accommodate for the batteries and circuitries. Picture of the capsule is shown below. (see Fig. A.2)

Figure A.2: Capsule of the module made out of Aluminum with two pressure sealed junctions

Legs and Legs holder: Although the capsule floats without other components attached, yet instability cannot be ruled out under operation. Similarly imbalance after loading with attachment cannot be avoided especially with the weight of the drive coupled on the cover. Therefore, the six legs in the previous version still have their stability function in addition to providing means of braking during slow down. The previously designed legs were maintained. In order to attach these legs to the casing, leg holders are designed with three hooks placed 120^{o} apart. Also three screws are provided at 120^{o} apart to attach the leg assembly the casing. This part is design to be detachable for (1) flexibility of positions where sensing module can be place i.e. the assembly orientation can be changed based on the requirements of the sensor to be attached. (2) For counter balance after loading other components (particularly the electronics). All the outer body components

are made out of Aluminum in order to reduce the overall weight of the system See the Fig. A.3 for description.

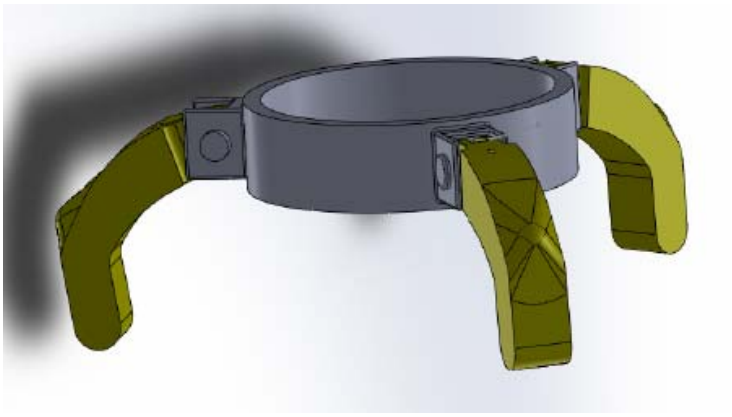

(a)

Figure A.3: Picture and solid work model of the legs and legs holder assembled.

Detachable for flexibility

Cover seal: One of the hemispheric ends of the casing is made the cover. A lip seal made out of Polytetrafluoroethylene (PTFE) – Glass reinforcement is used at the tip. PTFE has good application in lubrication, corrosion and wear resistance. The material is non-reactive and thus, it's acceptable in water and food processing. The sealing action of the part is energized by spring embedded at the internal groove of the seal. So as the shaft rotates around the seal, the springs ensure no passage of fluid from the pipe into the casing. The spring energized rotary seal works in fluid with pressure up to 150bars and temperature range of -40 to 260 degrees Celsius. Although, this sealing action generates addition friction into the system however, the lubrication power of the PTFE made the friction within affordable range. The seal is force fitted into one of the hemispheres in a way that the hydrodynamic external body of the cap is not significantly compromised. See figures showing the details below.

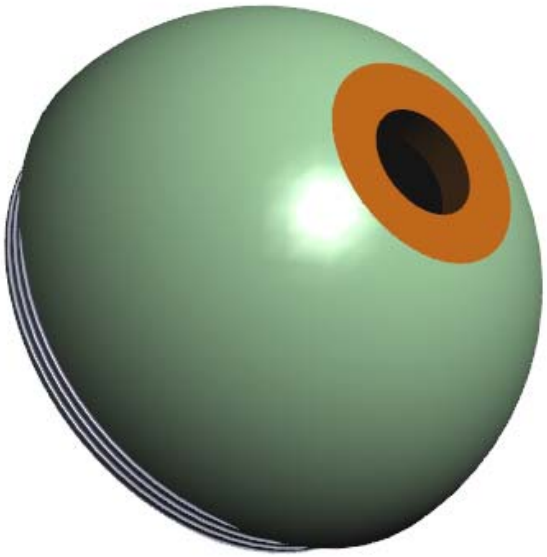

Figure A.4: Solid work model of the cap with the seal attached.

The drive: The drive of the module consists of a motor, a connecting shaft, motor and bearing holder, bearing and the propeller. The motor supplies the necessary rotational force through the shaft to the propeller which is designed to stir through the fluid either generate thrust to move or stop the mobility module. In order to reduce the friction due to the sealing action at on the shaft, a bearing is also placed at 10mm away from the lip seal. The bearing and the motor are secured on the cap using a holder. This holder increases the overall concentricity of the drive as it holds the motor and the bearing in place. The connecting shaft has a length of 30mm. 24mm of the length is 24mm diameter while the other 6mm is made into M4 thread coupling the propeller through the 6mm hub. Figures below show the solid models and the picture of the drive.

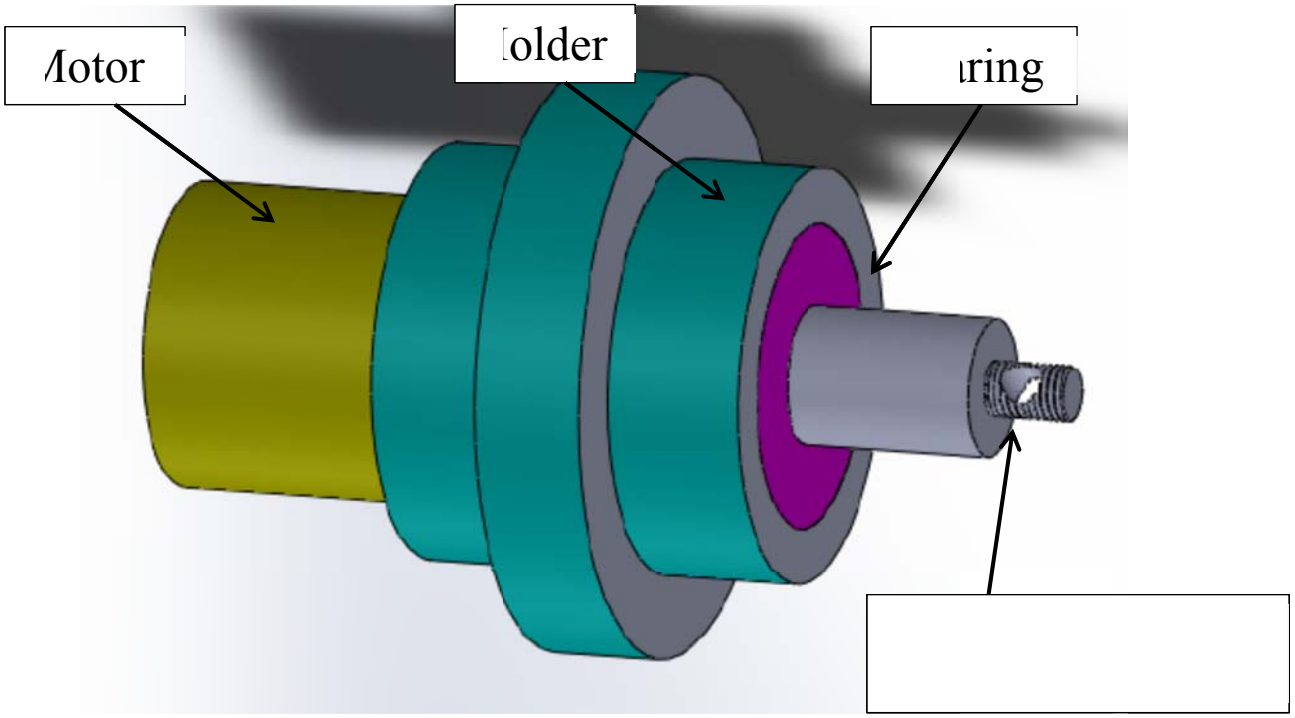

Figure A.5: Solid work model of drive without the propeller.

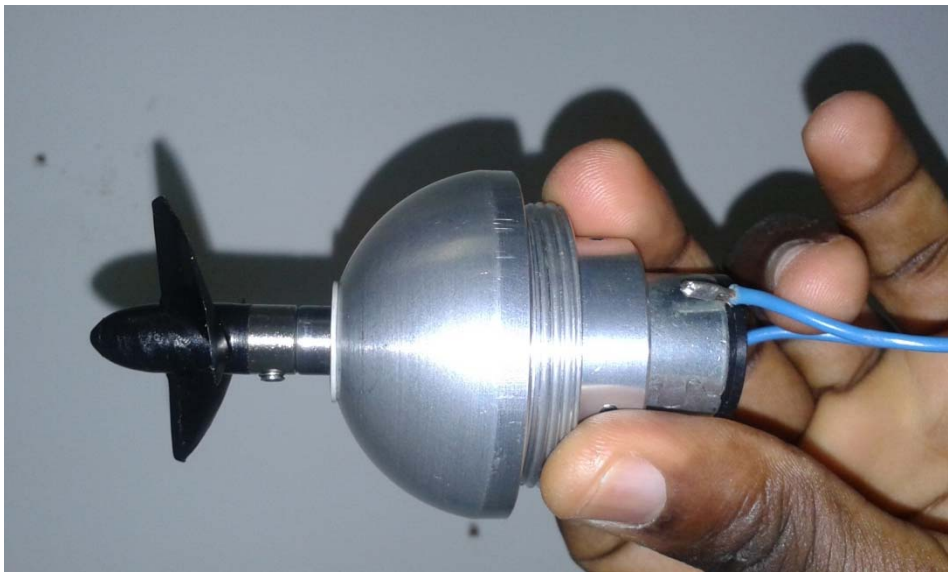

Figure A.6: Photograph of the drive with the propeller and the pressure sealed cover part.

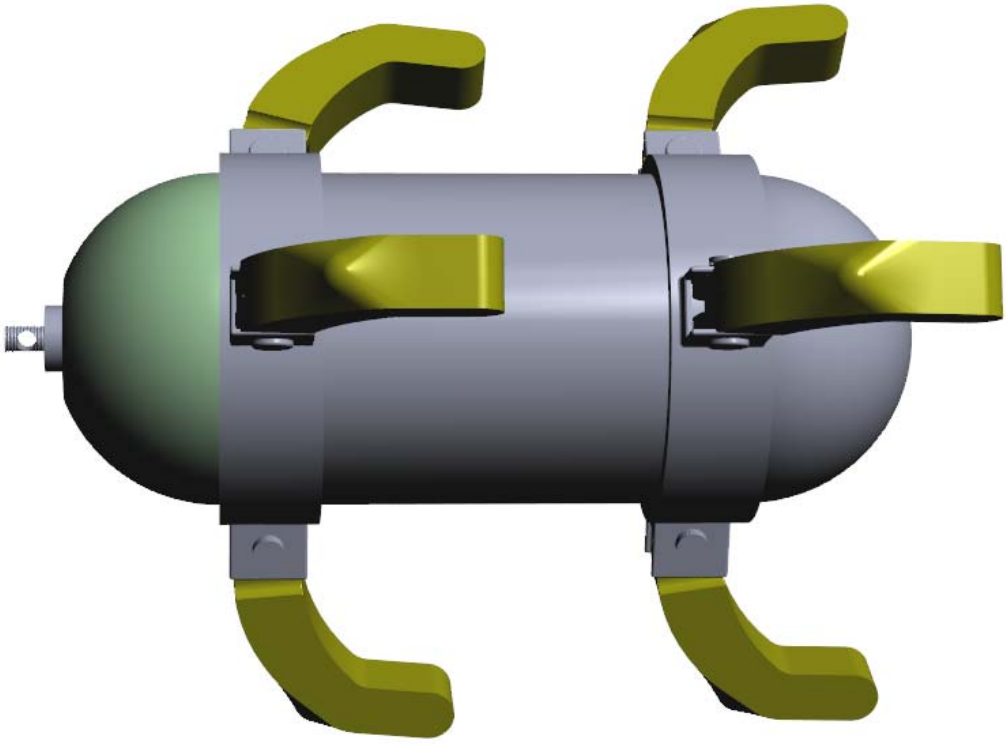

Figure A.7: Solid work model of the mobility module without the propeller

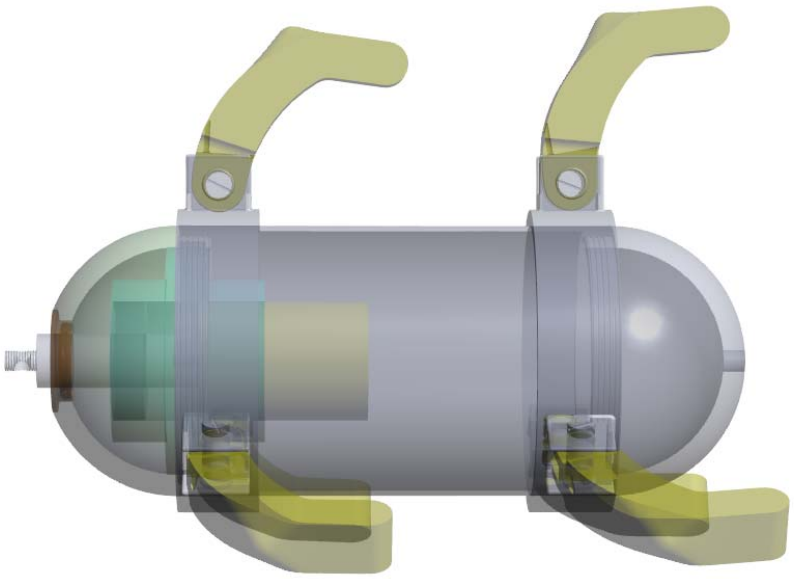

Figure A.8: Solid work model of the mobility module without the propeller showing inner details

Figure A.9: Picture of the assembled mobility module with parts made mostly out of Aluminum to reduce overall weight; shows the propeller at the tail end.

In conclusion after coupling the parts and seals, the mobility module is subjected to water proof test. Without attaching other components, the casing was packed with toilet paper. It was then kept in a pipe section with pressure over 45Psi for over 15miniutes. After removal, no trace of water was found on the tissue pressure; thus, the casing is water proofed and safe to accommodate the circuitry. We tested the rotation of the drive after incorporating the seal and we realized that there is enough rotational speed. This speed can further be manipulated by the electrical control to achieve the thrust-speed combination required to drive the mobility module in the pipe. Further test is water-proof test is recommended after incorporating the electronic to create rotation action under pressure.

In summary, a mobility module has been redesigned, constructed and tested for water-proof and rotation with lip seal. The design incorporated a propeller propulsion unit which is sealed at the shaft in order to avoid moist into the casing. The water proof test with no rotation was successful and test by powering the propeller directly from battery indicates that the drive has appreciable rotational speed despite the grip of the lip seal on the shaft.

REFERENCES

1. Mohan, K., Shankar, N., and Bhallamudi, S. (2008). State Estimate in Water Distibution Networks Using Graph-Theoretical Reduction Strategy. *Journal of Water Resources Planning and Management*, 134(5), 395-403
2. Control and Mitigation of Drinking Water Losses in Distribution Systems. (2011). Retrieved December 18, 2011, from United State Environmental Protection Agency (EPA): http://www.epa.gov/WaterSense/pubs/fixleak.html
3. Hunaidi, O., and Chu, T., (1999). Acoustic Characteristics of Leak Signals in Plastic Water Distribution pipes. *Applied Acoustics*, 58(3), pp. 235-254.
4. Urban Water Resources Management UWRM. Retrieved December 18, 2011, from UWRM: http://www.gdrc.org/uem/water/
5. Muggleton, J., Brennan, M. J., & and Pinnington, R. J. (2002). Wavenumber Prediction of Waves In Buried Pipes fFor Water Leak Detection. *Journal of Sound and vibration*, pp. 939-954.
6. Long R.,Cawley P. and Lowel M. (2003). Acoustic wave propagation in buried iron water pipes. *Proceedings of The Royal Society*, (pp. 2749-2770). London.
7. Yang Jin, Wen Yumei and Ping Li. (2008). Leak Acoustic Detection in Water Distribution Pipelines. *Proceedings of the 7th World Congress on Intelligent Control and Automation* (pp. 3057-3061). Chongqing: IEEE.
8. Matin, T., Allwright, D., Chapman, C., Howison, S., and Ockendon, J. Noise Generation by Water Pipe Leaks. Mecon Ltd.

9. Maninder, P., Neil. D., and James, F. (2010). Detecting & Locating Leaks in Water Distribution Polyethylene Pipes. *Proceedings of the World Congress on Engineering 2010.* London.

10. Wu, Z. Y., Sage, P., and Turtle, D. (2010). Pressure-Dependent Leak Detection Model and Its Application to a District Water System. *Journal of Water Resources Planning and Management*, 166(1), pp. 116-128.

11. Gao Y., Brennan M., Joseph P., Muggleton J. & Hunaida O. (2005). On the selection of acoustic/vibration sensors for leak detection in plastic water pipes. *Journal of Sound and Vibration*, pp. 927-941.

12. Hunaid O., Wang A., Bracken M., Gambino T., and Fricke C. (2004). Acoustic Methods for Locating Leaks in Municipal Water Pipe Networks. *International Water Demand Management Conference*, 1-14. Dead Sea – Jordan

13. Wilsky A. (1976). A Survey of Design Methods for Failure. Automatica, 601-611.

14. Fahmy M. and Moselhi O. (2009). Detecting and locating leaks in Underground Water Mains Using Thermography. *26th International Symposium on Automation and Robotics in Construction* (ISARC 2009), pp. 61-67.

15. Bimpas, M., Amditis A. and Uzunoglu N. (2010). Detection of water leaks in supply pipes esing continuous wave sensor operating at 2.45Hz. *Journal of Applied Geophysics*, 226-236.

16. Karney B., Khani D., Halfawy M. and Hunaidi O. (2009). A simulation Study on Using Inverse Transient Analysis for leak Detection in water distribution Networks. *Proceedings of the International Storm water and Urban Systems Modeling Conference*, (pp. 1-21). Toronto, Ontario.

17. Covas D., and Ramos H., (2010). Case Studies of Leak Detection and Location in Water Pipe Systems by Inverse Transient Analysis. *Journal of Water Resources Planning and Management,* 136(2), pp. 248-257.

18. Shinozuka M., Chou P., Kim S., Kim H., Yoon E., et al. (2010). Non-destructive Monitoring of a pipe network using MEMS-Based Wireless Network. *Proceedings of SPIE Conference on Smart Structures.* San Diego.

19. Mashford J., De-Silva D., Marney D. and Burn S., (2009). An Approach to Leak Detection in Pipe Networks using Analysis of Monitored Pressure Values by Support Vector Machine. *Proceedings of the 3rd International Conference on Network and System Security (NSS '09).* IEEE Computer Society Press.

20. Greyvenstien, B., and Van Zyl, J. (2007). An Experimental Investigation into the Pressure Leakage Relationship of some Failed Water Pipes. *Aqua- Journal of Water Supply: Research and Technology,* 56(2), pp.117-124.

21. Ben-Mansour R., Habib M., Khalifa A., Youcef-Toumi K., and Chatzigeorgiou D., (2012). Computational Fluid Dynamics of Small Leaks in Water Pipelines for Direct leak Pressure Transduction. Computers & Fluid, 57, pp. 110-123.

22. Khuleif Y., Khalifa A., Ben-Mansour R., and Habib M., (2012). Acoustic Detection of Leaks in Water Pipelines using Measurements inside Pipe. *Journal of Pipeline Systems Engineering and Practice.* 3(2), pp. 47-54

23. Reid J. and Michael P. (1966). Apparatus for Pinpointing Leaks in Buried Pipes. *Patent No. 3264864. United States American*

24. Choudhury, D., 1993, Introduction to the Renormalization Group Method and Turbulence Modeling. Fluent Inc., Technical Memorandum TM-107.

25. Sun, L. (2012). Mathematical modeling of the flow in a pipeline with a leak. *Mathematics and Computers in Simulation*, *82*(11), pp. 2253–2267.
26. Verde, C. (2001). Multi-leak detection and isolation in fluid pipelines. *Control and Engineering Practice 9*, pp. 673–682.
27. Misiunas, D., Vítkovský, J., Olsson, G., Simpson, A., & Lambert, M. (2005). Pipeline Break Detection Using Pressure Transient Monitoring. *Journal of Water Resources Planning and Managment*, 131(4). pp.316–325.
28. Larry W. (2000). Water Distribution System Handbook. McGraw Hill.
29. Fletcher R. and Chandrasekaran M. (2008). SmartBall^{TM}: A New Approach in Pipeline Leak Detection. *7th International Pipeline Conference (IPC2008).* ASME Conference Proceedings. 2008. pg: 117-33.
30. Chatzigeorgiou, D., Khalifa, A., and Youcef-toumi, K. (2011). An In-Pipe Leak Detection Sensor: Sensing Capabilities and Evaluation. *Proceedings of the 2011 ASME/IEEE International Conference on Mechatronic and Embedded Systems and Applications (MESA 2011).* Washington, DC, USA.
31. Chatzigeorgiou, D., Ben-Mansour, R., Khalifa, A., and Youcef-toumi, K. (2012). Design and Evaluation of an In-Pipe Leak Detection Sensing Technique Based on Force Transduction. IMECE2012-87493. *Proceedings of the ASME 2012 International Mechanical Engineering Congress & Exposition (IMECE 2012).*
32. Patankar, S. (1980). Numerical heat transfer and fluid flow. Hemisphere Publishing.

33. Shuja, S., Yilbas, B., and Budair O., (2001). Local Entropy Generation in Impinging Jet: Minimum entropy concept evaluating various turbulence models. *Computer Methods in Applied mechanics and engineering,* 190, pp. 3623-3644.
34. Fluent 12.1 User's Guide, Fluent Inc., Center Research Park, 10 Cavendish Court, Lebanon, NH 03766, USA, 2003.
35. D.M Chatzigeorgiou (2010). Analysis and Design of an In-pipe System for Water leak Detection. MIT, Thesis, 2010.
36. C. Changrak (2012). Robot Design for Leak Detection in Water-Pipe Sytsem. MIT, Thesis, 2012.

VITAE

Name: Suara, Kabir Adewale

Nationality: Nigerian

Date of Birth: January 16, 1987

Home Address: No 47, Majawe Street, Behind Nigerian Brewery PLC, Olubadan Estate II, Ibadan, Oyo State, Nigeria.

Email: suara@kfupm.edu.sa , suarakabir@gmail.com

Education with date

- Msc Mechanical Engineering (*Specialization: Thermofluid)*), King Fahd University of Petroleum and Minerals, KFUPM, Saudi Arabia. (GPA 3.893 out of 4.00) — April 2013
- B.Tech Mechanical Engineering, Ladoke Akintola Univeristy of Technology, Ogbomosho, Nigeria. (GPA 4.19 out of 5.00) — December 2009